Universidad de **Valladolid**

Facultad de Ciencias

Trabajo Fin de Master

Máster en Química Sintética e Industrial

Comb-like ionic complexes of biopolyacids and alkyltrimethylphosphonium soaps

Autor: Ana Gamarra Montes

Director: Prof. Sebastián Muñoz Guerra (UPC)
Tutor: Prof. Pablo Espinet Rubio (Uva)

Este trabajo ha sido realizado en los laboratorios del Grupo de Polímeros Industriales y Biotecnológicos del Departamento de Ingeniería Química de la UPC y ha sido dirigido por el Prof. Sebastián Muñoz Guerra.

La temática y objetivos del proyecto forman parte de la Tesis Doctoral que ha iniciado la autora en la Universidad Politécnica de Cataluña con el título "*Comb-like ionic complexes of biopolyacids and cation soaps*" y vinculada al proyecto MAT2012-38044-C03-03 titulado *"Bioplasticos derivados de carbohidratos para envasado y farmacia. Subproyecto II"*

Vº Bº Director del Proyecto

Sebastián Muñoz-Guerra

Vº Bº Tutor Académico del Proyecto

Pablo Espinet Rubio

ACKNOWLEDGMENTS

SUMMARY

This project is addressed to the study of comb-like polyelectrolyte-surfactant ionic complexes. This type of systems is currently object of intensive research in our group due to their fascinating features. They are able to be self-assembled in well-ordered nanostructures that can be exploited for building barrier films and core-shell nanoparticles with singular properties as biomaterials.

The synthesis and characterization of a series of alkyltrimethylphosphonium bromides (nATMP·Br) with the alkyl chain containing even numbers n of carbon atoms from 12 to 22 was first performed. The structural and thermal analysis of these novel surfactants were carried out and results were critically compared with those reported for the well-known alkyltrimethylammonium surfactants. The preparation of the ionic complexes was then undertaken by simple mixing stoichiometric quantities of the respective polyacid and surfactant solutions at the suitable temperature according to the surfactant used. The naturally-occurring poly (γ-glutamic acid) and hyaluronic acid were the polyelectrolytes of choice to be ionically coupled with the phosphonium surfactants. The structure and thermal properties of the complexes were examined by NMR and X-ray diffraction spectroscopies, calorimetry and optical microscopy. Results were interpreted on the basis of data available for similar alkyltrimethylammonium complexes previously reported, and they allow to preliminary concluding that an amphiphilic layered structure is also adopted for these new bio-based comb-like polymer-phosphonium surfactant ionic complexes.

INDEX

I. INTRODUCTION

1. Surfactants

Surfactants are molecules made of at least two counterparts differing in polarity and with opposite affinity for water which are called the hydrophilic and hydrophobic counterparts, respectively. The hydrophilic part is often called the head-group and the hydrophobic part is called the tail group. Amphiphile is sometimes used as a synonymous of surfactant. This word is derived from the Greek word amphi, meaning both. Furthermore, surfactants are also known as tensioactive agents.

The hydrophilic and hydrophobic parts make the surfactant surface active in the sense that it tends to be located at interfaces between polar and non-polar media, so that the hydrophilic part is solvated in the polar medium and the hydrophobic part in the non-polar medium. In fact, the word "surfactant" is an abbreviation for surface active agent.

Hydrophilic head group

Hydrophobic tail
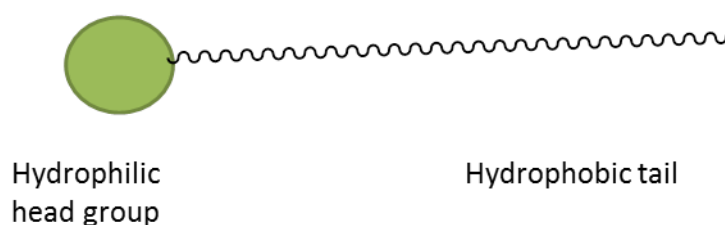
Figure I.1. Schematic illustration of a surfactant.

Surfactants absorption is caused in order to lower the free energy of the interface. So, surfactants reduce the surface tension of water, being the surface tension of water the interfacial free energy per unit area of boundary between water and the air above it. Surfactants are able to be absorbed in five types of interfaces, namely: solid-vapour, solid-liquid, solid-solid, liquid-vapour and liquid-liquid. The degree of surfactant concentration at an interface depends on the surfactant structure and also on the chemical nature of the two phases that meet at the interface. Therefore, there is not an universally good surfactant, suitable for all uses.[1]There is a limit to the surface and interfacial tension lowering effect by the surfactant. This limit is usually reached when micelles start to form in bulk solution.

1.1 Classification and structure of surfactants

Surfactants are usually classified according to the nature of their head-groups; thus, there are different types of surfactants:

Anionic surfactants. They have negatively charged head-groups. The cationic counterion is usually an alkaline metal or ammonium group. (*e.g.* salts of fatty acids).

Cationic surfactants. They have positively charged head-groups. The anionic counterion is generally an halide. (*e.g.* alkylamines or quaternary ammonium salts).

Zwitterionic surfactants. They are neutral molecules that are both, positively and negatively charged (usually depending on pH). (*e.g.* amino acids, betaines and phospholipid derived surfactants).

Nonionic surfactants. Their head-groups carry no charge and they do not suffer dissociation in water. (*e.g.* polyethylene oxide based surfactants).

A fundamental property of surfactants is their ability to form aggregates when mixed with water. The most common aggregates are micelles. At a given temperature they start to form at a certain concentration called the critical micelle concentration (*cmc*). The *cmc* is dependent on the surfactant structure. Below their *cmc* surfactants are dissolved in water as monomers in the solution. In the micellar aggregates the surfactant tail-groups will constitute the liquid-like hydrophobic interior phase while the head-groups form an outer hydrophilic layer in contact with the aqueous phase that prevents the interaction of the hydrophobic tails part with water. The micelles consist of a 50-150 surfactant molecules that self-assemble in a shape that is actually determined by on the v/v ratio of the head-group to tail-group. Israelachvili et al.[2] defined the "packing parameter" *p* in their micelle theory as the expression:

$$p = \frac{V}{al}$$

According to this expression, the micellar shape depends on different factors: the volume occupied in the micellar core by hydrophobic groups (V), the length of hydrophobic tails (l) and the optimal head-group area (α). Therefore, it will be formed different micelle structures according to the packing parameter value. (Table I.1).

Table I.1. Micelle structures depending on the packing parameter.

Packing parameter	Micelle shape	Picture
<1/3	Spherical	A
≈1	Lamellar	B
>1	Inverse	C
1/3<p<1/2	Cylindrical	D
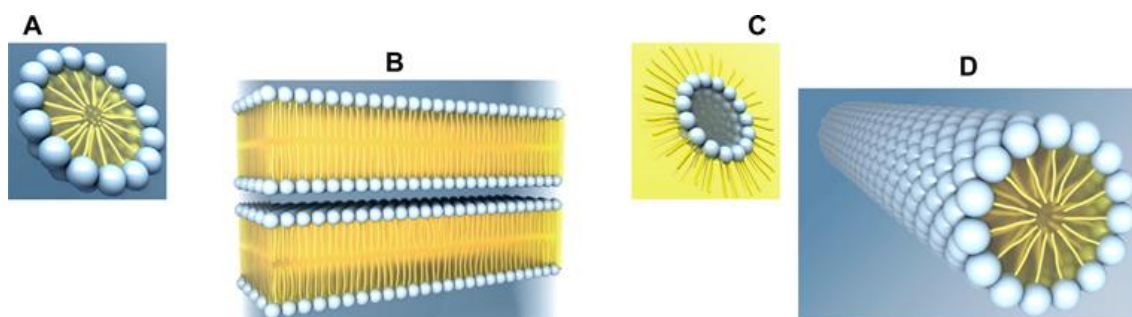
Figure I.2. Micelle structures.

Not only the size or length of hydrophobic tails influence on the geometry of the micellar shape, but also the surfactant concentration, temperature and additives.[3] The temperature is clearly one of the most influential in surfactant self-assembly. Therefore, there is a dramatic temperature-dependent solubility. While the solubility is usually poor at low temperatures, it increases by orders of magnitude in a relatively narrow temperature range. The temperature for the onset of the increase of solubility is called Krafft temperature. This temperature is strongly dependent on the alkyl chain length, the head-group and the counterion. Thus, Krafft temperature increases as the alkyl length increases and with salt addition. Another factor is the number of micelles in aqueous phase. When the number of micelles is high enough, they begin to pack together in a higher structural level. These structures have molecular order characteristic of crystals. However, they are not crystals because their molecular mobility is preserved. Consequently, they are called liquid-crystals. Furthermore, these structures have a specific geometric arrangement depending on the shape of individual micelles. Hence the spherical micelles give rise to cubic liquid crystals, the cylindrical micelles pack together into hexagonal liquid crystals, and the lamellar micelles form lamellar liquid crystals. (Figure I.3).
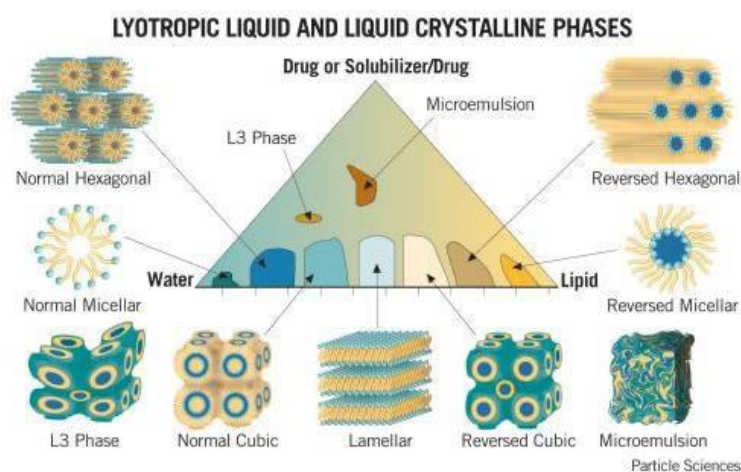
Figure I.3. Liquid crystal structures of surfactants.

I. INTRODUCTION

The concentration also plays an important role in the structural morphology of surfactants. While surfactants at low concentration have a good solubility, at high concentration high temperatures are required to achieve their dissolution. Between these concentrations liquid-crystals would be present, where the phases move from hexagonal structure to continuous cubic structures and further to lamellar assembly, as the concentration increases.

1.2 Alkyltrimethylphosphonium surfactants

Tetraalkylphosphonium surfactants are still a relatively unexplored field. However, they have recently become the focus of a good number of investigations because they offer superior properties when they are compared with tetraalkylammonium surfactants. Some of these properties are: their higher thermal stability,[4] antibacterial activity,[5] phase transfer capability[6] and electrostatic properties. Furthermore, tetraalkylphosphonium salts are generally less dense than water, which can be beneficial in processes that involve decanting steps.

Although using phosphonium salts presents several advantages, they are relatively expensive and they require cautious laboratory techniques due to alkylphosphines are often pyrophoric. These are common reasons for using the ammonium over the phosphonium functionality. Applications of tetraalkylphosphonium surfactants investigated in recent years include their use as extraction,[7] solvents,[8-10] electrochemical media,[11] phase transfer catalysts,[12-14] exfoliation agents for montmorillonite clays[15–17] and other smart materials applications.

Most attention in the literature has been given to the tetradecyltrihexylphosphonium halide surfactants[18-20] as they are commercially available within a range of different anions, and also relatively cheap. Furthermore, there are several publications dealing with alkyltrioctylphosphonium chorides,[21] one of them, the tetraoctylphosphonium bromide (CYPHOS IL 166), is also commercially available. Reports of alkyltributylphosphonium halides date back the 1980s, when Knifton published the use of some molten tetrabutylphosphonium bromide salts [22-25] which granted him several patents.[26-33] Then, alkyltributylphosphonium halides were applied in the late 80s as bioacides[34] or as compounds with microbiological activity.[35] Despite the impact of Knifton's studies, it was not until 1990 when tributylphosphine was started to be produced at large scale. Since then, not only tetrabutylphosphonium chlorides and bromides have become available on a multi-ton commercial scale, but many other alkylphosphonium compounds have been prepared. As a result, a large number of

compounds resulting from combining phosphonium cations with different four substituents and different anions may be designed. The majority of these tetraalkylphosphonium salts are available in Cytec Industries Inc.[18]

However, there are very few studies of the thermal and physicochemical properties of tetraalkylphosphonium surfactants bearing different substituents. As a detailed systematic evaluation of the basic physicochemical properties of tetraalkylphosphonium surfactants is necessary for future applications of these compounds, we have undertaken in this project the synthesis of a novel series of tetraalkylphosphonium surfactants and the study of their structure and basic properties. The surfactants of choice are alkyltrimethylphosphonium bromides (*n*ATMP·Br), which are represented in Scheme I.1. Specifically, the series includes the *n*ATMP·Br with the linear alkyl group being dodecyl, tetradecyl, hexadecyl, octadecyl, eicosyl and docosyl (*n* =12, 14, 16, 18, 20 and 22, respectively).
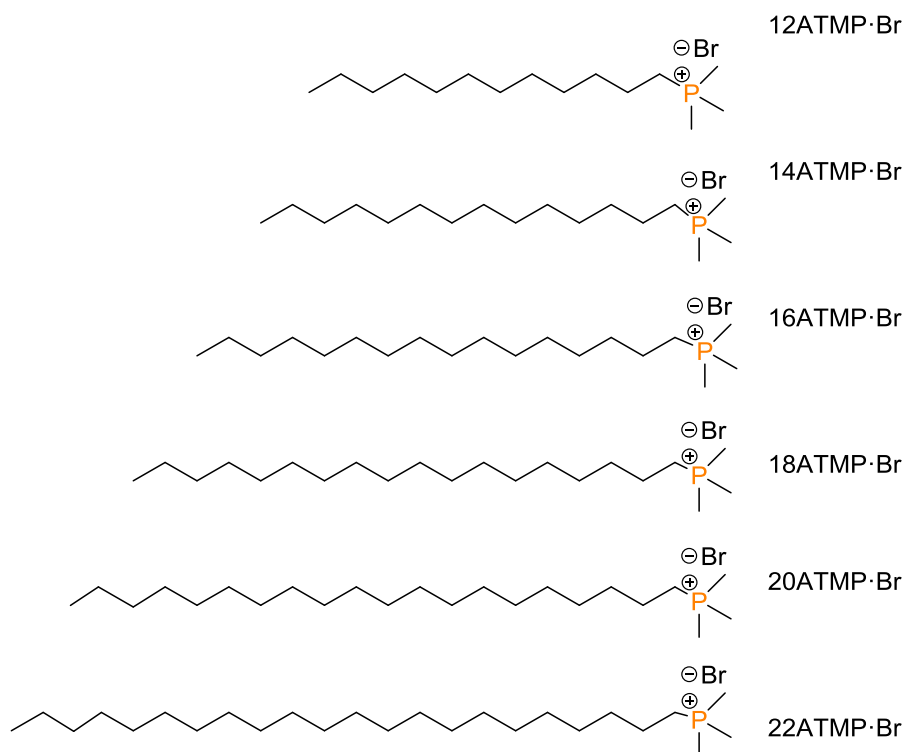
Scheme I.1. Alkytrimethylphosphonium bromides (*n*ATMP·Br).

2. Polyelectrolyte-surfactant complexes

The binding processes based on electrostatic interactions, hydrogen bond formation or charge transfer are those leading to the spontaneous formation of ordered structures. The wide variety of polyelectrolytes and tensioactives and the simple methodology for the synthesis of these stoichiometric complexes are clearly advantages that have recently motivated a high interest in this area.[36]

2.1 Structure of polyelectrolyte-surfactant complexes

Comb-like ionic complexes consisting of cationic tensioactives and oppositely charged polyelectrolytes are of prime interest due to different facts. On the one hand, spontaneous binding processes allow obtaining thermodynamically stable structures. Hence they are interesting to form **supramolecular assemblies**. Furthermore, **no covalent interactions** offer several advantages such as simple preparative procedures, fast reactions[37] and the resulting structures have tunable properties depending on medium changes. These complexes are generated spontaneously when the tensioactive and the polyelectrolyte are mixed in an aqueous solution. In this process, the counter ion of the polyelectrolyte is replaced by the surfactant ion so a neutral ion pair is formed. The strong electrostatic attraction in this association process makes binding extremely favorable. Moreover, the possibility of obtaining differently organized supramolecular structures by changing the binding process affords plenty of possibilities in the properties manipulation at the molecular scale, which is particularly important for the development of novel multifunctional materials. These complexes will be more or less stoichiometric depending mainly on the polymer to surfactant ratio used. Complexes are usually obtained by mixing the two components, the surfactant and the polyelectrolyte, in non-stoichiometric or stoichiometric quantities which results in the formation of a soluble or non-soluble complex, respectively.

Non-stoichiometric complexes containing an excess of polyelectrolyte are water soluble because uncoupled polyelectrolyte segments tend to surround the hydrophobic surfactant aggregate. These clusters are really interesting because they are able to solubilize hydrophobic organic molecules in water allowing several technological applications.[38] Furthermore; non-stoichiometric complexes have a great interest in gene therapy where DNA chains need to be compacted to be transferred into cells. In this sense, non-stoichiometric complexation of nucleic acids with cationic surfactants is a convenient approach.[39, 40]

Stoichiometric complexes are not soluble in water but in common organic solvents. These complexes present well defined self-assembled structures in both, in solution and in the solid state. In these complexes two fascinating facts are combined. On the one hand, surfactants are able to become structured and even able to crystallize. On the other hand, the polymers become suitable for being processed and to display mechanical properties. Furthermore, these systems have the ability to form different liquid-crystal phases such us lamellar,[41] columnar discotic [42] or cylinders.[43]

The type of mesophase structure is determined by the surfactant, whereas the polyelectrolite mainly plays a framework role although with significant effect on the structure due to its charge density.[44] However, it is the polyelectrolyte which has the major influence on the mechanical properties of the complex. [44]

Lamellar   Cylinder   Columnar discotic
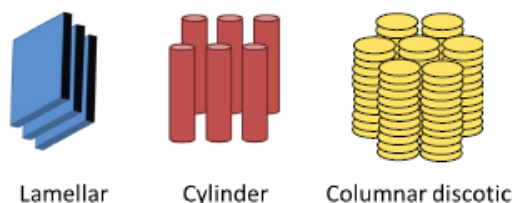
Figure I.4. Illustration of some mesophases of polyelectrolyte-surfactant complexes.

The surfactant-polyelectrolyte complexes show mechanical, electrical or optical behavior suitable for the development of new materials with unusual properties which is an issue of increasing interest. Thus, they have an exceptional potential as molecular composites with thermochromic properties and no lineal electro-optic or separation membranes in biomedicine.[45] Particularly noteworthy is the case in which the two components of the complex have a natural origin and are biocompatible and bioassimilable. These complexes are highly promising as biomaterials for drug-delivery, either as simple drug carriers or even as targeting systems with an active role.

2.2 Poly(γ-glutamic acid) complexes

Poly (γ-glutamic acid) (PGGA) is a naturally occurring polyelectrolyte which has the chemical structure of nylon 4 with a carboxylic group substituted in C4 (Scheme I.2).
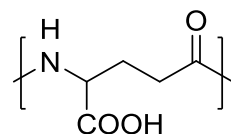
Scheme I.2. Chemical structure of PGGA.

In spite of the interesting properties of PGGA, such as non-toxicity and water affinity, the production and spreading of this polyacid is severely limited mainly due to its poor stability in humid environments and its incapacity for being processed. For this reason, diverse chemical modifications of PGGA have been explored with the purpose of increasing the potential industrial applications of its derivatives. One interesting modification of PGGA that has been object of much attention in recent years is ionic coupling with organic cations, mostly alkylammonium salts.

2.2.1. Poly(γ-glutamic) acid

Poly (γ-glutamic acid) (PGGA) is a water-soluble, biodegradable, and edible biopolymer produced by diverse *Bacillus subtilis*. Currently, it is the focus of plenty studies due to the potential properties that offers this biopolymer.

PGGA is a nylon 4 with a COOH group attached to the carbon 4. Usually, it is called poly (γ-glutamic acid) indicating that the peptide bond occurs between the amine group and the COOH in the γ position. The IUPAC nomenclature of this substance is Poly [imino[1-(2carboxy-ethyl)-2-oxo-1,2-ethanediyl]]. It is isomer of the poly (α-glutamic acid) which is one of the most interesting poly (α-aminoacids) due to its structure and biochemistry incidence.

Poly(γ-glutamic acid)
(PGGA)

Poly(α-glutamic acid)
(PAGA)
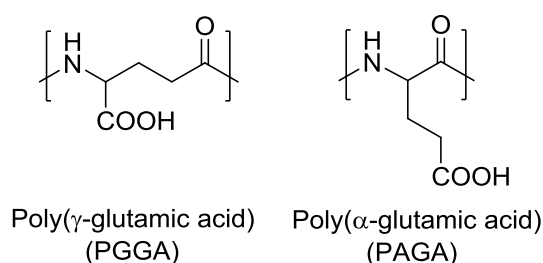
Scheme I.3. The PGGA and its isomer PAGA.

a) Biosynthesis and synthesis

PGGA was first discovered in 1935 by Ivánovics and Bruckner[47] as a capsule of *Bacillus anthracis* which was released into the medium on autoclaving, or on aging and autolysis of the cells. It was considered as a toxic polymer until it was discovered by Fuiji[50] in a Japanese traditional food called "natto" (fermented soybeans), which is a mixture of poly (glutamic acid) and fructan produced by *Bacillus natto*. This food is very beneficial because it increases the uptake in the small intestine of those physiological active substances, like vitamins, carotenoids or polyphenols eventually present in the digesting mass.[51]

Because of PGGA is a water-soluble, biodegradable, and edible biopolymer has become the focus of several researches. Therefore, PGGA could have potential applications in the industry of food, cosmetics or medicine. Consequently, several researchers have studied the production of PGGA.[49, 52]

Most of PGGA biosynthethic processes are carried out in aerobic conditions. Therefore, it has been shown that the presence of oxygen influences favorably in the production. Replacing aerobic conditions by nitrifying conditions means an economic

saving that has impulse the production of PGGA in these conditions. With the denitrification bacteria (B. licheniformis A35) and a M medium of cultive it was achieved a yield of 8.1 g/L.[53] The product obtained has got no polysacharides and the D/L ratio in the final polymer was highly affected by the Mn content. Thus, as the highest Mn concentration was, more increased the D-glutamic acid proportion. According to the production of PGGA at big scale, the most updated studies have achieved a PGGA concentration of 35 g/L with a production rate of 1g/L·h. These results were obtained when a cultive of B.locheniformis was used.[54] These results have been achieved after plenty of studies over years. [55-57]

According to the biosynthetic mechanism, the most consistent is that proposed by Kunioka.[58] The mechanism, which is illustrate in scheme I.4, is based on the L-glutamic acid that is generated in the tricarboxylic acid cycle (TCA cycle). This mechanism incorporate the pyruvic cycle proposed by Thorne et al.[38] in 1954 and explain polysaccharides formation from glucose. In brief, a partial stereochemical inversion leading to D-glutamic acid takes place by the action of pyruvic/ketoglucaric acid with the interactive concourse of the pair D/L-alanine. Polymerization of the glutamic acid D/L-enantiomeric mixtures finally occurs by the action of PGGA polymerase.
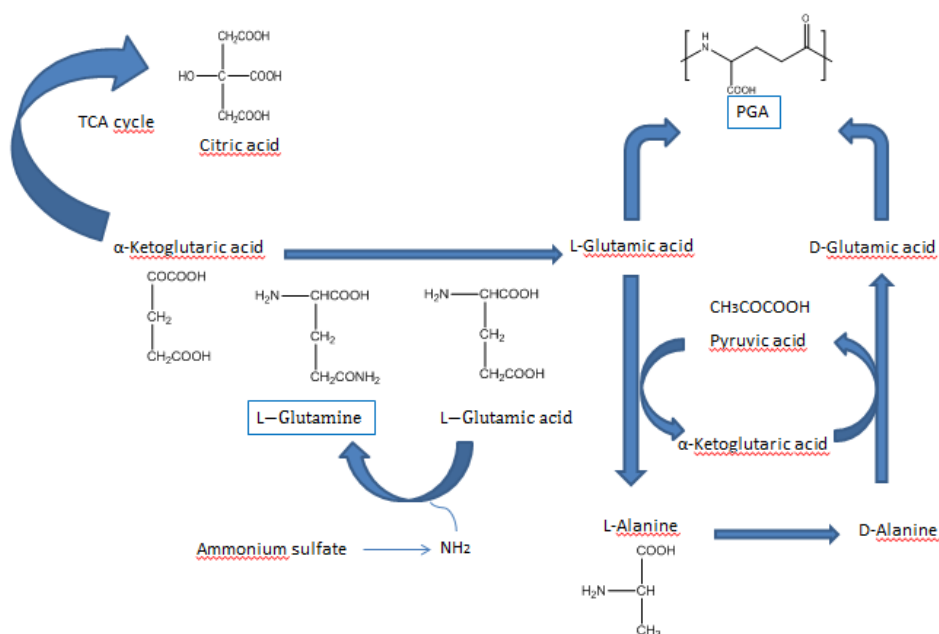
Scheme I.4. Biochemical mechanism of PGGA production by *Bacillus subtitlis*.[58]

The chemical synthesis of PGGA from glutamic acid is also feasible but through a so complex procedure that the method is not suitable for its production at industrial scale. For instance, Bruckner synthesis[59] was based on the polycondensation of glutamic acid with protected α-carboxyl groups and activated γ-carboxyl groups. However, glutamic acid derivatives tend predominantly to cyclize into pyroglutamate by intramolecular condensation; thus the use of γ-glutamyl-glutamic acid dimers is required in order to avoid undesirable cyclization (Scheme I.5).
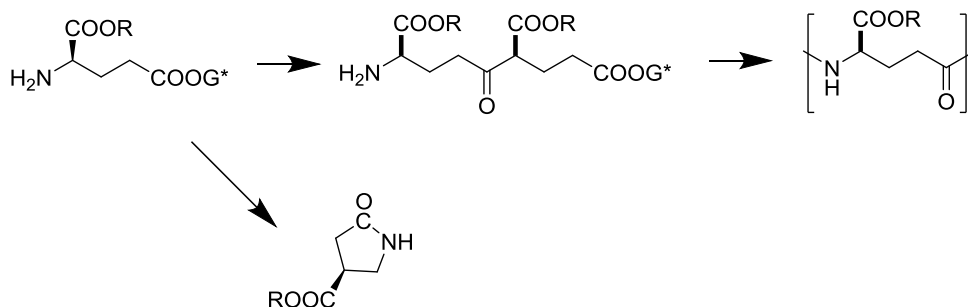
Scheme I.5. Chemical synthesis of PGGA.

On the other hand, Sanda et al.[60] have developed a new route to obtain the polymer that includes a previous transesterification followed by hydrogenation. Nevertheless, in these last years new biosynthetic procedures have been studied, such as the enzymatic synthesis using poly (γ-glutamate) synthetase.[61, 62]

b) Polyglutamic acid: structure and properties

PGGA is a polyamide which has a carboxyl group on the C4 of the principal chain. This means, this is a quiral carbon. So, there are available two different enantiomers: D-PGGA and L-PGGA. Usually biosynthetic PGGA contains a mix of both enantiomers. The D/L monomer ratio depends on the organism and the conditions employed in the process but it normally oscillates between 1/1 and 2/1. Enantiomerically pure D and L homopolymers are obtained from *B. anthracis* and *Natrialbaa egyptiaca*, respectively.[63,64]

PGGA is a polymer with a complex solubility. It is a polyelectrolyte with $pK_a = 2.27$ so it will be ionized or not depending on the pH. As a result, pH is a critical factor for the solubility and structure of the PGGA. At low pH values, PGGA is protonated and the polymer adopts a structure of α-helix. The protonated form is soluble in organic solvents such as DMSO (dimethylsulfoxide),[65] HMPA (hexamethylenphosphoramide),[66] or warm DMF (dimethylformamide) and NMP (*N*-methylpyrrolidone).[67] When the pH is higher, around 5.1, the PGGA is in ionized form. At this pH PGGA adopts the random coil arrangement. This PGGA is soluble in water but non-soluble in MeOH, EtOH or DMSO.
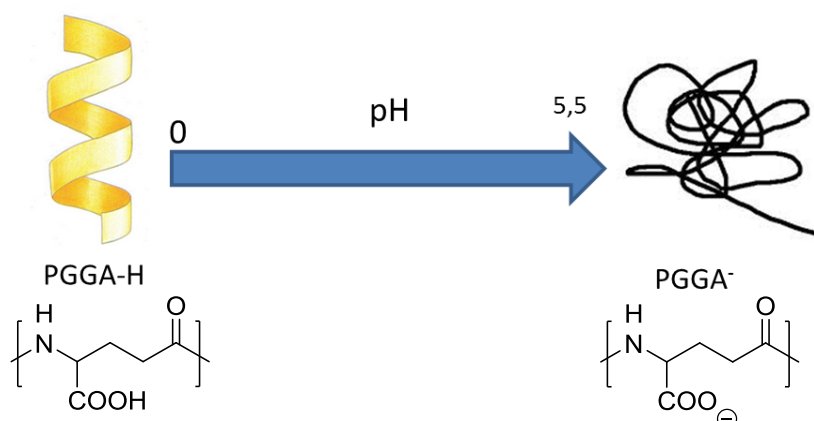
Figure I.5. PGGA structure depending on pH values.

PGGA is optically active and its specific rotation depends on the D/L ratio and has a T_g around 50 ºC. Regarding the thermal stability of PGGA, Kubota et al.[68] reported that PGGA experiments a loss of weight of around 10% at 236 ºC and that this polymer is stable to heating up to 210 ºC, where melting and decomposition happen at same time. The mechanism of the thermal degradation of PGGA was proposed by Portilla-Arias *et al.*[69] It was proposed to consist of an unzipping mechanism with generation of pyroglutamic acid (Scheme I.6).
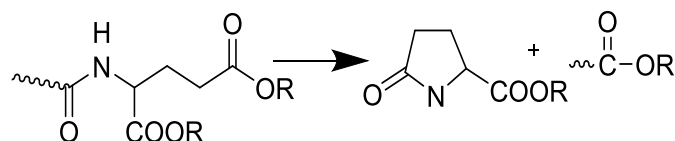
Scheme I.6. Thermal degradation mechanism of PGGA.

c) Applications of poly(glutamic acid)

PGGA is a potential candidate for replacing the actual flocculants in the market such as polyacrimalides and polyacrilic acids which degrade slowly in water releasing toxic substances. This is possible due to the solubility of PGGA in water and the possibility of interacting with cations, which is an important property of PGGA. Therefore, this property makes PGGA a suitable polymer for waste water treatment since both, inorganic and organic suspensions, can be removed by flocculation and coagulation.[70]

Furthermore, PGGA is interesting for applications in agriculture and, taking into account its biocompatibility, in cosmetics or dermatology.[71] These applications require hydrogels. Thus, PGGA is able to these applications due to the high density of hydrogen bonds in the structure of PGGA.

Another interesting outcome of this polymer is in the food field, not only as thickener or bun preservatives, but also as forming part of the food diet since it is easily biodegraded into the proteinogenic glutamic acid, which safety for our daily lifes.

Eventually, the most promising application of PGGA is in biomedical field due to PGGA is a biodegradable, edible, and non-toxic towards human and environment. Hence it has been suggested to be a good candidate for curable biological adhesive[72] and as drug, vaccine or gene carriers.[73]

2.2.2. Poly(γ-glutamic acid)-alkyltrimethylammonium surfactant complexes (nATMA·PGGA)

During the past decade, a deep research about complexes had been carried out. Among them, stoichiometric complexes study had been mainly focused on two polymer families: conventional synthetic charged polymers, such as modified polystyrene[75] or poly (acrylic acid), [43] and bio-polyelectrolytes, such as polypeptides.

In this project we will focus on the complexes with polypeptides which have been studied in the last years. Thus, the preparation and structural characterization of different complexes have been reported by Ponomarenko et al.[36, 76] : poly(α,L-glutamic acid) dodecyl- and cetyl-trimethylammonium and poly(L-lysine)/ dodecyl sulfate anions. It was found that both complexes displayed a similar behavior.

The complexes (nATMA·α,L-PGGA) described by Ponomarenko were obtained as precipitates when dodecyl, hexadecyl and octadecyl–trimethylammonium and PGGA were mixed in equal quantities. It was shown that the polypeptide in these complexes adopts the α-helical conformation, and that the long alkyl chains of the surfactant are able to crystallize separately in a hexagonal lattice inducing the formation of liquid-crystal phases, [36] whereas the shorter ones (below 16 carbon atoms) remain in a disordered state.

nATMA·poly(γ,D-glutamic) acid or nATMA·poly(γ,DL-glutamic) acid complexes were prepared by Pérez-Camero et al.[78, 79] and García-Álvarez et al.[80] two decades ago in the Chemical Engineering Department of the ETSEIB (UPC).
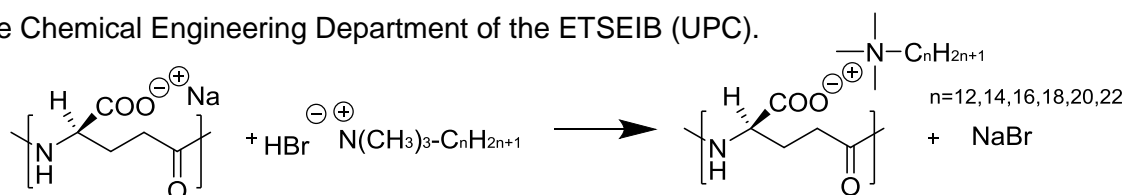
Scheme I.7. Formation of the ionic nATMA·PGGA complexes.

All these stoichiometric or quasi-stoichiometric complexes are obtained by precipitation when aqueous solutions of Na·PGGA and alkyltrimethylammonium bromides are mixed. Moreover, it was found that all complexes adopt the layered biphasic structure typical of comb-like polypeptides, which is schematically depicted in Figure I.6.
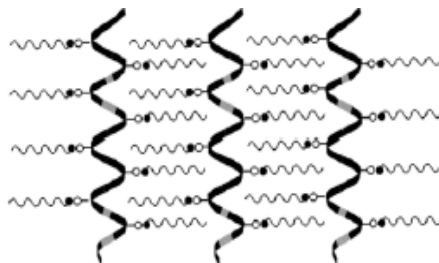
Figure I.6. Lamellar biphasic structure characteristic of comb-like ionic complexes of PGGA.[80]

Moreover, it was ascertained by X-ray diffraction measurements that the chains are alternating with the crystalline surfactant which is partially crystallized in a pseudo-hexagonal lattice. The window spacing of the layered ranged between 3.0 and 4.5 nm depending on the length of the alkyl chain.

Crystallization of hydrocarbon tails takes place for alkyl chains containing at least 18 carbon atoms for both D and D,L-PGGA enantiomorphs. Thus, the DSC analysis of the shortest alkyl chains did not show any thermic transition from 0 ºC to degradation temperature. Conversely, a well-defined pick between 50 and 80 ºC, depending on the alkyl chain length, appeared in the thermograms of nATMA·PGGA with n=18, 20 and 22. This is the melting temperature of the crystallized paraffin phase.

More recently Portilla-Arias et al.[82] have described nATMA·PMLA complexes made of poly (L-malic acid) and the same surfactants; these complexes display almost exactly the same structure and properties than those made of PGGA.

Tolentino et al.[83] have recently described the first comblike ionic system entirely made of biobased components. These complexes, nACh·PGGA, were made from PGGA and alkanoylcholines (nACh) derived from fatty acids. Alkanoylcholines have been proved to be hydrolyzed by butyrylcholine esterase producing common components of human metabolisms and they are therefore considered to be less toxic than alkyltrimethyl ammonium compounds.[46]
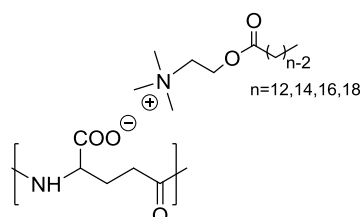
Scheme I.8. Chemical structure of nACh·PGGA.

These systems were motivated by both structural and functional reasons. On the one hand, they are able to adopt a lamellar structure similar to that typical of the *n*ATMP·PGGA complexes although slight differences in the crystallization of the paraffinic phases produce slight differences in the thermal properties of the complexes. Such differences are caused by the presence of the relatively flexible ethylenoxycarbonyl group which allows a higher mobility of the alkyl chain favoring its crystallization. Furthermore, these compounds are antimicrobial agents and have proven to display therapeutic activity in the treatment of the Alzheimer disease[84] and certain gastro-intestinal disorders. [85] The extremely easy of preparation of the *n*ACh·PGGA complexes combined with their unique biocharacteristics and their amphiphilic nanostructure made these compounds outstanding candidates for building bioactive materials of potential utility in diverse biomedical applications.

2.3 Hyaluronic acid complexes

Hyaluronic acid (HyalA) is a carbohydrate, more specifically a polysaccharide belonging to the glycosaminoglycans group (GAG). It is a linear polyanion, with a repeating disaccharide structure [(1→3)-β- D-*N*-acetylglucosamine (GlcNAc) and (1→4)-β- D-glucuronic acid (GlcA) which can be several thousands of sugar units long.
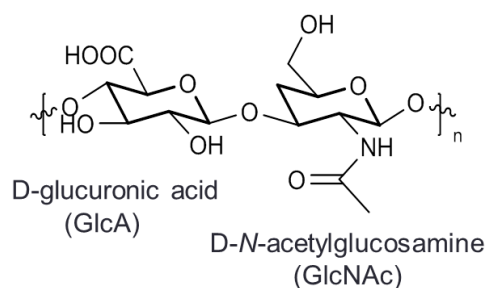
Scheme I.9. Chemical structure of hyaluronic acid.

This polysaccharide suffers rapid enzymatic degradation due to its sensitivity to hyaluronidase.[86]Some chemical modifications of hyaluronic acid have been performed to get new derivatives that broaden its range of applications. It can be stabilized by crosslinking or by chemical modifications. In this project we will focus on the modification of HyalA by forming ionic complexes with *n*-alkyltrimethylphosphonium salts.

2.3.1. Hyaluronic acid

a) Hyaluronic acid: Origin and biosynthesis

In 1934, Karl Meyer and his colleague John Palmer isolated a new substance from the vitreous body of cows' eyes. They found that the substance contained two sugar molecules, one of which was uronic acid. Therefore, they proposed the name "hyaluronic acid". The popular name is derived from "hyalos", which is the Greek word for glass + uronic acid.[87] HyalA was first used commercially in 1942 when Endre Balazs[88] applied for a patent to use it as a substitute for egg white in bakery products. The first medical application of HyalA for humans was as a vitreous substitution/replacement during eye surgery in the late 1950s. The used HyalA was initially isolated from human umbilical cord, and shortly thereafter from rooster combs in a highly purified and high molecular weight form.[87]The structure of the disaccharide is energetically very stable. Moreover, this structure is conserved throughout all mammals, suggesting that HyalA is a biomolecule of considerable importance.[89] In the body, HyalA occurs in the salt form, hyaluronate, and is found in high concentrations in several soft connective tissues, including skin, umbilical cord, synovial fluid, and vitreous humor. Significant amounts of HyalA are also found in lung, kidney, brain, and muscle tissues.

Thus, HyalA has been successfully produced on an industrial scale using several bacteria of the Streptococcus. [90, 91]

Nowadays, microbial production by fermentation is gathering strength for commercial production, especially in pharmaceutical field, since these preparations will avoid the allergy responses usually provoked by products coming from animal sources. [92-94]

b) Hyaluronic acid: structure and properties

The structure of hyaluronic acid, as previously mentioned, consists of an alternating disaccharide repeat of D-glucuronic acid and D-N-acetylglucosamine, and are linked together through alternating beta-1,4 and beta-1,3 glycosidic bonds (see scheme I.9). Both sugars are spatially related to glucose which in the beta configuration allows all of its bulky groups (the hydroxyls, the carboxylate moiety and the anomeric carbon on the adjacent sugar) to be in sterically favorable equatorial positions while all of the small hydrogen atoms occupy the less sterically favourable axial positions. When not bound to other molecules, it binds to water giving it to it a stiff viscous quality. Thus, in a physiological solution, the backbone of a HyalA molecule assumes a stiffened helical configuration, which can be attributed to hydrogen bonding

between the hydroxyl groups along the chain. Therefore, the axial hydrogen atoms form a non-polar, relatively hydrophobic face creating a twisting ribbon structure. As a result, a coil structure is formed that traps approximately one thousand times its weight in water.[95] Thus, in the solid state HyalA is a flaky substance but its aqueous solutions show high viscosity and elasticity.

Solutions of HyalA display very unusual rheological properties and are exceedingly lubricious and very hydrophilic. Therefore, the HyalA chain takes up the form of an expanded, random coil. At low concentrations these chains entangle with each other, which may contribute to the unusual rheological properties displayed by this biopolymer; when concentration is increased, an enhancement of the viscoelasticity behavior is observed for hyaluronan solutions. An 1% aqueous solution of HyalA still retains its characteristic viscosity and elasticity, a property that makes it an interesting biomaterial.[96]

The pKa of this polysaccharide is around 3.0. Thus, changes in the pH will provide different ionization grades which will affect rheological properties due to chain interactions will be altered.[97]

c) Applications of -hyaluronic acid.

The distinguishing properties of HyalA such as biocompatibility, non-immunogenicity, biodegradability, viscoelasticity and hydrophilicity have made that this polysaccharide has highly used in skin-care products as an excellent moisturizer and biomedical fields. Therefore, its function in the body is, amongst other things, to bind water and to lubricate movable parts of the body, such as joints and muscles.

The unique viscoelastic nature of HyalA along with its biocompatibility and non-immunogenicity has led to its use in a number of clinical applications, including the supplementation of joint fluid in arthritis,[98-100] as a surgical aid in eye surgery, and to facilitate the healing and regeneration of surgical wounds. More recently, HyalA has been investigated as a drug delivery agent for various administration routes, including ophthalmic, nasal, pulmonary, parenteral and topical.[101] As other polysaccharides, HyalA is a suitable component for drug delivery systems both as an inert matrix or by HyalA-drug covalently or ionically attached conjugates.[102, 103]

In those biomedical applications HyalA is used alone, in combination with other polymers or slightly crosslinked to avoid it´s enzymatic degradation and because of crosslinking reduces its solubility giving not only more durable materials but also better mechanical effects, which are appropriate for filling tissue engineering applications.

2.3.2. Hyaluronic acid-alkyltrimethylammonium surfactant complexes (*n*ATMA·HyalA)

In these last years it has been revealed that coupling of polyelectrolytes with ionic surfactants is a convenient method for the preparation of ionic complexes with remarkable structure and properties.[36,77] Specifically, coupling polyacids with alkylammonium surfactants bearing long alkyl chains which are known to lead to amphiphilic comb-like systems displaying a layered biphasic structure, (Figure I.6). Moreover, it was reported by Portilla-Arias, García-Alvarez, Martínez de Ilarduya, Holler and Muñoz-Guerra [82, 108-110], that these systems are able to lodge agents with chemical or biomedical activity. In this sense, the preparation, structure and thermal behavior of complexes made of hyaluronic acid with alkyltrimethylammonium surfactants, abbreviated as *n*ATMA·HyalA, with alkyl chains containing 18, 20 and 22 carbon atoms (Scheme I.10) have been recently reported.[107.] The purpose of this coupling was on the one hand broaden the HyalA potential as biomaterial, and to appraise how the alternating ionic structure of Hyal may affect the formation of these comb-like ionic complexes.
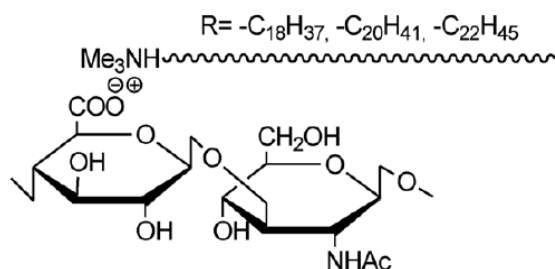
Scheme I. 10. Chemical structure of *n*ATMA·HyalA.

The complexes were prepared following a similar methodology initially reported by Ponomarenko et al.[36] and later applied by us with some minor modifications to the preparation of other complexes. [82,108-111] Moreover, these complexes had similar properties than previous complexes. Thus, they were non-water soluble but they dissolved in organic solvents and are stable to heating up to above 200 ºC. In addition, these complexes also self-organized in a biphasic layered structure characteristic of comb-like amphiphilic systems with the polyacid and the alkyl side chains phases alternating periodically with a repeating distance of ~4.5 nm. They displayed melting of the paraffinic phase in the 50–70 ºC range without appreciable changes in the layered spacing. However, the degree of order attained by the alkyl chains in these complexes was significantly lower than usually found in other similar comb-like ionic complexes.

II. EXPERIMENTAL

1. Materials

The sodium salt of poly (γ-glutamic acid) (Na·PGGA) sample used in this work was kindly supplied by Dr. Kubota of Meiji. Co. (Japan). It was obtained by biosynthesis and has a molecular weight of ≈ 300,000 Da and a D:L enantiomeric composition of 59:41. 1-bromododecane (97%), 1-bromohexadecane (97%), 1-bromooctadecane (96%), 1-bromoeicosane (98%), 1-bromodocosane (96%), trimethylphosphine solution in toluene (1M) were supplied from Sigma-Aldrich and 1-bromotetradecane (97%) from Merck. They all were used as received. Chloroform, hexane, toluene and acetone were supplied from Panreac and used without further purification.

2. Synthesis of alkyltrimethylphosphonium bromides

The synthesis of the alkyltrimethylphosphonium surfactants (nATMP·Br) was carried out   as reported elsewhere.[81] Thus, 5 mL of a 1.0 M solution of trimethylphosphine (TMP) in toluene (5 mol) was slowly added to 1-bromoalkane (5.5 mol) preheated at 120 ºC and under nitrogen. Then, the mixture was heated in a silicone oil bath between 130-145 ºC and maintained under stirring for a period of 12 to 20 h depending on the bromoalkane used. After the reaction was completed a white precipitate was formed, which was collected by filtration. In order to remove the slight excess of 1-bromoalkane, the precipitate was repeatedly washed with toluene and dried under vacuum for 48h. Their chemical structure is represented in scheme III.1, which was ascertained by ^{1}H and ^{13}C NMR, FT-IR and elemental analysis. δ_H (300.1 MHz; CDCl$_3$) 4.47 (2H, m, RC**H**$_2$P$^+$), 2.25 and 2.20 (9H, d, P$^+$(C**H**$_3$)$_3$), 1.5 (2H, m, RC**H**$_2$CH$_2$P$^+$),1.26 (nH, m, CH$_3$-(C**H**$_2$)$_n$-CH$_2$ CH$_2$P$^+$), 0.89-0.88 (3H, t, C**H**$_3$-(CH$_2$)$_n$-P$^+$), δ_C (75.5 MHz; CDCl$_3$) 31.9 (CH$_3$-CH$_2$-**C**H$_2$-(CH$_2$)$_n$-P$^+$), 29.5-29.0 (CH$_3$-CH$_2$-CH$_2$-(**C**H$_2$)$_n$-P$^+$), 24.2-24.1 (RCH$_2$ **C**H$_2$CH$_2$P$^+$), 23.5 (RC**H**$_2$ CH$_2$P$^+$), 22.7 (CH$_3$**C**H$_2$-(CH$_2$)$_n$-P$^+$), 21.8 and 21.7 (RC**H**$_2$P$^+$), 14.1 (**C**H$_3$-(CH$_2$)$_n$-P$^+$), 9.4 and 8.6 (RP$^+$(**C**H$_3$)$_3$).

3. Synthesis of complexes

Complexes of alkyltrimethylphosphonium surfactants with both Poly (γ-glutamic acid) (nATMP·PGGA) and hyaluronic acid (nATMP·HyalA) were prepared following the methodology described by Ponomarenko *et al.*[36] for the synthesis of complexes of alkyltrimethylammonium surfactants with poly(α,L-glutamic acid).

In brief, 100 mL of an aqueous 0.01 M solution of the *n*ATMP surfactant of choice was added to the same volume of a 0.01 M Na·PGGA solution in water under stirring, and the mixture was left to rest at the suitable temperature. This temperature **oscillated between 25 and 60 ºC** depending on the length of the alkyl chain so higher temperatures are required as the alkyl length increases. A white precipitate appeared after several hours of standing, which was isolated by filtration or centrifugation, washed several times with water, and dried under vacuum for at least 48 h.

4. Methods

FT-IR spectra were recorded on a FT-IR Perkin Elmer Frontier spectrophotometer provided with a universal ATR sampling accessory from solid samples and within the 4000-600 cm-1 interval. Four scans were accumulated for each spectrum which was registered with a resolution of 0.5.1H and 13C NMR spectra were recorded on a Bruker AMX-300 NMR instrument and using TMS as reference. The spectra were registered at 300.1 MHz for 1H-NMR and 75.5 MHz for 13C-NMR MHz and samples were dissolved in chloroform.

Elemental analyses were carried out at the Servei de Microanàlisi at IQAC (Barcelona). The tests were made in a Flash 1112 elemental microanalizer (A5) which was calibrated with several standards of known composition. The determination of C and H was made by the dynamic flash combustion method using He as portador gas. Results were given in weight/weight percentage and in duplicates.

Krafft temperatures were estimated visually. Samples were prepared as follows: 1% mixtures of *n*ATMP·Br in water were heated until dissolution and then cooled down to room temperature and kept in a refrigerator at 5 ºC for 24 hours. The cooled samples were then introduced in a water bath provided with a magnetic stirring and heated up in steps of 1 ºC every 15 min. The temperature at which turbidity disappeared was taken as the approximate Krafft temperature.

Thermogravimetric analyses were performed under an inert atmosphere with a Perkin-Elmer TGA6 thermobalance at heating rates of 10 ˚C min-1. Calorimetric measurements were performed with a Perkin-Elmer Pyris DSC instrument calibrated with indium and zinc. Sample weights of about 2–5 mg were used to obtain heating-cooling cycles at heating and cooling rates of 10 ºC min-1 within the temperature range of -30 ºC to 290 ºC and under a nitrogen atmosphere.

Optical microscopy was carried out on an Olympus BX51 polarizing microscope equipped with a digital camera and a Linkam THMS-600 hot stage provided with a nitrogen gas circulating system to avoid contact with air humidity. Samples for observation were prepared by casting from 1% (w/v) chloroform solutions on a microscope glass cover slide and then covered with another slide.

X-ray diffractograms (XRD) were obtained in two specialized centers. Firstly, in the University of Sevilla, specifically in the department of Organic and Pharmaceutical Chemistry where XRD were obtained following a repetitive protocol which consisted on several heating-cooling cycles where samples were heated and cooled at heating and cooling rates of 10 ºC min^{-1} within the temperature range of 25 ºC to 280 ºC. Diffractograms were registered at the selected temperatures using a diffractometer with a monochromatized of Cu(α) radiation (λ= 1.544390). The reflections collected were those appearing in the range 1º $\leq \theta \leq$ 15º. Secondly, in the University of Barcelona, where the XRD were registered at room temperature using two types of samples: that coming from the synthesis, which are white powders, and others which had been previously heated up to 290 ºC and cooled again to room temperature.

II. EXPERIMENTAL

III. RESULTS AND DISCUSSION

1. Alkyltrimethylphosphonium salts (*n*ATMP·Br)

1.1 Synthesis of alkyltrimethylphosphonium salts

The *n*ATMP·Br surfactants, (Scheme III.1), were prepared by a nucleophilic substitution reaction of the appropriate 1-bromoalkane with trimethylphosphine (TMP). As TMP is highly inflammable it was supplied in 50% (v/v) toluene solution to reduce handling risks. Furthermore, manipulation of TMP must be conducted under an inert atmosphere to avoid its oxidation. The temperature and reaction time depended on the number of carbon atoms (*n*) of the bromoalkane so the longer the alkyl chain length, the higher the temperature or the longer the reaction time required for completion. Yields oscillated between 70 and 90% and all of the *n*ATMP·Br salts were recovered as white powders. They all were soluble in a variety of organic solvents such as chloroform and methanol, and also in water at temperatures 20-60 ºC depending on the value of *n*. Main synthesis data of these compounds are given in Table III.1.

$$Br^{-}$$
$$(CH_2)_{n-1} - P^{+}(CH_3)_3$$

n=12,14,16,18,20,22
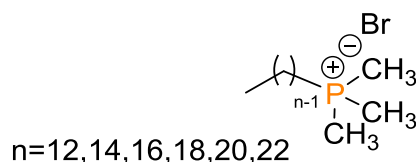
Scheme III.1. Chemical structure of *n*ATMP·Br.

Table III.1. Synthesis data of *n*ATMP·Br surfactants.

n	*t* (h)	*T* (ºC)	Yield (%)	Elemental analysis[a]	
				C (%)*	H (%)*
12	16	134	70	55.53 (55.53)	10.50 (10.59)
14	17	136	80	58.03 (57.92)	10.79 (10.9)
16	18	138	85	60.06, (59.96)	11.00 (11.16)
18	20	140	70	61.56 (61.73)	11.22 (11.38)
20	22	145	80	63.12 (63.26)	11.37 (11.58)
22	24	150	70	64.70 (64.61)	11.65 (11.75)

[a] In brackets, values calculated for the observed compositions

1.2 Chemical Characterization

The chemical composition and purity of *n*ATMP·Br were ascertained by elemental analysis and their chemical constitution by both FTIR and NMR spectroscopies.

Elemental analysis obtained by combustion essays for carbon and hydrogen were in satisfactory agreement with the calculated values (see table III.1). The FT-IR spectra recorded from the whole series of *n*ATMP·Br are compared in Figure III.1b. The bands appearing on these spectra can be grouped into two categories: those arising from the trimethylphosphonium cation head-group which has characteristic bands at 970 cm^{-1} and 712 cm^{-1}, and those attributed to the alkyl tail appearing around 2920 cm^{-1}, 2850 cm^{-1} and 1470 cm^{-1}. The 970 cm^{-1} band has been attributed to either phenyl phosphorus or activated phenyl vibrations.[112, 113] However, this band is present in spectra of both phenyl phosphonium and tetraalkylphosphonium salts, **but this band is quite limited since its intensity is highly variable.** The band at 712 cm^{-1} is another band characteristic of phosphonium salts. For carrying out a comparative evaluation of the *n*ATMP·Br spectra the 970 cm^{-1} band was taken as reference due to it is not overlapped with any band related to the 1-bromoalkane spectrum (Figure III.1a) Thus, the intensity of this band was fixed and compared with the intensity showed by the band at 2890 cm^{-1}, which is characteristic of methylene stretching. As expected, the longer the alkyl chain length, the more intense are the observed methylene bands.
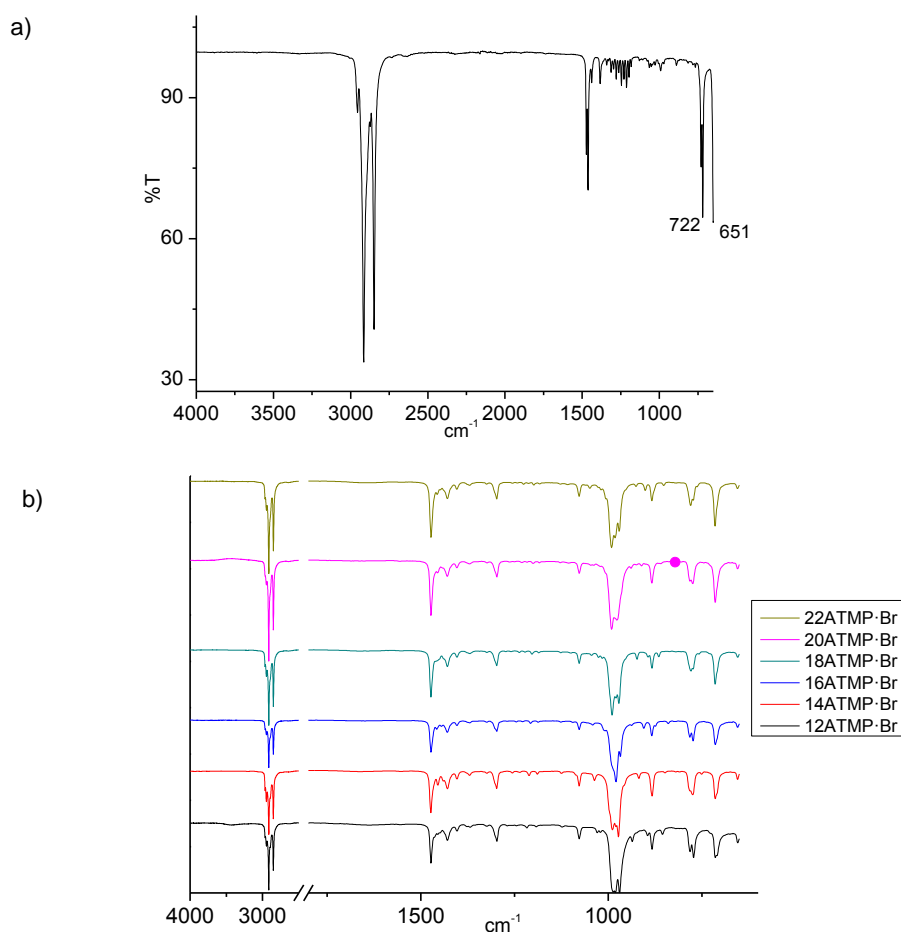
Figure III.1. a) FTIR of 1bromooctadecane b) FTIR of *n*ATMP·Br surfactants.

III. RESULTS AND DISCUSSION

The NMR results were consistent with FT-IR data and ascertained the chemical structure of the *n*ATMP·Br surfactants. A detailed assignment of the peaks is given in the experimental section. The ^{1}H and ^{13}C NMR spectra of 18ATMP·Br are depicted in Figure III.2 for illustrative purposes. The spectra of all other salts are provided in the Supplementary Information section (SI).
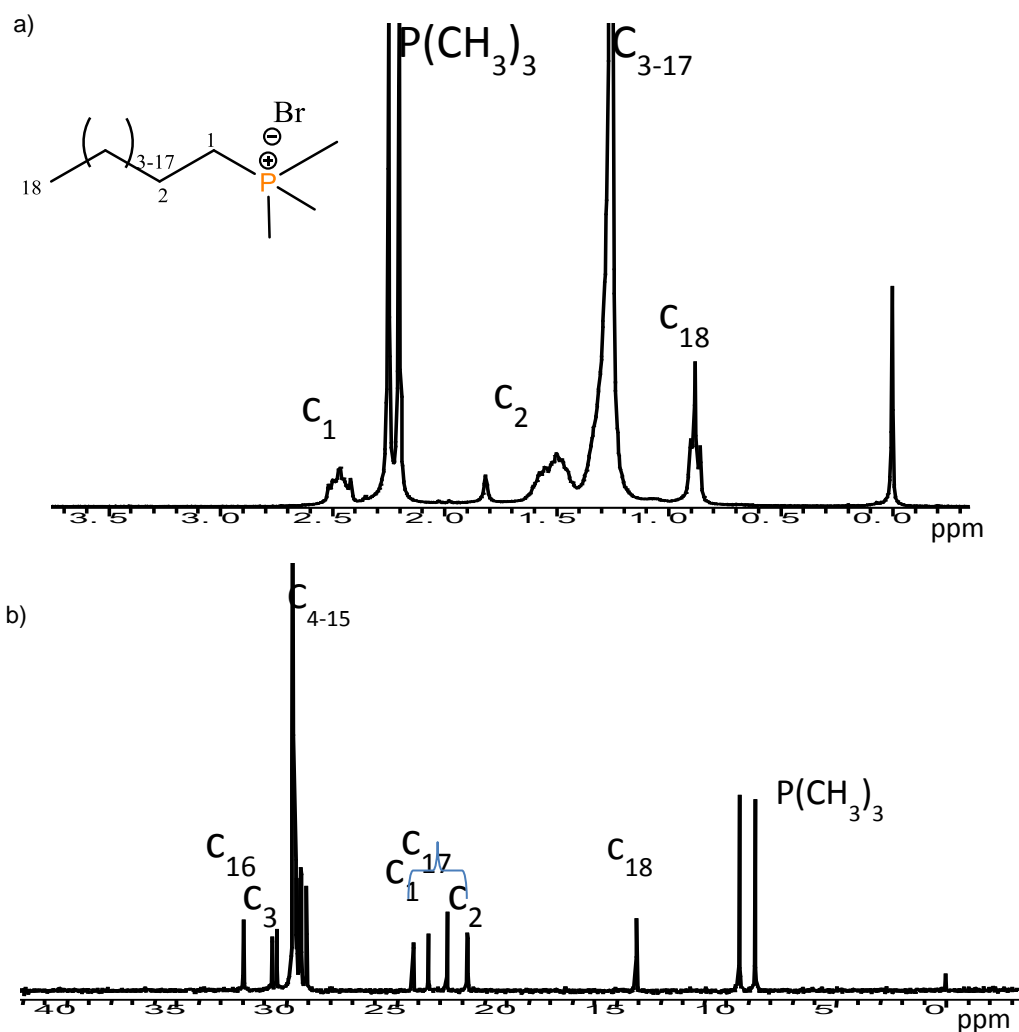
Figure III.2. a) ^{1}HNMR and b) ^{13}C NMR spectra of *n*ATMP·Br recorded at 25 ºC.

1.3 Solubility and thermal stability

The Krafft temperatures (T_{Krafft}) values were determined only for the *n*ATMP·Br with *n* = 18, 20 and 22 since salts with *n* <18 are soluble in water at room temperature. The T_{Krafft} values obtained for *n*ATMP·Br are compared in Table III.2 where it is observed that they steadily increase with the value of *n*. When these Krafft temperatures are compared with those reported for *n*ATMA·Br[116] we can see that significantly lower values are displayed by the phosphonium salts according to the higher water solubility observed for these compounds.

The thermal stability of *n*ATMP·Br surfactants was evaluated by TGA. The TGA curves obtained by heating the samples from room temperature up to 600 ºC under an inert atmosphere are depicted in Figure III.3. Decomposition was found to start around 370-400˚C with onset temperatures decreasing slightly with the length of the alkyl chain. Therefore, it is demonstrated that *n*ATMP·Br surfactants thermal stability is higher than those of *n*ATMA·Br surfactants.[74]
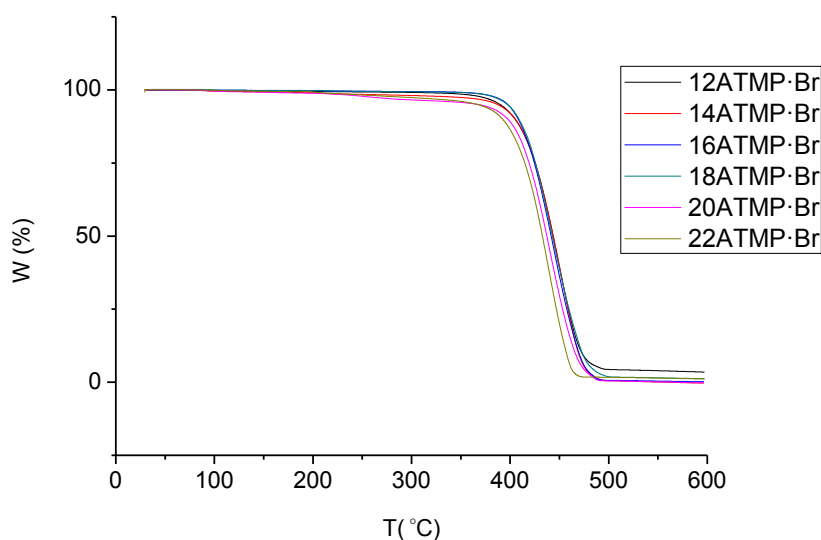
Figure III.3. TGA traces of *n*ATMP·Br recorded under an inert atmosphere.

It was explored if the surfactants were thermally stable at 290 ºC, which is the selected temperature to record DSC traces. For that, the percentage of lost weight was measured when the samples were heated at 290 ºC for 3 h. The results were favorable due to the percentage of weight holds over the time (Fig. III.4a). Furthermore, TGA derivative curves (Figure III.4b) revealed that the decomposition process proceeded through an one-step mechanism in one-step which has the maximum decomposition rate temperature located within the 435-450 ºC interval. After heating most of the samples had no residues left, with some irrelevant exceptions due to some of them had between 1-4 %. Moreover, it was observed a slightly deformation at high temperatures which may be it is consequence of a second decomposition process. Provided that it cannot be explain, we assume that the decomposition is through one-step. The onset and maximum decomposition rate temperatures as well as the remaining weight percentages for every *n*ATMP·Br surfactants are listed in Table III.2.
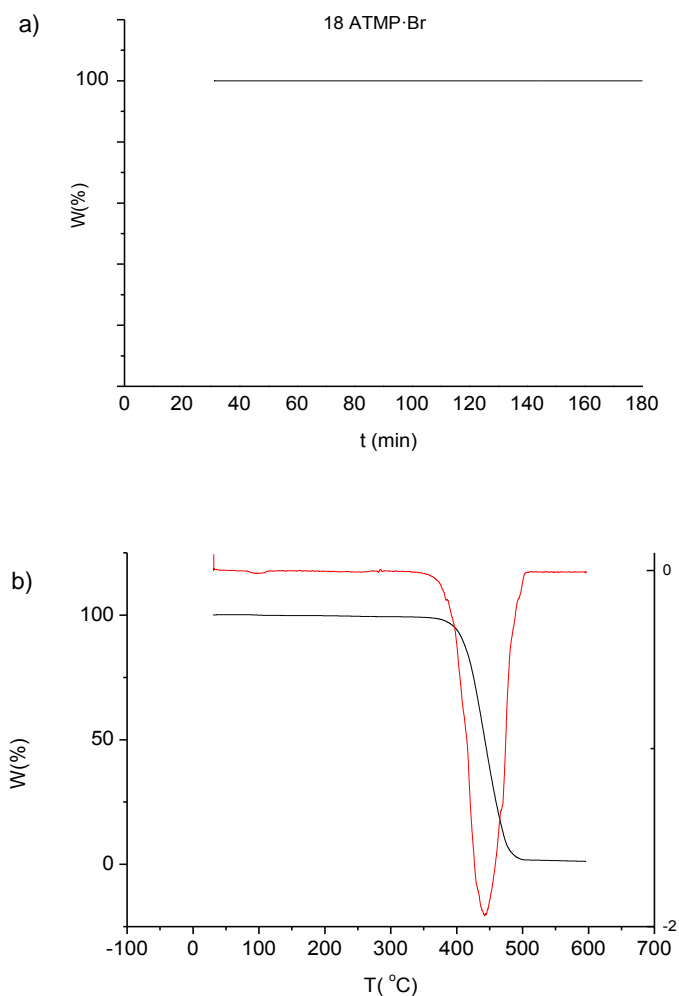
Figure III.4. a) Isotherm trace at 290 ºC of the 18ATMP·Br salt, b) TGA trace of 18ATMP·Br salt and its derivative curve.

1.4 Thermal transitions

The DSC study has been confined within temperatures well below the onset decomposition temperature. Thus, DSC traces were recorded within the interval going from -30 ºC to 290 ºC applying several heating-cooling cycles. They are depicted in Figure III.5 for the whole series of *n*ATMP·Br and the temperatures and enthalpies recorded at the first heating and cooling and the second heating are listed in Table III.2.
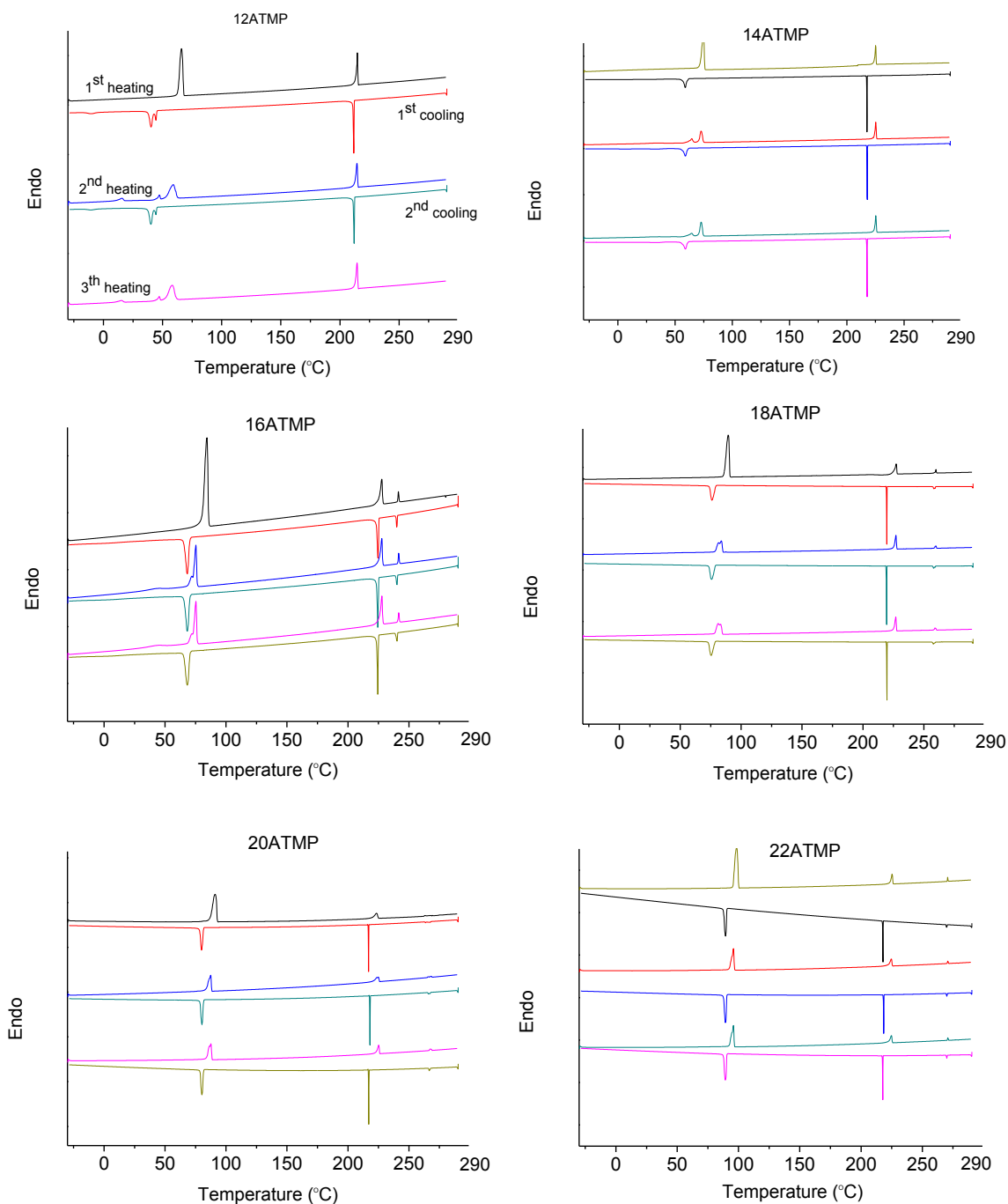
Figure III.5. DSC traces of *n*ATMP·Br at successive heating-cooling cycles over the -30 ºC to 290 ºC interval.

While only two transition temperatures are observed for 12ATMP·Br and 14ATMP·Br, there are three for the others. This means that surfactants, with n = 12 and 14 should display three thermal phases whereas four phases should be expected for n = 16, 18, 20 and 22.

III. RESULTS AND DISCUSSION

Specifically, the first phase (**Phase I**) appears at low temperatures, the second phase (**Phase II**) in the intermediate region and the third and fourth phases (**Phases III and IV**) at high temperatures. Thus, for surfactants with $n<16$ the third phase, correspond to the isotropic liquid whereas in the others it is the fourth phase. In either case, all the surfactants exhibit a variety of thermal transitions and present endothermal peaks at heating as well as their respective exothermal peaks at cooling, which means that all of them take place reversibly. Nevertheless, it is invariably observed that exothermal peaks appear at slightly lower temperatures than their respective endothermal ones. The magnitude of the supercooling is indicative of the nature of the involved transition.

Tabla III.2. Thermal properties of nATMP·Br surfactants.

n	TGA[a]				DSC[b]								
	T_{krafft} (ºC)	T_d (ºC)	$^{max}T_d$ (ºC)	W (%)	T (ºC) and ΔH (kCal·mol^{-1}) (in parenthesis)								
					1st Heating			Cooling			2nd Heating		
					I/II	II/III	III/IV	II/I	III/II	IV/III	I/II	II/III	III/IV
12	<25	444	449	3.5	65.9 (9.3)	214.8 (2.9)	-	40.2 (-3.9)	211.6 (-2.7)	-	59.1 (6.1)	214.4 (2.9)	-
14	<25	387	455	0	74.8 (10.1)	225.2 (2.7)	-	58.8 (-3.0)	217.6 (-2.7)	-	72.7 (5.5)	225.3 (2.6)	-
16	<25	398	443	0	84.4 (11.8)	227.4 (2.5)	241.4 (0.4)	68.2 (-4.1)	227.7 (-2.2)	240 (-0.4)	75.3 (4.6)	227.8 (2.6)	241.6 (0.4)
18	35	397	443	1.2	89 (14.5)	227.3 (2.4)	260 (0.4)	75.9 (-5.4)	219.6 (-2.7)	258.2 (-0.4)	83.7 (5.6)	227 (2.4)	260.1 (0.4)
20	45	367	442	0	91.1 (16.5)	223.4 (2.4)	263.1 (0.4)	80.0 (-7.2)	216.9 (-2.7)	263.5 (-0.4)	87.44 (6.7)	224.4 (2.5)	268.4 (0.4)
22	55	367	438	0	98.5 (17.1)	225.3 (2.4)	270.7 (0.4)	89.6 (-7.3)	217.9 (-2.2)	270.7 (-0.3)	96.0 (7.2)	224.6 (2.3)	270.7 (0.3)

[a]Thermal stability of nATMP•Br surfactants being T_d the onset decomposition temperature calculated by measuring the 5% loss of weight, $^{max}T_d$ the maximum rate decomposition temperature for each decomposition step and W the remaining weights after the respective decomposition stages.
[b] Thermal transitions study through some heating-cooling cycles being I, II, III and IV the phase I,II,III and IV, respectively. The transition temperatures (ºC) and in parenthesis their enthalpies (kCal·mol^{-1}).

The plot of transition temperatures against n is shown in Figure III.6a revealing that a linear trend is followed for all nATMP·Br although noteworthy differences are observed among them. Regarding the I/II transition that takes place at the lowest temperature (in blue color) it can be observed that temperatures increase with a similar slope for the whole series. The supercooling associate to this transition is noticeable especially in the first heating where it varies between 2 and 10 ºC. The II/III transition observed at temperatures slightly above 200 ºC (in pink color) occurs essentially at the

same temperature along the whole series and displays a moderate supercooling of about 1 ºC. The transition taking place at the highest temperature (III/IV transition) (in green color) is only observed for nATMP·Br with n>14 and it is distinguished that both, the exotherm and endotherm processes, are practically coincident. This means that the supercooling required for reversing this transition is practically negligible. For n<14 this transition is not appreciate due to some possible reasons. First, these surfactants have only three mesophases, so they only exhibit two temperature transitions. Alternatively the tendency of the T vs. n plot seems to indicate that this transition may overlap with the II/III transition due to both peaks should appear at the same region.

All in all, from the features commented, while the I/II transition implies a slight supercooling that produce a material whose heating peak, thus the second heating, appears at about 2-10 ºC lower than in the first heating. However, the II/III and III/IV transitions are well reproduced in the second heating traces appearing at the same temperature and intensity. This means that an effective nucleation takes place in the recovery of these phases. Therefore, it can be suggested that the I/II transition must involve a crystal melting process, where take place a slightly supercooling due to the nucleation process is slow; whereas the II/III and III/IV transitions must correspond to a transition between two mesophases which belong to liquid crystal phases. To study in detail the thermal transitions the plot of enthalpies and entropies involve in the transitions have been represented against n in figure III.6b and c.

Values of the enthalpy and entropy involved in the transitions are plot against n in Figures III.6b and III.6c, respectively. Due to enthalpy and entropy values are directly related we will study them together. Thus, the tendencies observed are: on the one hand, the values associated to the I/II transition increase slightly linearly with the length of the chain with a noticeable slope which is a clear indication that the alkyl chain takes active part in the molecular rearrangement. Furthermore, the values associated to this transition in the first heating takes values between 14-41 kJ mol^{-1} higher than in the second heating. This means that the phase adopted by the surfactant coming from solution is more ordered than the phase formed upon cooling from the melt. Therefore, two phases (tentatively called phases Iα and Iβ can be assumed to exist in nATMP·Br at room temperature since the longer is the chain the larger is the enthalpy difference between the phases Iα and Iβ. It can be inferred that the methylene contribution to the stability of Phase Iα is greater than in Phase Iβ, and therefore a more efficiently packed structure should be expected to occur in Phase Iα.

This behavior is similar to that described for the *n*ACh·I soaps in which a well-ordered in the three dimensions structure was proven to exist in Phase Iα.[105] On the other hand, the enthalpy and entropy values of the II/III and III/IV transitions appear to be practically independent of *n*. These results are consistent with the similar values found along the series for II/III and III/IV transitions enthalpies and entropies values. Furthermore, it is suggested that the alkanoyl chain must not participate actively in the molecular rearrangement involved in these transitions.
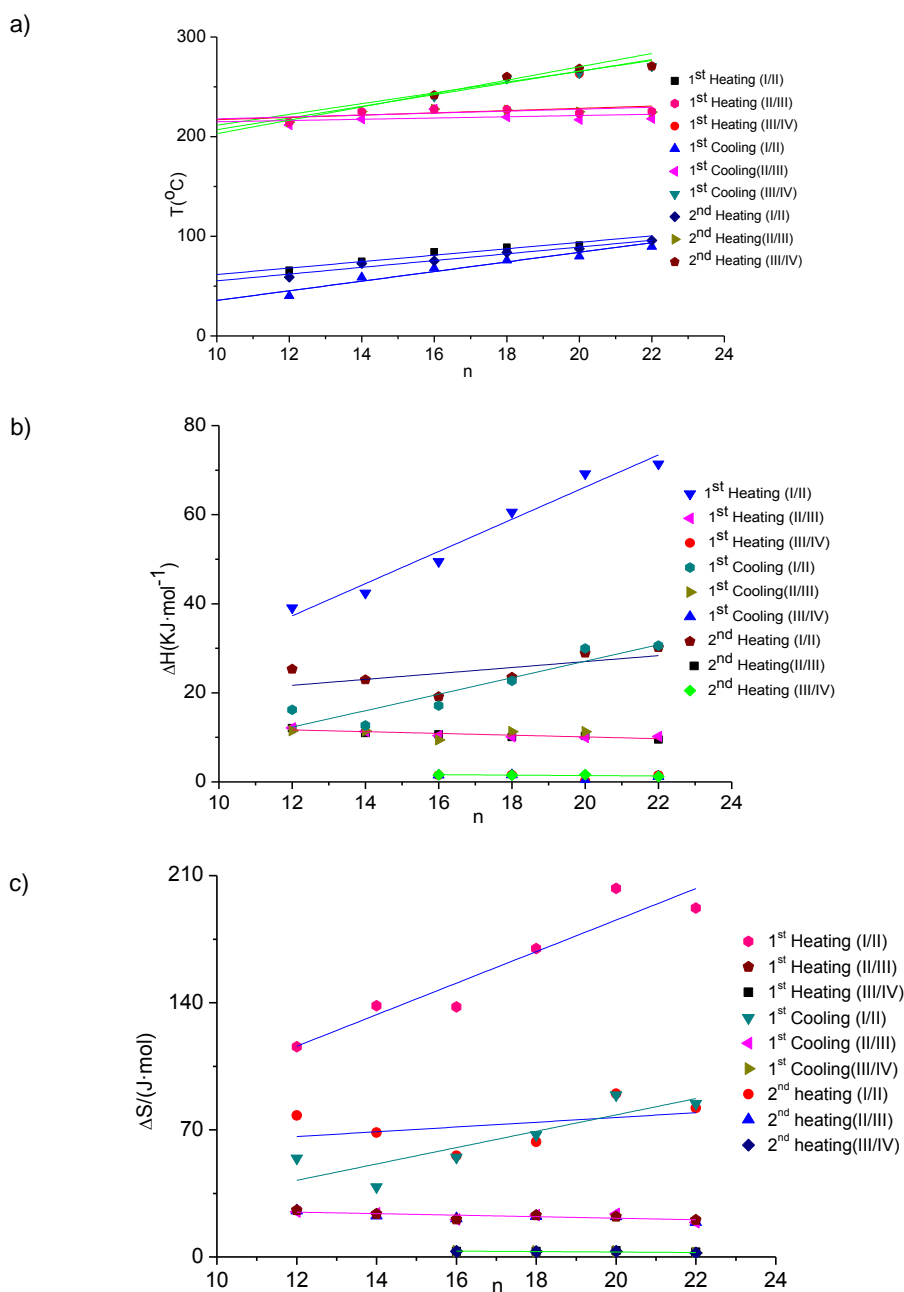
Figure III.6. Phase transition temperatures a), enthalpies b), and entropies c) of *n*ATMP·Br surfactants as a function of *n*. In b) the negative H registered at cooling are represented in positive values for a closer comparison with the H registered at heating.

III. RESULTS AND DISCUSSION

The thermal transitions characterized by DSC have also been studied by polarizing optical microscopy at both heating and cooling. According to DSC results, 12ATMP·Br and 14ATMP·Br show under the polarizing microscope three clear different textures at both increasing and decreasing temperatures within the 20-300 ⁰C range corresponding to the three phases described above. Illustrative pictures are shown in Figure III.7 for 12ATMP·Br. Phase Iα is shown at 25 ⁰C by the original. As it has been mentioned before, a high crystallinity is adopted by this phase as it is revealed by the uniform color and high birefringence displayed in the picture. At temperature of 150 ⁰C, the texture shown is characteristic of a smectic crystal-liquid phase (Phase II), which is the structure, reasonably expected to be adopted upon heating Phase I. The smectic texture is much better revealed at cooling probably due to the more favorable mobility of the molecules when come from higher temperatures. At temperatures above 210 ⁰C a black picture is obtained corresponding to the isotropic phase (Phase III). After cooling down to room temperature a high birefringent texture is recovered but clearly less ordered than that observed in the unheated sample. This would correspond hypothetically to Phase Iβ. X-ray diffraction data will be later presented in support of the occurrence of these optically detected phases.
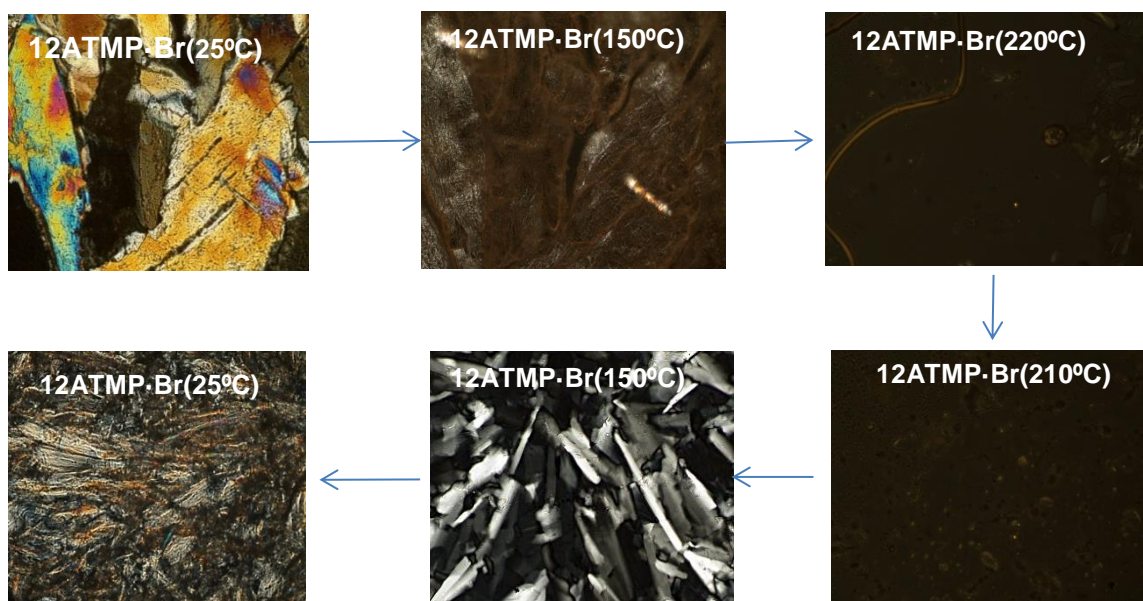
Figure III.7. Micrographs recorded by POM from 12ATMP·Br at the indicated temperatures.

Furthermore, four different phases can be distinguished under the polarizing microscope for surfactants with n = 16,18, 20 and 22 at both increasing and decreasing temperatures within the 20-300 ºC range, which correspond with the DSC results. A selection of pictures taken from 20ATMP·Br is shown in figure III.8 to illustrate the texture changes occurring in the surfactants with n>14. Phase Iα is shown at 25 ºC, which corresponds to the texture before heating and displays a high birefringence due to its high crystallinity. Similarly to the 12ATMP·Br, at temperature of 150 ºC, the texture shown is characteristic of a smectic crystal-liquid phase (Phase II), which is also much better appreciate at cooling. However, in this case an additional phase is obtained above 210 ºC. This phase (Phase III) is very similar to that observed at 150 ºC but with a lower birefringence due to its lower crystallinity. Probably, differences between these two phases (Phase II and Phase III) concern the order degree of the ionic layer, which is crystallized at 150 ºC but disordered at 210 ºC. At temperatures above 250 ºC a black picture is obtained corresponding to the isotropic phase (Phase IV). As occurs in 12ATMP·Br, after cooling down to room temperature a high birefringent texture is recovered but clearly less ordered than that observed in the unheated sample (Phase Iα). Therefore, this phase correspond to Phase Iβ, which is less crystalline than Phase Iα.
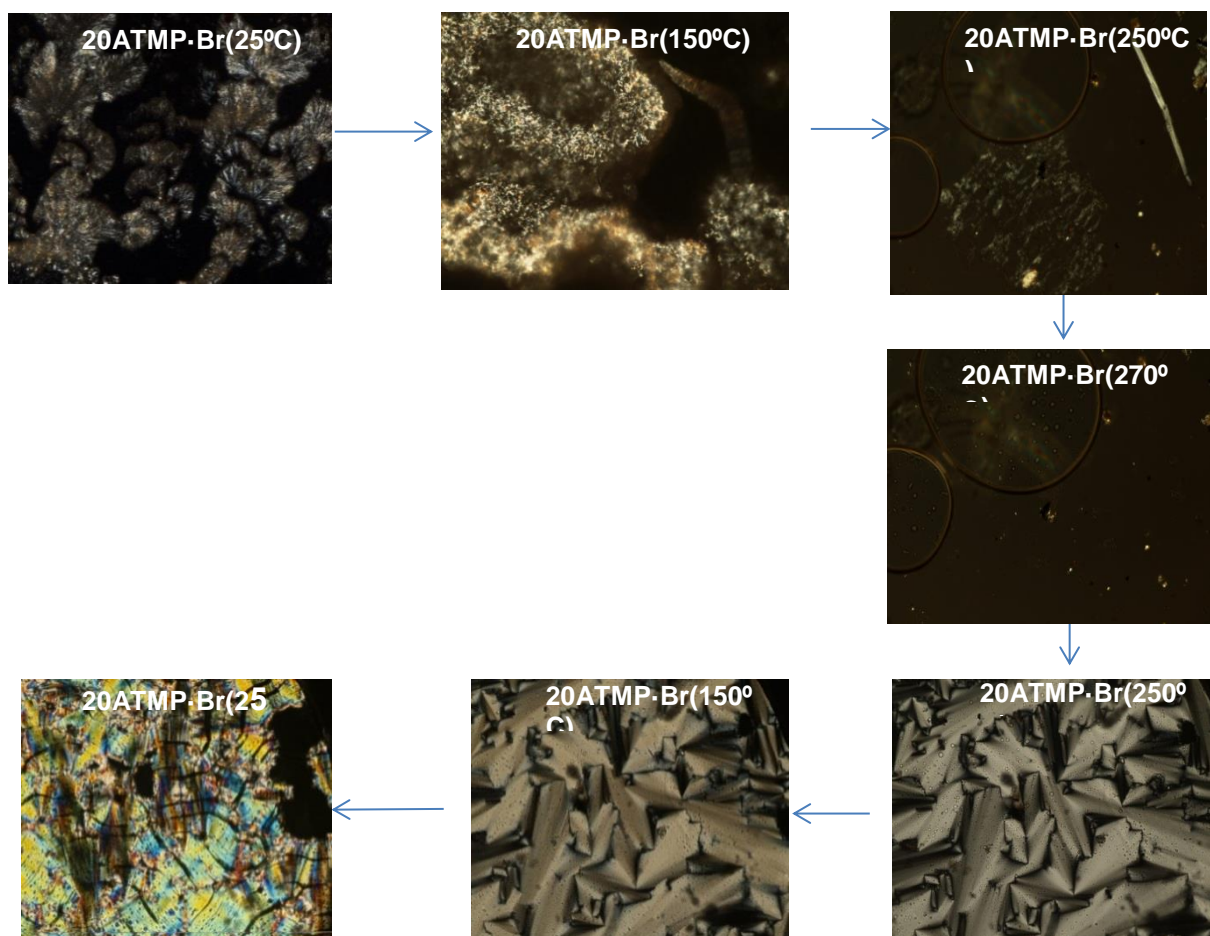
Figure III.8. Micrographs recorded by POM from 20ATMP·Br at the indicated temperatures.

III. RESULTS AND DISCUSSION

1.5 X-ray diffractograms

The SAXS and WAXS profiles from 20ATMP·Br are compared in Fig.III.9 and the most characteristic spacings of the pattern are listed in table III.3. As mentioned, the XRD profiles obtain in the University of Barcelona, were registered at room temperature using two types of 20ATMP·Br samples: that coming from the synthesis, which are white powders, and other which had been previously heated up to 290 ºC and cooled again to room temperature. Thus, two facts were ascertained by the results obtained. On the one hand, the 20ATMP·Br crystallizes when it is cooling from the molten. Moreover, it was found that this crystalline structure generated is different than the initial.
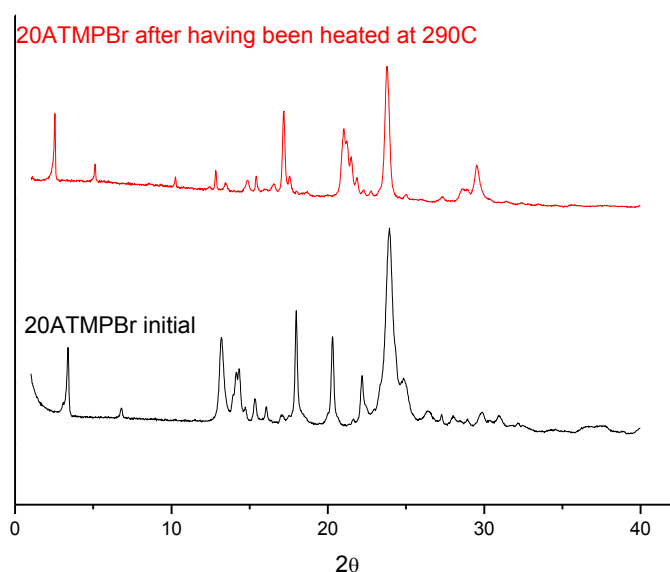
Figure III.9. XRD profile of 20ATMP·Br obtained in the University of Barcelona after having been heated at 290 ºC and before heating (initial).

Furthermore, it can be ascertained that it is a layered structure due to the strong reflection appearing in the SAXS region (Fig.III.9) at a spacing of 26.0 Å or 34.7 Å depending on if it is the initial sample or the sample after having been heated at 290 ºC, respectively. As occurred in Ach·I[105], it is expected that this layered structure was shared by the whole series of surfactants and that all the surfactants displayed similar patterns in the WAXS region. In this particular case, a fair number of sharp peaks in the 6.7-3.7 Å interval with the strongest one corresponding to the 3.7 Å spacing was found. According to these results, we can conclude that 20ATMP·Br has a layered structure and its paraffinic chain is crystallized.

.   **Table III.3**. The most characteristic spacings of the 20ATMP·Br pattern

20ATMP·Br After heating		20ATMP·Br Initial	
2θ	d(Å)	2θ	d(Å)
2.6	34.7	3.42	26.0
5.1	17.2	6.8	13.0
13.2	8.6	13.2	6.7
12.8	6.9	14.2	6.2
17.2	5.2	18.1	4.9
20.8	4.2	20.2	4.4
23.5	3.7	22.5	4.0
29.8	3.0	24.2	3.7

Eventually, it has been demonstrated that the heat treatment affects significantly to the surfactant structure due to it changes with the temperature changes. In these sense, in the figure III.9 it is assessed that the phase I involves two phases: the phase Iα, which is the phase adopted from the synthesis and is the most crystalline phase, and the phase Iβ, which appears after having been heated at 290 °C. Moreover, in figure III.10, where are illustrated the XRD profiles obtain in the University of Sevilla, the different peaks characteristic of each phase can be distinguished for nATMP·Br samples with n = 20 and 22 along the different temperatures. As we have mentioned, this behavior is expected to occur for the whole series of surfactants. However, we have not yet obtained the rest of XRD from the others surfactants so it is only a prediction.
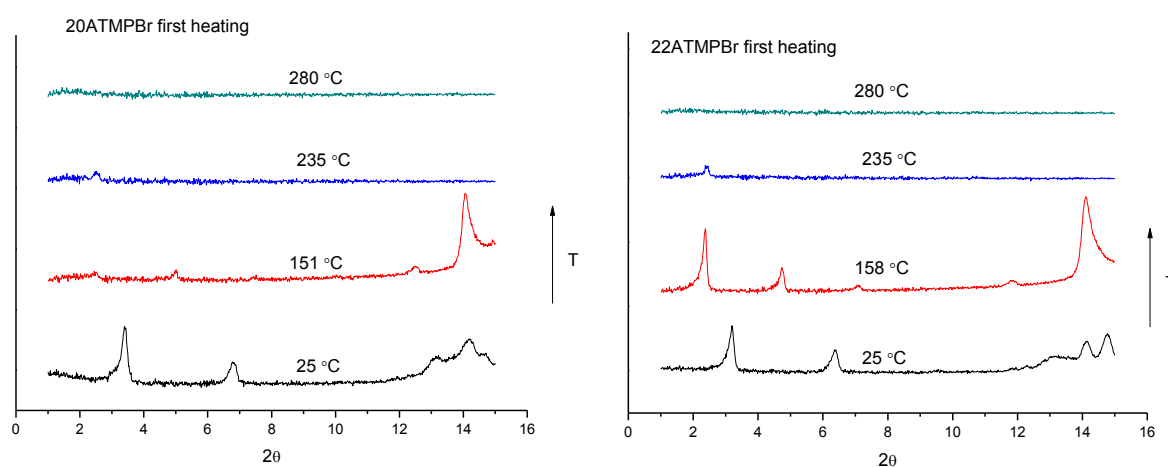
Figure III.10. XRD profiles of nATMP·Br with n= 20 and 22 obtained in the University of Sevilla for the indicated temperatures.

III. RESULTS AND DISCUSSION

2. Ionic complexes of poly(γ-glutamic) acid and alkyltrimethylphosphonium surfactants (*n*ATMP·PGGA)

2.1. Synthesis of the complexes

The *n*ATMP·PGGA with *n*= 12, 14, 16, 18, 20 and 22 (Scheme III.2), were synthesized by mixing aqueous solutions of equimolecular amounts of Na·PGGA and the corresponding *n*ATMP·Br at the minimum temperature required to dissolve the surfactant. After standing for a few hours a white precipitate appeared that was collected by filtration and dried under vacuum for several days to render a white to pale powder.
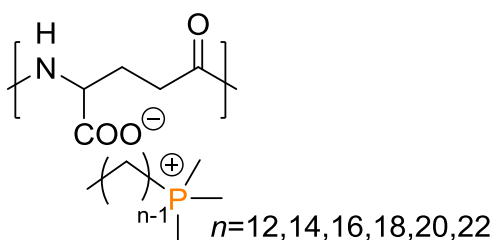
Scheme III.2. Chemical structure of *n*ATMP·PGGA complexes.

The results obtained for the six complexes examined in this work are compared in Table III.4. Yields were found to oscillate between 60 and 90% being the lower yields those of the shortest surfactants probably due to their high solubility reduce their precipitation. Consequently, more concentration solutions have been used in order to improve their precipitation and their yields. The solubility behavior displayed by *n*ATMP·PGGA was similar to that observed for other complexes of *n*ATMA·PGGA, *e.g.* they are soluble in organic solvents such as, methanol, ethanol, TFE or DMSO. A feature worth of mention in this regard is that they appear to be readily soluble in chloroform, whereas they cannot be dissolved by water, which is exactly the opposite of the behavior showed by Na·PGGA.

Table III.4. Synthesis results of *n*ATMP·PGGA complexes.

$R(CH_3)_3P^+$	Complex	Reaction conditions		Yield (%)	Composition[c]
		Conc (M)[a]	$T^a(°C)^b$		
-$C_{12}H_{25}$	12ATMP·PGGA	0.075	25	58	1.03:1
-$C_{14}H_{29}$	14ATMP·PGGA	0.05	25	68	1.11:1
-$C_{16}H_{33}$	16ATMP·PGGA	0.01	30	70	1.16:1
-$C_{18}H_{37}$	18ATMP·PGGA	0.01	45	70	1.16:1
-$C_{20}H_{41}$	20ATMP·PGGA	0.01	55	72	1.2:1
-$C_{22}H_{45}$	22ATMP·PGGA	0.01	65	93	1.3:1

[a] Concentration of the two solutions before mixing to form the complex
[b] Temperature selected according to the surfactant solubility in water.
[c] Ratio of ATMP to PGGA in the obtained complex.

III. RESULTS AND DISCUSSION

2.2. Chemical characterization

The composition and constitution of *n*ATMP·PGGA complexes were assessed by both FT-IR and ^{1}H and ^{13}C NMR spectroscopies. FT-IR spectrum of the *18*ATMP·PGGA complex is represented together with the PGGA spectrum in the ionized form (Figure III.11a) in order to compare them regarding the characteristic groups of the surfactant at around 2900 cm^{-1}, 2850 cm^{-1},1400 cm^{-1}, 970 cm^{-1} and 712 cm^{-1} and the characteristic bands of the polyacid (the amide stretching) at 1580 and 1530 cm^{-1}. Moreover, if the whole series of the of *n*ATMP·PGGA complexes are represented (figure III.11b) it can be observed again that the longer the alkyl chain length, the more intense are the observed methylene bands (those appearing at 2900 and 2850 cm^{-1}).
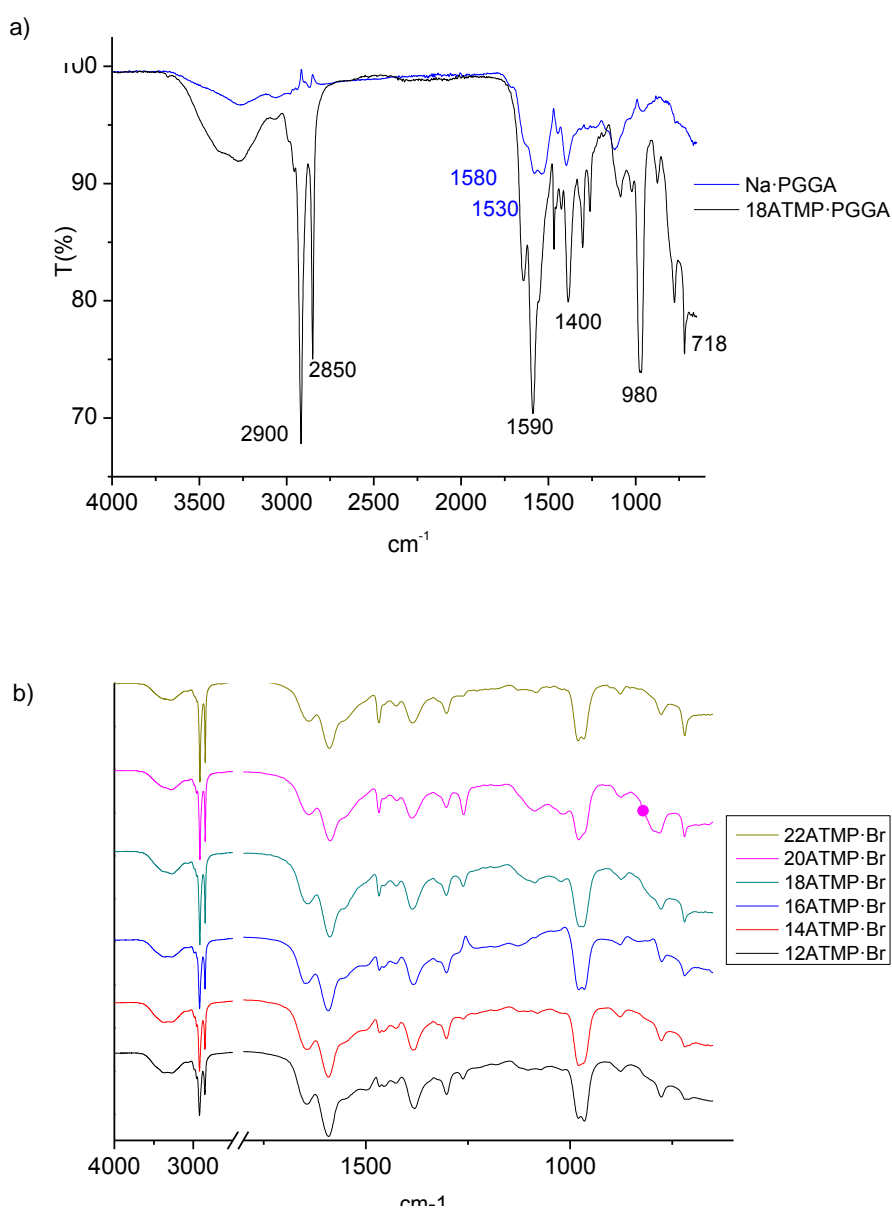
Figure III.11. a) FTIR of 18ATMP·PGGA and PGGA and b) FTIR of the *n*ATMP·PGGA

^{1}H and ^{13}C NMR spectra of nATMP·PGGA (Figure III.12) allow estimating the composition of the complexes by comparing the peak area of the α-methylene proton of PGGA (CH, δ = 4.1 ppm) with that of the peak arising from inner protons of the alkyl chain attached to the phosphonium ion ($^{3-17}$CH$_2$, δ= 1.2–1.4 ppm, ^{2}CH$_2$, δ = 1.5 ppm, ^{18}CH$_3$, δ = 0.9 ppm). The results afforded by this analysis revealed that the surfactant to the polyacid ratio increases from 1.0 to 1.3 with the length of the alkyl side group (table III.4).This excess of surfactant found in the longest surfactants may be cause due to their lower solubility that makes them precipitate together with the complex when the complex is forming. Consequently, the surfactant holds within the complex structure.
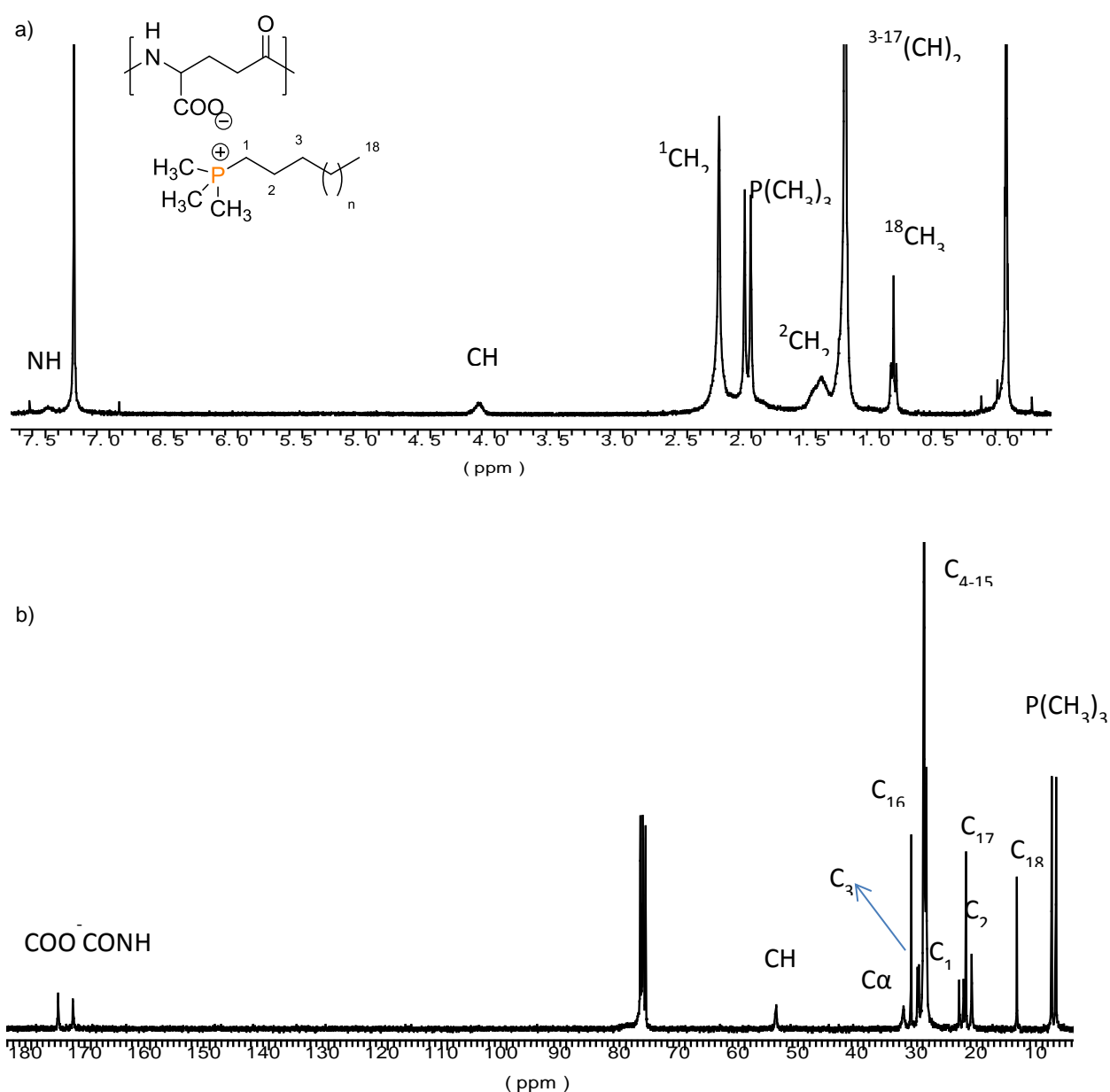
Figure III.12. a) ^{1}HNMR and b) ^{13}C NMR spectra of 18ATMP·PGGA recorded at 25 °C.

III. RESULTS AND DISCUSSION

2.3 Structural Characterization

The thermal behavior of *n*ATMP·PGGA complexes was examined by TGA and DSC. The TGA trace recorded from the whole series of *n*ATMP·PGGA complexes are qualitatively similar to those reported for *n*ATMA·PGGA. As we can see in figure III.13, decomposition takes place within the temperature range of 250–350 ºC.
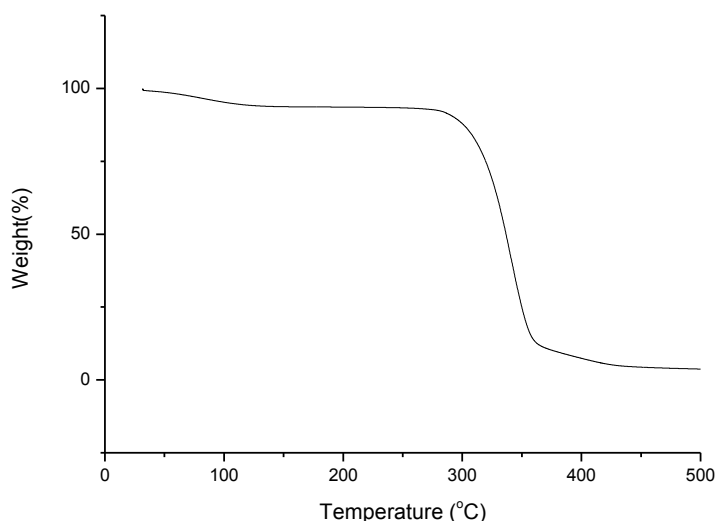
Figure III.13. TGA trace of 22ATMP·PGGA complex.

Furthermore, it was found that *n*ATMP·PGGA DSC traces (figure III.14) were similar to those shown in the *n*ATMA·PGGA complexes.[78, 80] Therefore, we can conclude that *n*ATMP·PGGA complexes have the DSC behavior characteristic of comb-like polypeptides bearing flexible side chains that are able to crystallize for a sufficient length. Thus, an endothermal peak at a temperature around 60 ºC was observed for $n \geq 18$, which is perfectly reversible and largely reproducible regarding both, position and intensity. This peak is associated to the melting of the separate paraffinic phase, which is made of crystallized alkyl side chains.
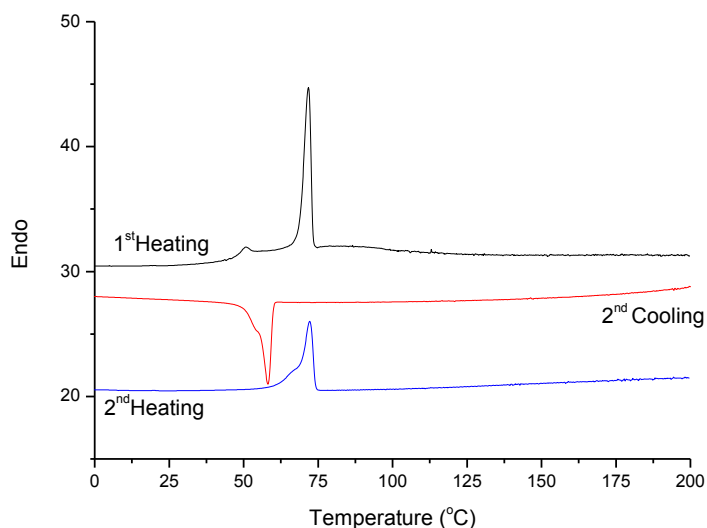
Figure III.14. DSC traces of 20ATMP·PGGA complex.

All in all, we can assume that nATMP·PGGA complexes adopt the layered biphasic structure typical of comb-like polypeptides with the polyacid and the alkyl side chains phases alternating periodically with a repeating distance of ~4.5 nm. This structure are going to be investigated by both polarizing optical microscope and X-ray diffraction to study the different phases at increasing temperatures and to measure the characteristic spacings, respectively.

3. Ionic complexes of hyaluronic acid and alkyltrimethylphosphonium surfactants (*n*ATMP·HyalA)

3.1 Synthesis of trimethylphosphonium complexes

The complexes *n*ATMP·HyalA with *n* =12, 14, 16, 18, 20 and 22 (Sheme III.3), were formed when equal quantities of aqueous solutions of polyacid and surfactant were mixed and the mixture was left to stay between 25-65 ⁰C, depending on the length of the alkyl chain, for a few hours. As a result of ionic coupling between the polyacid and the surfactant, complexes precipitated from the mixed aqueous solution after several hours of standing. The complexes obtained were transparent to white hygroscopic fibrous solids that were soluble in methanol but non-soluble either in chloroform or ethyl ether. Yields were found to oscillate between 60 and 90%. These results are compared in Table III.5. Their composition and constitution have been assessed through the Chemical characterization and their thermal stability and thermal transitions are going to be studied soon with their structural characterization.

n=12,14,16,18,20,22
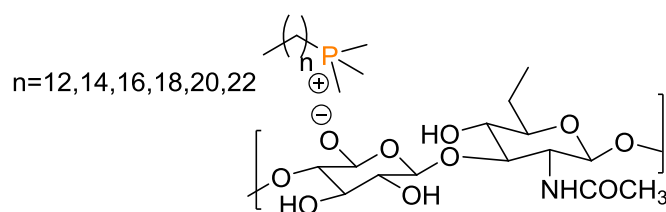
Scheme III.3. Chemical structure of *n*ATMP·Hyal complexes.

Table III.5. Synthesis results of *n*ATMP·HyalA complexes.

R(CH$_3$)$_3$P$^+$	Complex	Reaction conditions		Yield (%)	Composition[c]
		Conc (M)[a]	T^a(⁰C)[b]		
-C$_{12}$H$_{25}$	12ATMP·HyalA	0.075	25	58	2:1
-C$_{14}$H$_{29}$	14ATMP·HyalA	0.05	25	67	2:1
-C$_{16}$H$_{33}$	16ATMP·HyalA	0.01	30	70	2:1
-C$_{18}$H$_{37}$	18ATMP·HyalA	0.01	45	71	2:1
-C$_{20}$H$_{41}$	20ATMP·HyalA	0.01	55	77	2:1
-C$_{22}$H$_{45}$	22ATMP·HyalA	0.01	65	93	2:1

[a] Concentration of the two solutions before mixing to form the complex
[b] Temperature selected according to the surfactant solubility in water.
[c] Ratio of ATMP to PGGA in the obtained complex.

3.2 Chemical Characterization

The composition and constitution of *n*ATMA·HyalA complexes were checked by both FTIR and ^{1}H/^{13}C NMR.

Infrared bands characteristic of the HyalA with the carboxyl groups in the ionized state along with those arising from the characteristic groups of one of the surfactant cation (*e.g* 18ATMP·HyalA) are represented in order to compare them (figure III.15). Moreover, if we compared the spectra of the whole series of surfactants we would see a similar tendency as before: the longer the alkyl chain length, the more intense are the observed methylene bands.
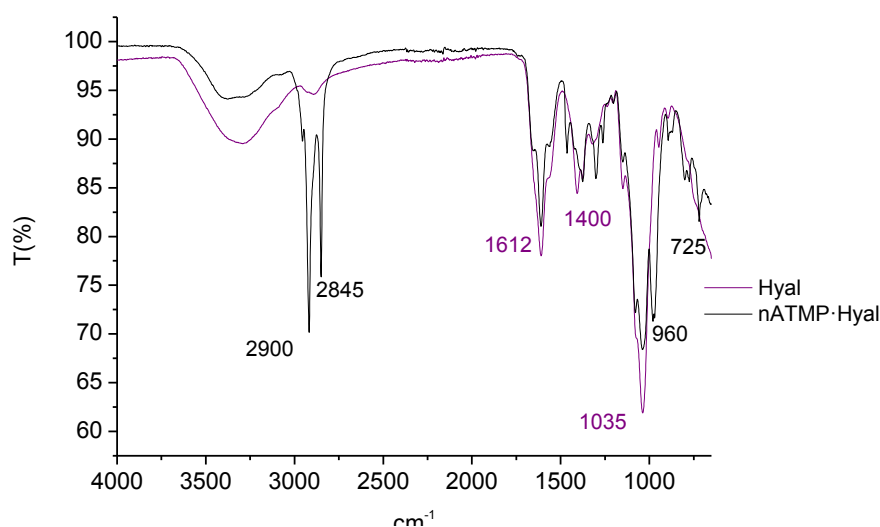
Figure III.15. FTIR of the *n*ATMP·HyalA complexes and HyalA.

Results consistent with infrared data were obtained in the NMR analysis. The ^{1}H and ^{13}C NMR spectra of 18ATMA·HyalA are depicted in Figure III.16 for illustrative purposes. In ^{13}C NMR spectrum can be distinguished the surfactant signals from those corresponding to the polyacid (*) simply by comparing their intensity due to while surfactant signals are extremely intense the others not. The chemical slight shifts observed for the six complexes can be checked in the supplementary information and the composition of the complexes was accurately determined by ^{1}H NMR. In this sense, the peak areas measured for the hyaluronic acid methyl protons signal (CH, δ = 4.3 ppm) to the alkylammonium interior methylene accumulative signal ($^{3-17}$CH$_2$, δ = 1.2–1.4 ppm and ^{18}CH$_3$ δ = 0.9 ppm). These results are given in Table III.4 where it is seen that the surfactant to hyaluronic acid ratio is around 2:1 for the whole series of *n*ATMP·HyalA complexes.

a)

b)

Figure VI.16. a) ^{1}HNMR and b) ^{13}C NMR spectra of *18*ATMP·HyalA recorded at 25 ºC. * HyalA carbons .
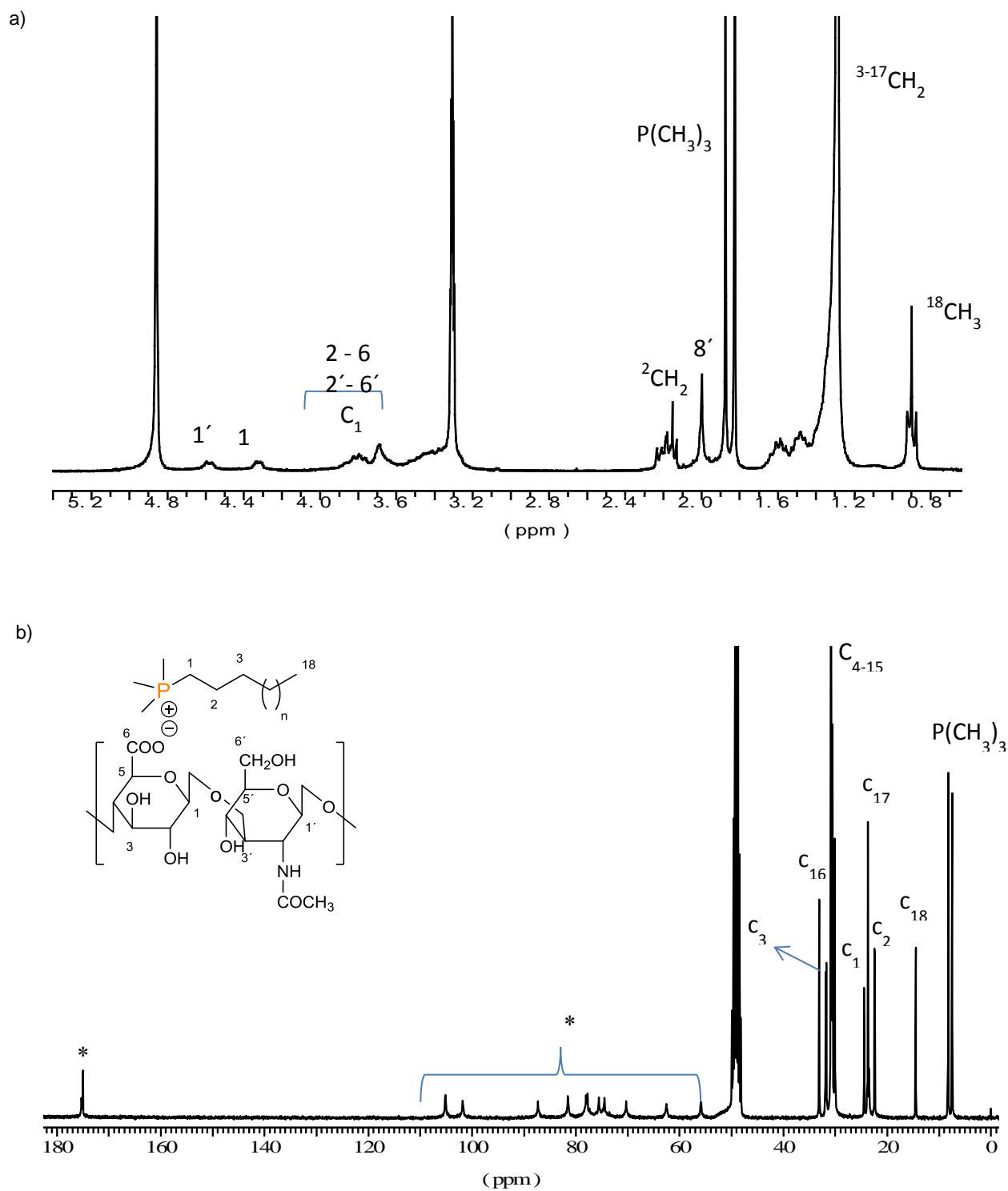
IV. CONCLUSIONS

IV. CONCLUSIONS

A series of alkyltrimethylphosphonium bromide surfactants (*n*ATMP·Br) have been prepared from trimethylfosfine and 1-bromo alkanes with *n* = 12, 14, 16, 18, 20 and 22, and their thermal and structural properties have been studied as a function of temperature. Cytotoxicity of investigated surfactants has been demonstrated several times that is strongly influenced by alkyl chain length and alkyl substitution on the cations. In general, phosphonium surfactants are less cytotoxic compared with ammonium surfactants. This work reveals that these surfactants offer superior properties when they are compared to ammonium surfactants as well as their suitability to prepare bio-based comb-like polymers by ionic coupling with naturally occurring polyelectrolytes. This general conclusion is supported by the following partial conclusions:

1) Firstly, in the thermal stability study of *n*ATMP·Br surfactants evaluated by TGA it was found that their decomposition starts around 370-400°C with onset temperatures decreasing slightly with the length of the alkyl chain, but that are higher than those shown for the *n*ATMA·Br surfactants. Consequently, it is clear that phosphonium surfactants are more thermal stable than ammonium surfactants.

2) Secondly, while *n*ATMP·Br surfactants with *n*<18 are soluble in water at room temperature, those with n>18 are soluble in warm water showing Krafft temperatures between 35 and 65 °C depending on *n*. These Krafft temperatures are lower than those shown for *n*ATMA·Br surfactants, so phosphonium surfactants are more soluble than ammonium surfactants.

3) Thermal transitions have been studied by DSC and polarizing optical microscopy. Several thermal transitions involving crystalline, semicrystalline and liquid-crystal phases were characterized for these soaps at temperatures increasing with the value of n. Hence it was found that, while only two transition temperatures were observed for 12ATMP·Br and 14ATMP·Br surfactants, there are three for the higher members of the series. This means that they display three or four thermal phases, respectively.

IV. CONCLUSIONS

Ionic complexes of alkyltrimethylphosphonium bromide surfactants and poly (□-glutamic acid) (nATMP·PGGA) have been prepared and characterized. These complexes have a composition from 1.0:1.0 to 1.3:1.0 with the length of the alkyl side group. According to preliminary DSC data and based on antecedents available on similar systems, these complexes are expected to be self- organized in biphasic layered structure characteristic of comb-like amphiphilic systems with the polyacid and the alkyl side chains phases alternating in a periodically layered structure. The preparation of other comb-like ionic complexes of these phosphonium surfactants and other biopolyacids is also possible. In these sense, we have prepared complexes of hyaluronic acid and ATMP·Br (nATMP·HyalA). Although their thermal characterization has not been carried out yet, we were able to assess their composition and constitution through their chemical characterization. Thus, we found that the surfactant to hyaluronic acid ratio is around 2:1 for the whole series of nATMP·HyalA complexes. Consequently, more studies of these systems are going to be carried out and other potential systems will be searched.

IV. CONCLUSIONS

V. REFERENCES

1. Holmberg, K.; Jönsson, B.; Kronberg, B.; Lindman, B. *Surfactants and polymers in aqueous solution*; JW.A, LTD: Chichester, England, 2003.

2. Israelachvili, J. N.; Mitchell, D. J.; Ninham, B. W. Theory of self-assembly of hydrocarbon amphiphiles into micelles and bilayers. *J. Chem. Soc.- Faraday Trans. II.* **1976**, *72*, 525-1568.

3. Winsor, P. A. Binary and multicomponent solutions of amphiphilic compounds. Solubilization and the formation, structure, and theoretical significance of liquid crystalline solutions. *Chem. Rev.* **1968**, *68*, 1–38.

4. Xie, W.; Xie, R.; Pan, W.-P.; Hunter, D.; Koene, B.; Tan, L.-S. ; Vaia, R. Thermal stability of quaternary phosphonium modified montmorillonites. *Chem. Mater.* **2002**, *14*, 4837.

5. Kanazawa, A.; Ikeda, T; Endo.T. Novel polycationic biocides: synthesis and antibacterial activity of polymeric phosphonium salts. J. Polym. Sci. Part A: Polym. Chem. **1993.** 31:335-343.

6. Harikumar, K.; Rajendran, V. Synthesis of a new NP multi-site phase-transfer catalyst and its application to dichlorocarbene addition reactions. J. Chem. & Cheml. Sci. Vol.2. **2012**, 1, 21-29.

7. Wellens, S.; Goovaerts, R.; Möller, C.; Luyten,J.; Thijs,B.; Koen Binnemans. A continuous ionic liquid extraction process for the separation of cobalt from nickel. Green Chem. **2013**, 15, 3160–3164

8. Gerritsma, D.A.; Robertson, A.; McNulty, J.; Capretta, A. Heck reactions of aryl halides in phosphonium salt ionic liquids: library screening and application. *Tetrahedron Lett.* **2004**, *45*, 7629.

9. Ito, N.; Arzhantsev, S.; Heitz, M.; Maroncelli, M. Solvation dynamics and rotation of coumarin in alkylphosphonium ionic liquids. *J. Phys. Chem. B.* **2004**, *108*, 5771.

10. McNulty, J.; Capretta, A.; Wilson, J.; Dyck, J.; Adjabeng, G.; Robertson, A. Suzuki cross-coupling reactions of aryl halides in phosphonium salt ionic liquid under mild conditions *Chem. Commun.* **2002**, 1986.

11. Gorodetsky, B.; T. Ramnial, T.; Branda, N. R.; Clyburne, J. A. Electrochemical reduction of an imidazolium cation: a convenient preparation of imidazol-2-ylidenes and their observation in an ionic liquid. C. *Chem. Commun.* **2004**, 1972.

12. Ramnial, T.; Ino, D. D.; Clyburne, J. A. C. Phosphonium ionic liquids as reaction media for strong bases. *Chem. Commun.* **2005**, 325.

13. Landini, D.; Maia, A.; Podda, G. Nonhydrated anion transfer from the aqueous to the organic phase: enhancement of nucleophilic reactivity in phase-transfer catalysis. *J. Org. Chem.* **1982**, *47*, 2264.

14. Landini, D.; Maia, A.; Rampoldi, A. Stability of quaternary onium salts under phase-transfer conditions in the presence of aqueous alkaline solutions. *J. Org. Chem.* **1986**, *51*, 3187.

15. Panek, G.; Schleidt, S.; Wolkenhauer, M.; Spiess, H. W.; Jeschke, G. Heterogeneity of the surfactant layer in organically modified silicates and polymer/layered silicate composites. *Macromolecules.* **2006**, *39*, 2191.

16. Hedley, C. B.; Yuan, G.; Theng, B. K. G. Thermal analysis of montmorillonites modified with quaternary phosphonium and ammonium surfactants. *Appl. Clay Sci.* **2007**, *35*, 180.

17. Byrne, C; McNally, T. Ionic liquid modification of layered silicates for enhanced thermal stability. *Macromol. Rapid Commun.* **2007**, *28*, 780.

18. Bradaric, C. J.; Downard, A.; Kennedy, C.; Robertson A. J.; Zhou Y. H. Industrial preparation of phosphonium ionic liquids . Green Chem., **2003**, 5, 143–152.

19. Chowdhury, S. A.; Scott J. L.; MacFarlane ,D. R.. Ternary mixtures of phosphonium ionic liquids + organic solvents + water. Pure Appl. Chem.**2008**, 80, 1325–1335.

VI. REFERENCES

20. Freire, M. G.; Carvalho, P. J.; Gardas, R. L.; Santos,L; Marrucho I. M.; Coutinho J. A. P. Solubility of water in tetradecyltrihexylphosphonium-based ionic liquids. J. Chem. Eng. Data. **2008**, 53, 2378–2382.
21. Adamová, G.; Gardas, R. L.; Rebelo, L. P. N.; Robertson A. J.; Seddon, K. R. Alkyltrioctylphosphonium chloride ionic liquids: synthesis and physicochemical properties. Dalton Trans. **2011**, 40, 12750–12764.
22. Knifton, J. F. Homogeneous transition metal catalysis in molten salts. *Aspects Homogeneous Catal.* **1988**, *6*, 1.
23. Knifton, J. F; Grigsby R. A.; Jr; Lin, J. J. Syngas reactions. 6. Aliphatic alcohols and esters from synthesis gas. *Organometallics* **1984**, *3*, 62.
24. Knifton, J. F. Ethylene glycol from synthesis gas via ruthenium melt catalysis.*J. Am. Chem. Soc.* **1981**, *103*, 3959.
25. Knifton, J. F. Vicinal glycol esters from synthesis gas. *J. Chem. Soc. Chem. Commun.* **1981**, 188.
26. Knifton, J. F. Manufacture of ethylene glycol from synthesis gasUS Patent 4265828, **1981**.
27. Knifton, J. F. Alkanols from synthesis gasUS Patent 4339545, **1982.**
28. Knifton, J. F. Manufacture of alkanols from synthesis gas. US Patent 4332914, **1982.**
29. Knifton, J. F. Process for preparing acetic and propionic acids and their esters. US Patent 4362822, **1982.**
30. Knifton, J. F. Manufacture of alkanols from synthesis gas. US Patent 4315994, **1982.**
31. Knifton, J. F.Process for producing ethylene glycol using a ruthenium-copper catalyst. US Patent 4518715, **1985.**
32. Knifton, J. F. Process for C.sub.1 -C.sub.4 alkanol production from synthesis gas. US Patent 4605677, **1986.**
33. Knifton, J. F ; Grice, N. J. Process for C.sub.1 -C.sub.4 alkanol production from synthesis gas using a trimetallic catalyst. US Patent 4622343, **1986.**
34. Donofrir, D. K.; Whitekettle, W. K. Biocidal compositions and use there of containing a synergistic mixture of tetraalkyl phosphonium halide and n-alkyl dimethylbenzyl ammonium chloride. US Patent 4835143, **1989.**
35. Grade, R.; Thomas, B. M. Using phosphonium compound. US Patent 4874526, **1988.**
36. Ponomarenko, E.A.; Waddon, A.J.; Bakeev, K.N.; Tirrell, D.A.; Macknight, W.J. *Self-assembled complexes of synthetic polypeptides and oppositely charged low molecular weight surfactants. Solid-state properties.* Macromolecules. **1996**, 29, 4340-4345.
37. Macknight, W.J.; Ponomarenko, E.A.; Tirrell, D.A. *Self-assembled polyelectrolyte surfactant complexes in nonaqueous solvents and in the solid state.* Ac. Chem. Res. **1998**, 31, 781-788.
38. Goddard, E. D.; Ananthapadmanabhan, K. P. *Interactions of surfactants with polymers and proteins*; CRC Press: Boca Raton, FL, **1993.**
39. Mel'nikov, S. M.; Dias, R.; Mel'nikova, Y. S.; Marques, E. F.; Miguel, M.G.; Lindman, B. DNA conformational dynamics in the presence of catanionic mixtures. *FEBS Lett.* **1999**, *453*, 113–118.
40. Langevin, D. Complexation of oppositely charged polyelectrolytes and surfactants in aqueous solutions. A review. *Adv. Colloid. Interfac. Sci.* **2009**,*147-148*, 170–177.
41. Thünemann, A. F.; Schnoller, U.; Nuyken, O.; Voit, B. Self-assembled complexes of diazosulfonate polymers with low surface energies. *Macromolecules* **1999**, *32*, 7414-7421.
42. Thünemann, A. F. Polyelectrolyte – surfactant complexes (synthesis, structure and materials aspects). *Progr. Polym. Sci.* **2002**, *27*, 1473–1572.

VI. REFERENCES

43. Antonietti M.; Conrad, J. Synthesis of very highly ordered liquid crystalline phases by complex-formation of polyacrylic-acid with cationic surfactants. *Angew. Chem. Int. Edit.* **1994**, *33*, 1869-1870.

44. Antonietti, M.; Neese, M.; Blum, G. Dielectric and mechanic relaxation in polyelectrolyte-supported bilayer stacks: a model for the dynamics of membrans. *Langmuir.* **1996**, *12*, 4426-4441.

45. Loos, K., Muñoz-guerra, S. *Microestructure and crystallization of rigid coil comb-like polymers and block copolimers.* New york, Ed. Marcel Dekker. **2000**, 263-320.

46. Tischer, M.; Pradel, G.; Ohlsen, K.; Holzgrabe, U. Quaternary ammonium salts and their antimicrobial potential: targets or nonspecific interactions. *Chem. Med. Chem.* **2012**, *7*, 22–31

47. Bruckner, V.; Ivanovics, G.Chemishe und immunologiche Studien uber den Mechanismus der milzbrandinfektin und Immunitat; die chemische Struktur der Kapselsubstanz des Milzbrandbazillus und der serologisch identischen spezifischen Subtanz des Bazillus mesentericus. Z. Immunitatsforsch. 1937, 90, 304–318.

48. Bovarnick, M. The formation of extracellular D(γ-glutamic) acid polypeptide by Bacillus subtilis. J. Biol. Chem. **1942**, 145, 415-424.

49. Thorne, C.B.; Gómez, C.G.; Noyes, H.E.; Housewright, R.D. Production of glutamic polypeptide by Bacillus subtilis. J. Bacteroil. **1954**, 68, 307-315.

50. Fuiji,H. Formation of mucilage by Bacillus natto. Effects of some cultural conditions on the chemical constituents of mucilage. Nippon Nogei Kagaku Kaishi. **1963,** 37, 615-618.

51. Kashim, N.; Furuta, K.; Tanabe, I. Permeability enhancer. US Patent 20060025346, **2006.**

52. Ashiuchi, M.; Misono, H. Poly (γ-glutamic acid). A. Steinbuchel, R.H. Biopolymers for medical and pharmaceutical applications. Wiley–VCH, Weinheim**.** Marchessault (Eds.), **2005,** 1, 619–634.

53. Cheng C, Asada Y; Aida T. Production of gamma-polyglutamic acid by Bacillus licheniformis A35 under denitrifying conditions. Agric. Biol. Chem. **1989,** 53, 2369-2375.

54. Yoon, S.H. ; Do, J.H.; Lee, S.Y.; Chang, H.N. Production of poly- *γ* -glutamic acid by fed-batch culture of Bacillus licheniformis. Biotechnol. Lett. **2000,** 585–588.

55. Sawa, S.; Murakawa, T.; Murao, T.; Omata. Isolation and purification of polyglutamic acid produced by Bacillus subtilis. Nippon Nogeikagaku Kaishi. **1973**, 5, 47, 159-165.

56. Kubota, H; Matsunobu, T; Uotani, K; Takebe, H; Satoh, A; Taniguchi, M. Large scale production of poly(γ-glutamic acid) by Bacillus subtillis F-2-01. Sci Report Meiji Seika Kaisha. **1992**, 31, 41-50.

57. Wu, Q.; Xu, H.; Zhang, D.; Ouyang, P. A novel glutamate transport system in poly (γ-glutamic acid)-producing strain Bacillus subtilis. Appl. Biochem. Biotechnol. **2011**,164,1431-1443.

58. Kunioka, M. Biosynthesis and chemical reactions of poly(amino acid)s from microorganisms. *Appl. Microbiol. Biotechnol.* **1997**, *47*, 469–475.

59. Kajtar, M. Bruckner, V. *Improved synthesis of stereoisometric poly (γ-glutamic acid)s.* Acta Chim. Academ. Scie. Hung. **1969**, 62, 191.

60. Sanda, F.; Fuyiyama, T. *Chemical synthesis of poly (γ-glutamic acid) by polycondensation of γ-glutamic acid dimmer: Synthesis and reaction of poly(γ-glutamic acid) methyl ester.* J. Polym. Sci. Part A. Polym. Chem.**2001**, 35, 2001, 732-741.

VI. REFERENCES

61. Ashiuchi, M.; Kamei, T.;Baek, D. H.; Shin, S. Y.;Sung, M. H.; Soda, K.; Yagi, T.; Misono, H. Enzymatic synthesis of high molecular weight poly gamma-glutamate and regulation of its stereochemistry. Appl. Environ. Microbiol. **2004**, 70, 4249–4255.

62. Ashiuchi, M.; Kamei, T.; Misono, H. Poly-gamma-glutamate synthetase of Bacilllus Subtilis. J. Mol. Cat. B Enzym. **2003**, 23, 101-106.

63. Pérez-Camero, G.; Congregado, F.; Bou, J. J.; Muñoz-Guerra, S. Biosynthesis and ultrasonic degradation of bacterial poly(gamma-glutamic acid). *Biotechnol. Bioeng.* **1999**, *63*, 110–115.

64. Borbély, M.; Nagasaki, Y.; Borbély, J.; Fan, K.; Bhogle, A.; Sevoian, M. Biosynthesis and chemical modification of poly(γ-glutamic acid). *Polym. Bull.***1994**, *32*, 127-132.

65. Kubota, H.; Fukuda, H.; Takebe, H.; Endo, T. Poly-gamma-glutamic acid ester and shaped body thereof. US Patent 5118784, **1992.**

66. Gross, R. A.; McCarthy, S. P.; Shah, D. T. Gamma-poly (glutamic) acid esters. US Patent 5378807, **1995.**

67. Kubota, H.; Nambu, Y.; Endo, T. Some properties of poly (γ-glutamic acid) produced by microorganism. *Nippon Kagaku Kaishi*, **1993**, *8*, 973-977.

68. Kubota, H.; Nambu, Y.; Endo, T. Convenient esterification of poly (γ-glutamic acid) produced by microorganism with alkyl halides and their thermal properties. *J. Polym. Sci. A Polym. Chem*. **1995**, *33*, 85-88.

69. Portilla-Arias, J. A.; García-Alvarez, M.; Martínez de Ilarduya, A.; Muñoz-Guerra, S. Thermal decomposition of microbial poly (γ-glutamic acid) and poly-glutamate)s. *Polym. Degrad. Stab.* **2007**, *92*, 1916–1924.

70. Shih, I. L.; Van, Y. T.; Yeh, L. C.; Lin, H. G.; Chang, Y. N. Production of a biopolymer flocculant from Bacillus licheniformis and its flocculation properties. *Bioresource Technol.* **2001**, *78*, 267-272.

71. Fukazu, F.; Taguchi, Z. *Cosmetics containing crosslinked poly (γ-glutamic acid);* Kokai Tokyo Koho: Japan, **2003.**

72. Richard, A., Margaritis, A. Poly (glutamic acid) for biomedical applications. Crit. Rev. Biotechnol. **2001**.21, 219–232.

73. Bajaj, I.; Singhal, R. Poly (glutamic acid) – An emerging biopolymer of commercial interest. *Bioresource Technol.* **2011**, *102*, 5551–5561.

74. Melis, J.; Morillo, M.; Martínez de Ilarduya, A.; Muñoz-Guerra, S. Poly (α-alkyl γ-glutamate) s of microbial origin : I. Ester derivatization of poly (γ-glutamic acid) and thermal degradation. Polymer **2001**, 42, 9319–9327.

75. Ruokolainen, J.; Brinke, G.T.; Ikkala, O. Supramolecular polymeric materials with hierarchical structure-within-structure morphologies. *Adv. Mater.* **1999**, *11*, 777-780.

76. Thünemann, A. F.; Müller, M.; Dautzenberg, H.; Löwen, J. J. H. Polyelectrolyte complexes. Adv. Polym. Sci. **2004**, 166, 113–171.

77. Ponomarenko, E.A.; Waddon, A.J.; Tirrell, D.A.; Macknight, W.J. Structure and properties of stoichiometric complexes formed by sodium poliy*(α,L-glutamate) and oppositely charged surfactants.* Langmuir. **1996**, 12, 2169-2172.

78. Pérez-Camero, G.; García-Alvarez ,M.; Martínez de Ilarduya, A.; Fernández,C.; Campos,L.; Muñoz-Guerra,S. Comblike complexes of bacterial poly(gamma,D-glutamic acid) and cationic surfactants Biomacromolecules. **2004**, 5, 144.

79. Pérez-Camero, G.; Martínez de Ilarduya, A.; García-Álvarez, M., Muñoz-Guerra, S. Stoichiometric complexes made of naturally occurring poly (γ,D-glutamic acid) and cationic surfactants. *Abs. Pap. Amer. Chem. Soc.* **1999**, *218*, U532.

80. García-Alvarez, M.; Alvarez, J.; Alla, A.; Martínez de Ilarduya, A.; Muñoz-Guerra, S. Comb-like ionic complexes of cationic surfactants with bacterial poly(γ-glutamic acid) of racemic composition. *Macromol. Biosci.* **2005**, *5*, 30–38.

VI. REFERENCES

81. Horner, L.; Oediger, H. Phosphororganische verbindungen phosphinimino-verbindungen aus phosphindihalogeniden und primaren aminen. Ann. Chem. Liebigs **1959**, 627, 142.

82. Portilla-Arias, J. A.; García-Alvarez, M.; Martínez de Ilarduya, A.; Holler, E.; Muñoz-Guerra, S. Nanostructurated complexes of poly(β,L-malate) and cationic surfactants: synthesis, characterization and structural aspects. *Biomacromolecules* **2006**, *7*, 161–170.

83. Tolentino, A.; Salvador, L.C.; Abdelilah, A.; Martinez de Ilarduya, A.; Muñoz Guerra, S. Comblike Ionic Complexes of Poly(gamma-glutamic acid) and Alkanoylcholines Derived from Fatty Acids. Macromolecules. **2013**, 46, 1607−1617.

84. Carelli,V.; Liberatore, F.; Scipione, L.; Cardellini, M.; Rotiroti, D.; Rispoli, V. Enhancement of absorption of drugs from gastrointestinal tract using choline ester salts. U.S. Patent 4, 822, 773,**1989.**

85. Ponder, J.W.; Richards, F.M. An efficient Newton-like method for molecular mechanics energy minimization of large molecules. J.Comp.Chem.**1987**, 8, 1016-1024.

86. Volpi, N.; Schiller, J.; Stern, R.; Soltés, L. Role, metabolism, chemical modifications and applications of hyaluronan. *Curr. Med. Chem.* **2009**, *16,* 1718–1745.

87. Meyer K.; Palmer J.W. The polysaccharide of the vitreous humor. JBC.**1934**, 107,629–634.

88. Balazs E.A.; Laurent T.C.; Jeanloz R.W. Nomenclature of hyaluronic acid. Biochem. J. **1986**, 235, 903.

89. Chen W.Y.J.; Abatangelo G. Functions of hyaluronan in wound repair. Wound Repair and Regen. **1999**, 7, 79–89.

90. Liu, L.; Liu, Y.; Li, J.; Du, G.; Chen, J. Microbial production of hyaluronic acid: current state, challenges, and perspectives. Microb. Cell Fact. **2011**, 10, 99,144.

91. Izawa, N.; Hanamizu, T.; Iizuka, R.; Sone, T.; Mizukoshi, H.; Kimura, K.; Chiba, K. Streptococcus thermophilus produces exopolysaccharides including hyaluronic acid. J. Biosci. Bioeng. **2009**, 107, 119–123.

92. Kreil G. Hyaluronidases-a group of neglected enzymes. Protein Sci.**1995**, 4, 1666–1669.

93. Hidemichi, A.; Hisayuki, K.; Mitsuo, Y. Shiseiso Co LTD. Preparation of hyaluronic acid. JP Patent 58056692, **1983**.

94. Balazs, E. A. Ultrapure hyaluronic acid and the use thereof. US Patent 4141973, **1979**.

95. Cowman M.K.; Matsuoka S. Experimental approaches to hyaluronan structure. Carbohyd. Res. **2005**, 340, 791–809.

96. Hargittai, I.; Hargittai, M. Molecular structure of hyaluronan: an introduction. *Struct. Chem.* **2008**, *19,* 697–717.

97. Kobayashi, Y.; Okamoto, A.; Nishinari, K. Viscoelasticity of hyaluronicacid with different molecular-weights. *Biorheology.* **1994**, *31*, 235–244.

98. Neo H.; Ishimaru J.I.; Kurita K.; Goss A.N. The effect of hyaluronic acid on experimental temporomandibular joint osteoarthrosis in the sheep. J. Oral Maxil. Surg. **1997**, 55, 1114–1119.

99. Barbucci R.; Lamponi S.; Borzacchiello A.; Ambrosio L.; Fini M.; Torricelli P.; Giardino R. Hyaluronic acid hydrogel in the treatment of osteoarthritis. Biomaterials. **2002**, 23, 4503-4513.

100. Uthman I.; Raynauld J.P.; Haraoui B. Intra-articular therapy in osteoarthritis. Postgrad. Med. J. **2003**, 79, 449–453.

101. Brown M.B.; Jones S.A. Hyaluronic acid: a unique topical vehicle for the localized delivery of drugs to the skin. JEADV. **2005**, 19, 308–318.

VI. REFERENCES

102. Duranti, F.; Salti, G.; Bovani, B.; Calandra, M., Rosati, M. L. Injectable hyaluronic acid gel for soft tissue augmentation – a clinical and histological study. Dermatol. Surg. **1998**, 24, 1317–1325.

103. Shu, X. Z.; Liu, Y.; Palumbo, F. S.; Luo, Y.; Prestwich, G. D. In situ crosslinkable hyaluronan hydrogels for tissue engineering. Biomaterials. **2004**, 25, 1339–1348.

104. Lin, K.; Bartlett, S. P.; Matsuo, K.; Livolsi, V. A.; Parry, C.; Hass, B. Hyaluronic acid-filled mammary implants – an experimental study. Plast. Reconstr. Surg. **1994**, 94, 306–315.

105. Tolentino, A.; Alla, A.; Martínez de Ilarduya, A.; Font-Bardía, M.; León, S.; Muñoz-Guerra, S. Thermal behavior of long-chain alkanoylcholine soaps. RSC Adv. **2014**, 4, 10738–10750.

106. Davey, T. W.; Ducker, W. A.; Hayman, A. R.; Simpson, J. Krafft temperature depression in quaternary ammonium bromide surfactants. Langmuir, **1998**, 14, 3210–3213.

107. Adamová, G.; Gardas, R.L.; Nieuwenhuyzen, M.; Puga, A.V.; Rebelo, L. P. N.; Robertson A.J.; Seddona, K.R. Alkyltributylphosphonium chloride ionic liquids: synthesis, physicochemical properties and crystal structure. Dalton Trans. **2012**, 41, 8316–8332.

108. Portilla-Arias, J. A.; García-Alvarez, M.; Martínez de Ilarduya, A.; Holler, E.; Muñoz- Guerra, S. Thermal decomposition of fungal poly(beta,L-malic acid) and poly(beta,L-malate)s. Biomacromolecules. **2006**, 7, 3283–3290.

109. Portilla-Arias, J. A.; García-Alvarez, M.; Martínez de Ilarduya, A.; Muñoz-Guerra, S. Ionic complexes of biosynthetic poly(malic acid) and poly(glutamic acid) as prospective drug-delivery systems. Macromol. Biosci. **2007**, 7, 897–906.

110. Tolentino, A.; Alla, A.; Martínez de Ilarduya, A.; Muñoz-Guerra, S. Comblike ionic complexes of pectinic and alginic acids with alkyltrimethylammonium surfactants. Carbohyd. Polym. **2011**, 86, 484–490.

111. Tolentino, A.; Alla, A.; Martínez de Ilarduya, A.; Muñoz-Guerra, S. Comb-like ionic complexes of hyaluronic acid with alkyltrimethylammonium. Carbohyd. Polym. **2013**, 92, 691– 696.

112. Daasch, L. W.; Smith, D. C. Infrared spectra of phosphorus compounds. Amal. Chem. **1951**, 23, 858.

113. Rao, C. N. R.; Ramachandran, J.; Balasubramanian, A. Infrared and near-ultraviolet absorption spectra of polyphenyl derivatives of elements of groups ivb and vb. Can. J. Chem. **1961**, 39, 171.

VI. REFERENCES

VI.   SUPLEMENTARY INFORMATION

*

1. Alkyltrimethylphosphonium salts (*n*ATMP·Br)

1.1 Chemical Characterization
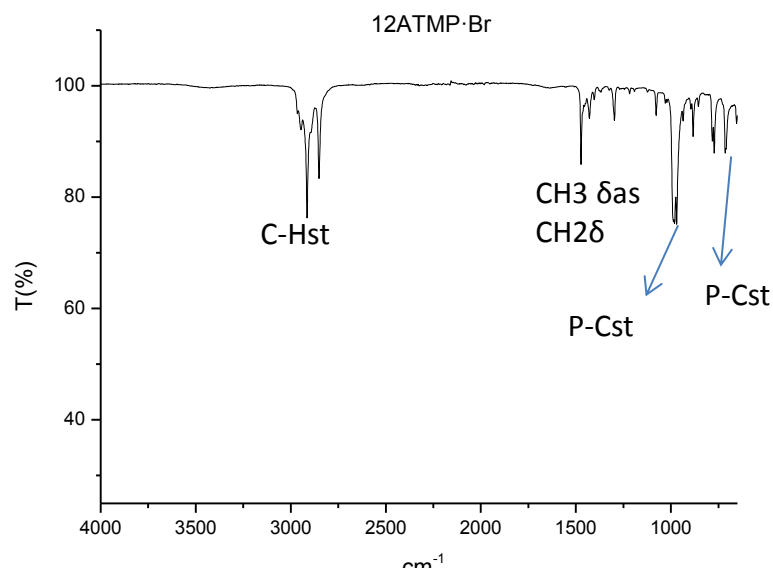
Figure VI.1. FTIR of 12ATMP·Br.

Figure VI.2. (a) ^{1}HNMR and **(b)** ^{13}C NMR spectra of *12*ATMP·Br recorded at 25 °C.   ppm

VII. SUPPLEMENTARY INFORMATION
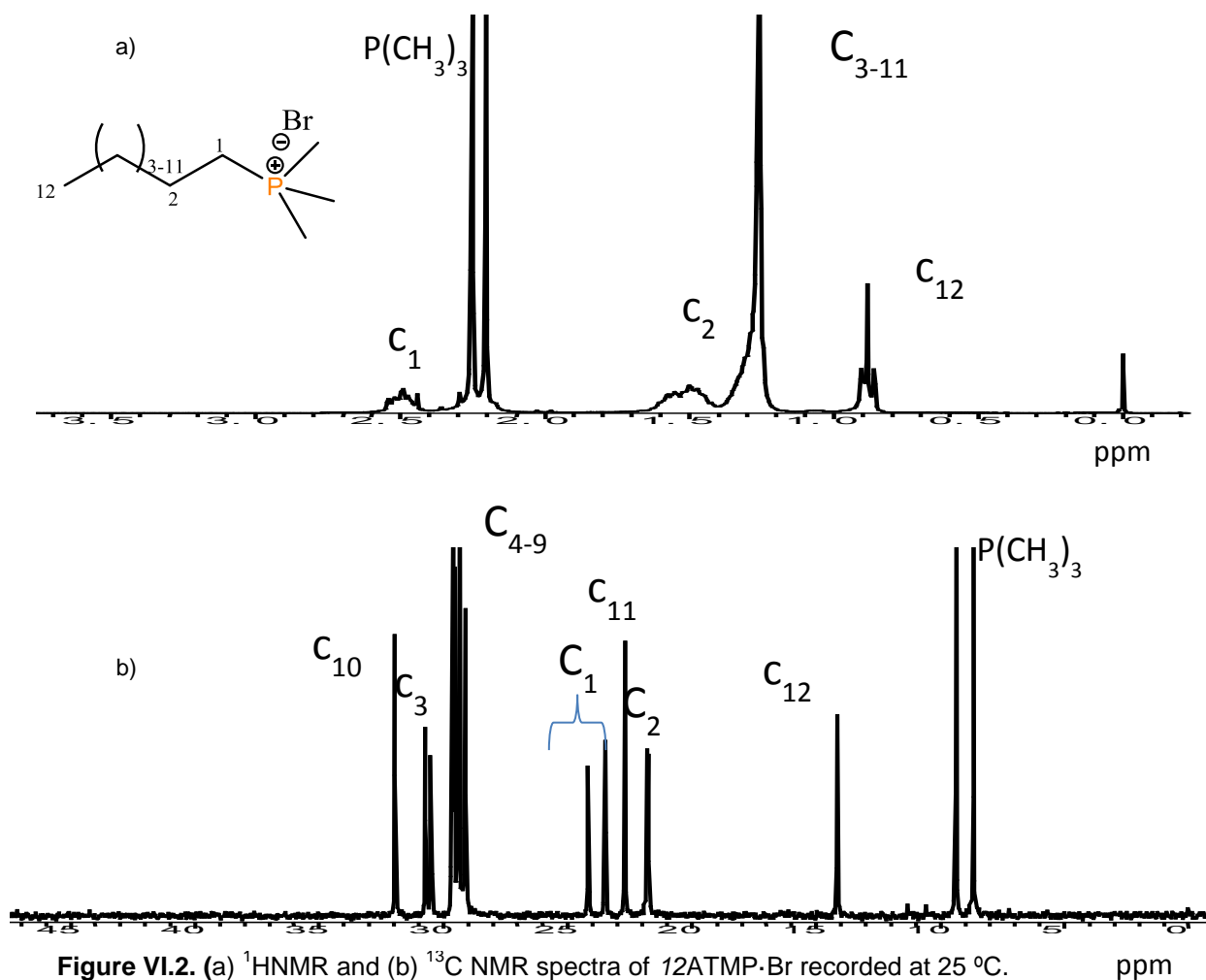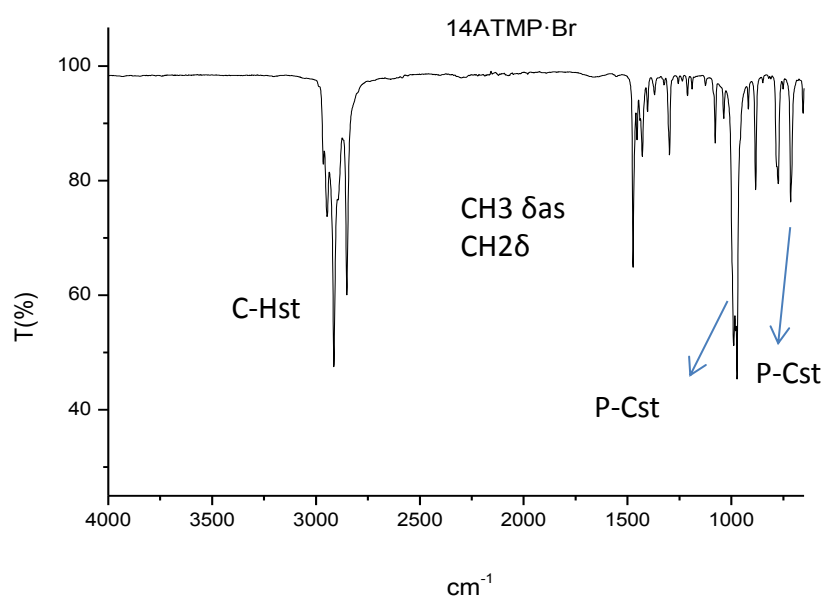
Figure VI.3. FTIR of 14ATMP·Br.
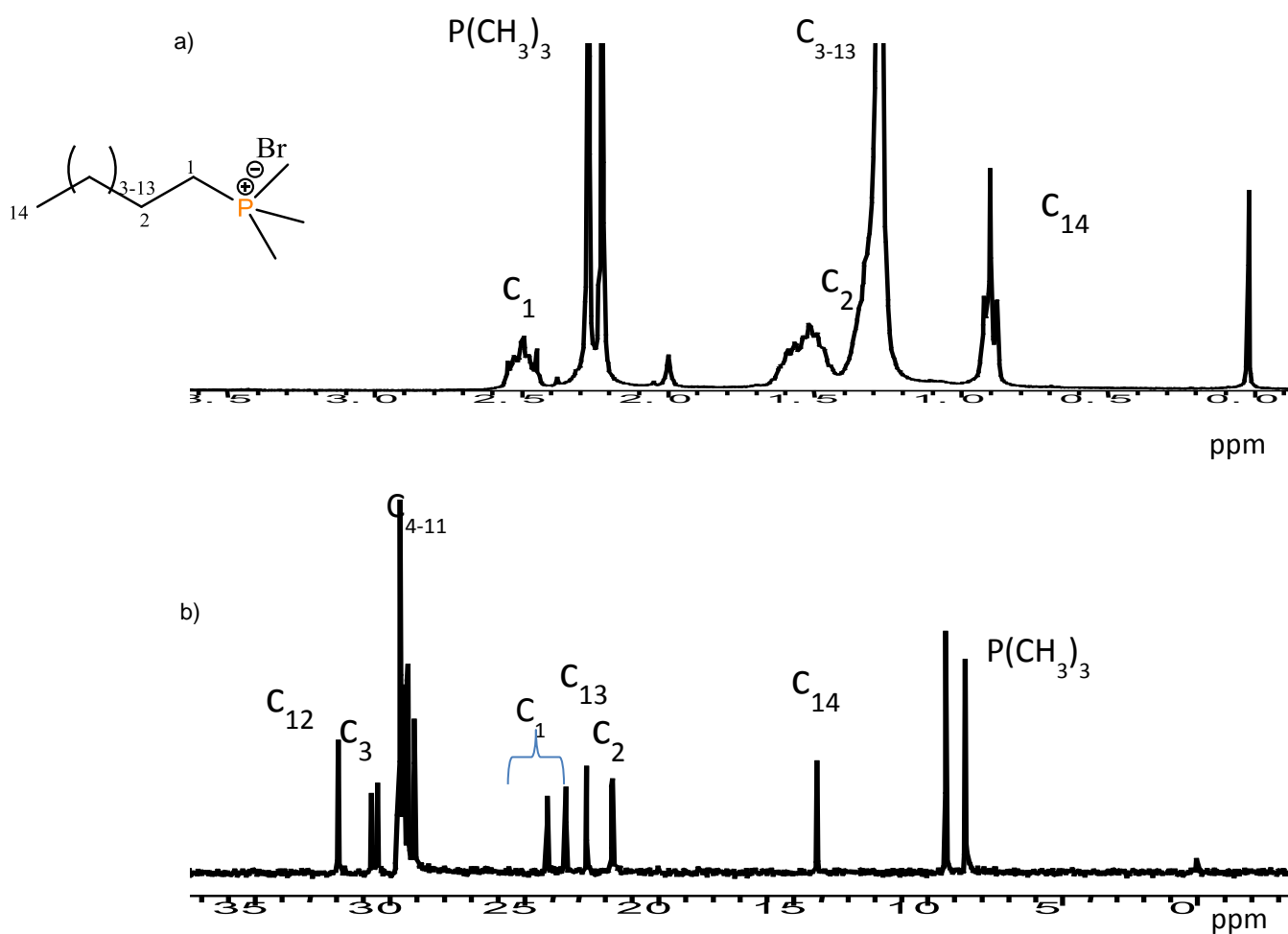
Figure VI.4. (a) ^{1}HNMR and (b) ^{13}C NMR spectra of *14*ATMP·Br recorded at 25 °C.

VII. SUPPLEMENTARY INFORMATION
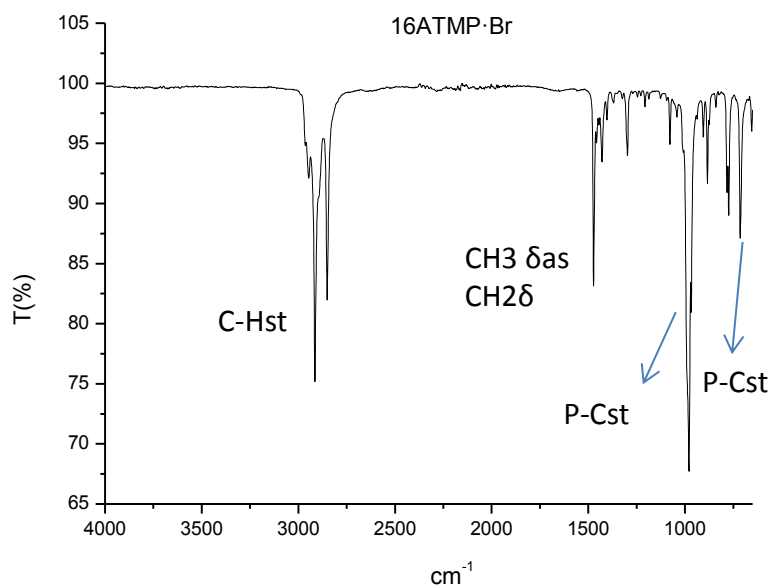
Figure VI.5. FTIR of 16ATMP·Br.
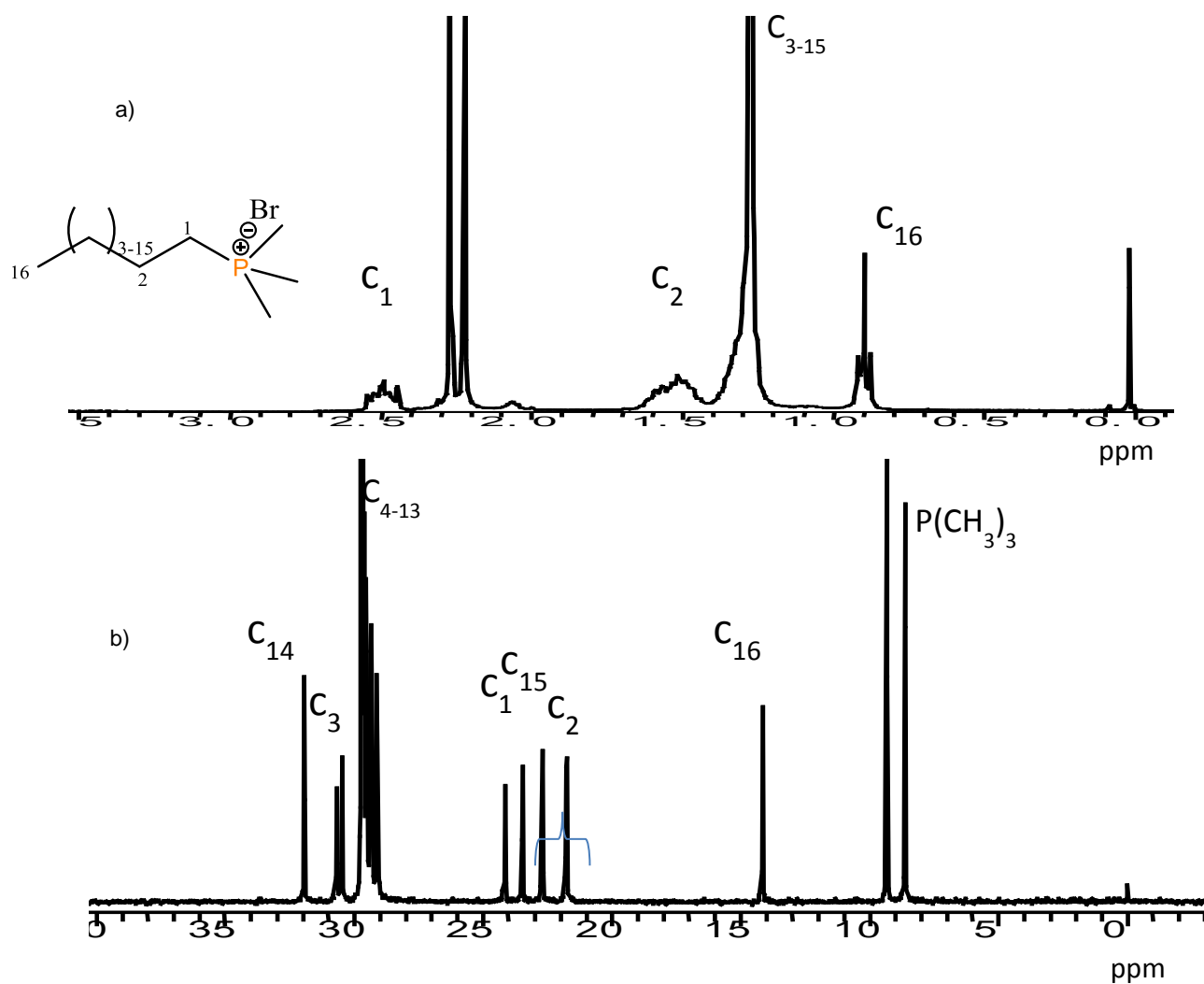
Figure VI.6. (a) ^{1}HNMR and **(b)** ^{13}C NMR spectra of *16*ATMP·Br recorded at 25 ºC.

VII. SUPPLEMENTARY INFORMATION
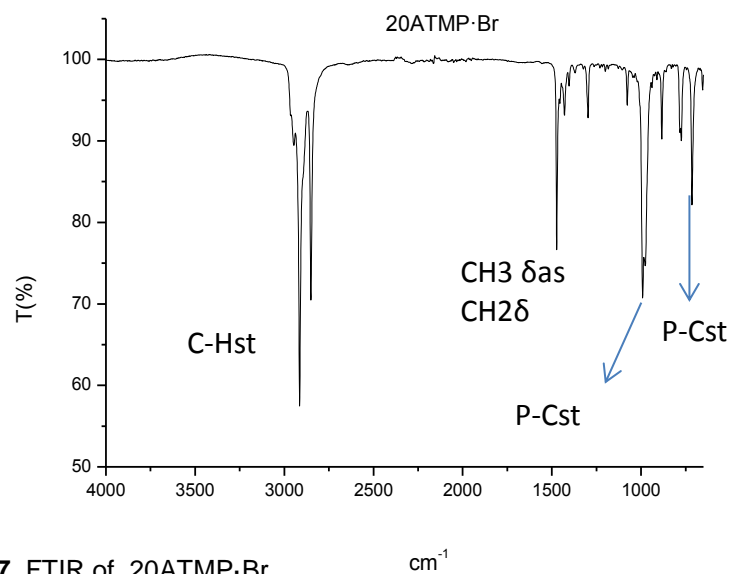
Figure VI.7. FTIR of 20ATMP·Br.
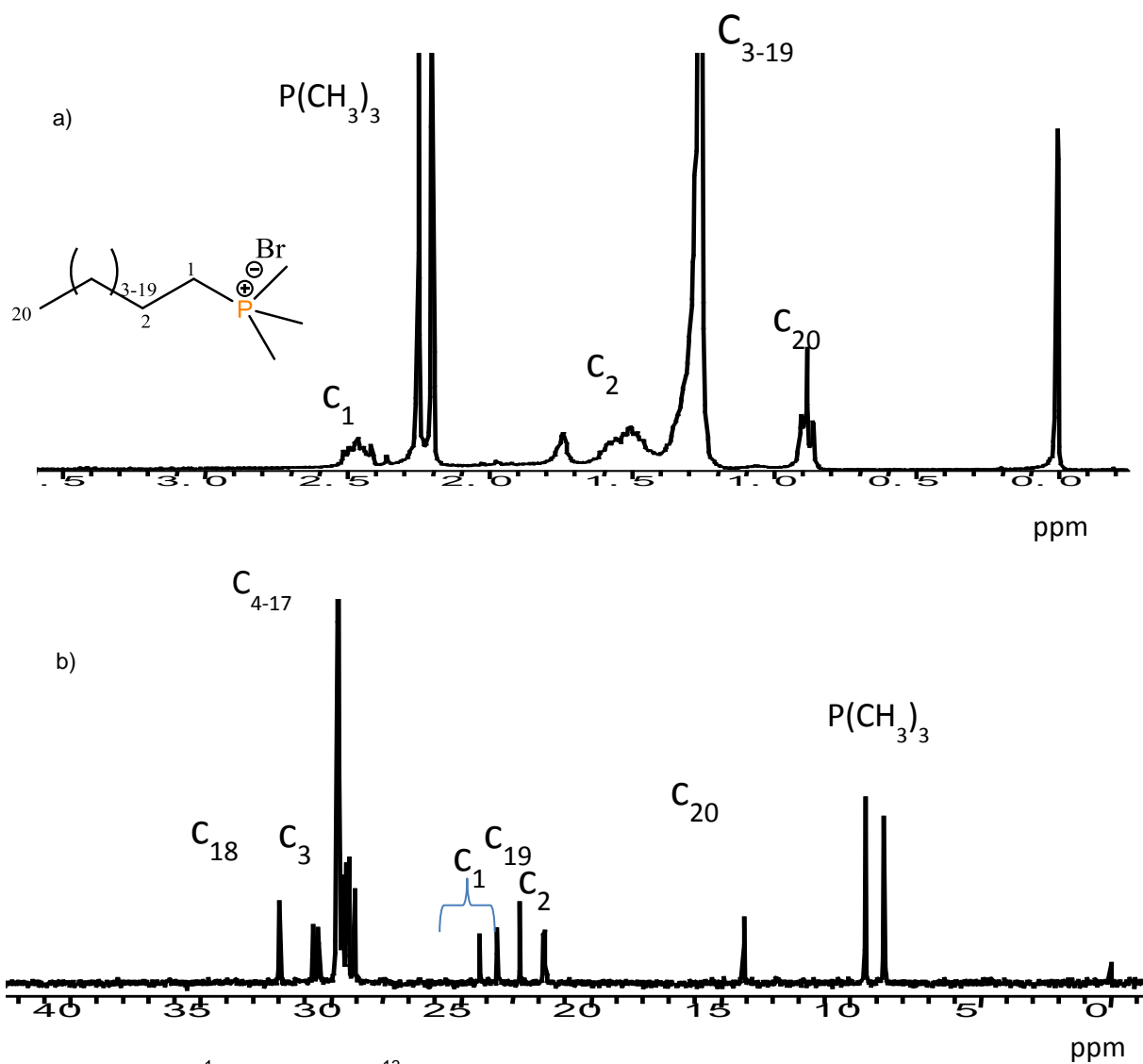
Figure VI.8. (a) ^{1}HNMR and (b) ^{13}C NMR spectra of *20*ATMP·Br recorded at 25 ºC.

VII. SUPPLEMENTARY INFORMATION
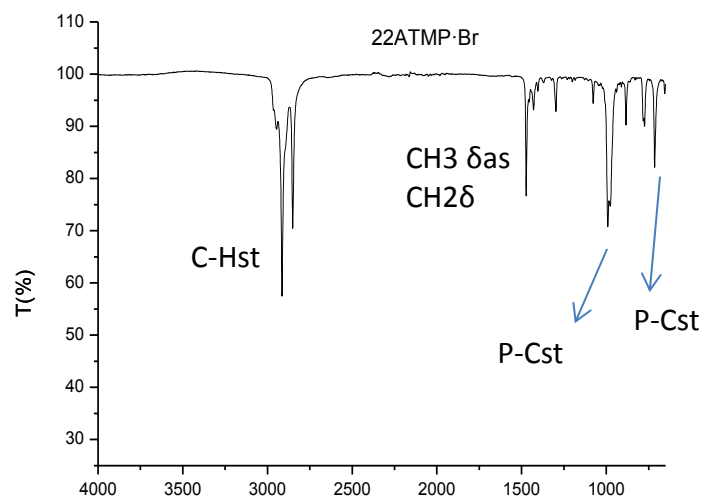
Figure VI.9. FTIR of 22ATMP·Br.
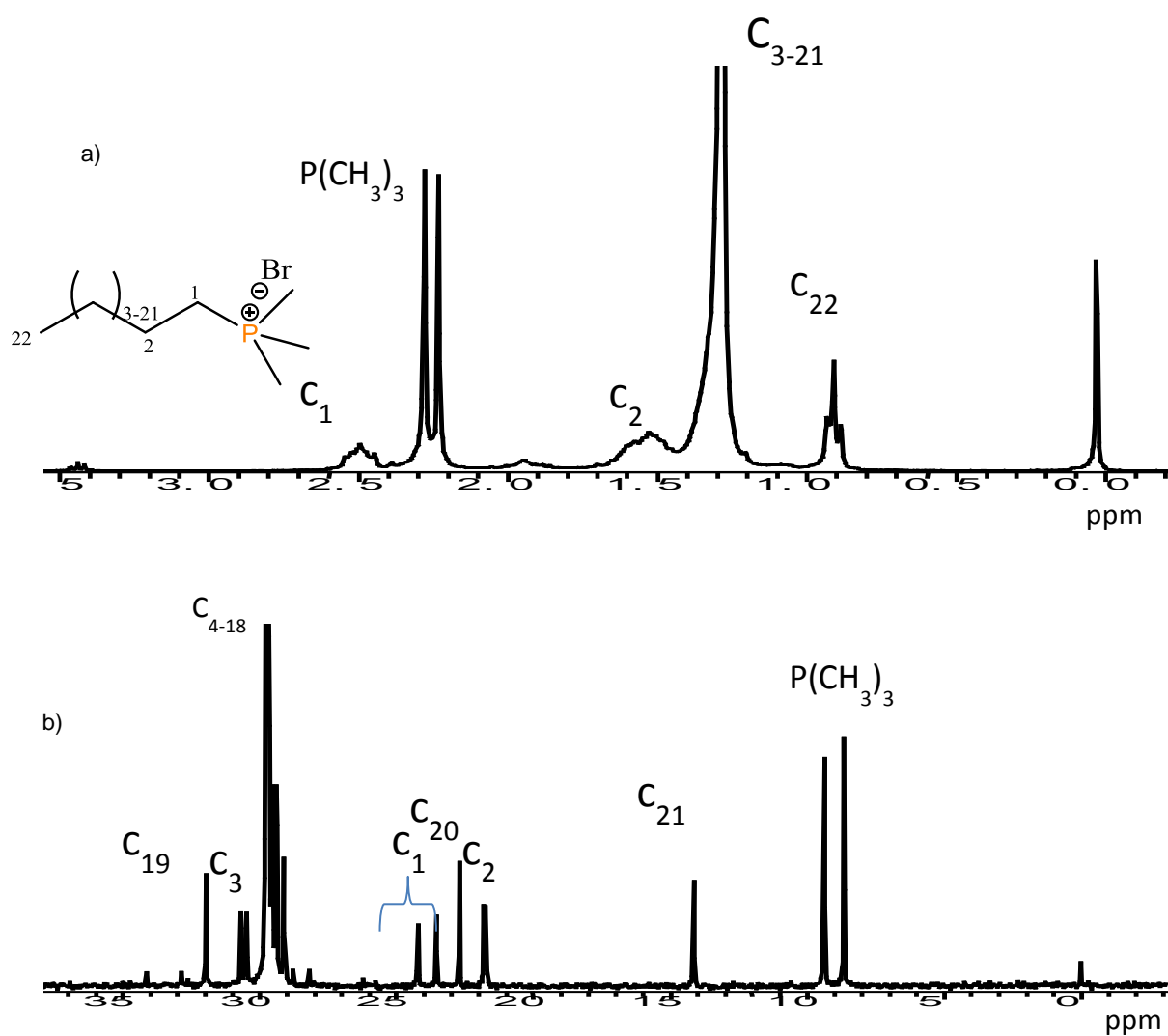
Figure VI.10. (a) ^{1}HNMR and (b) ^{13}C NMR spectra of 22ATMP·Br recorded at 25 ºC.

VII. SUPPLEMENTARY INFORMATION

2.2 Thermal transitions
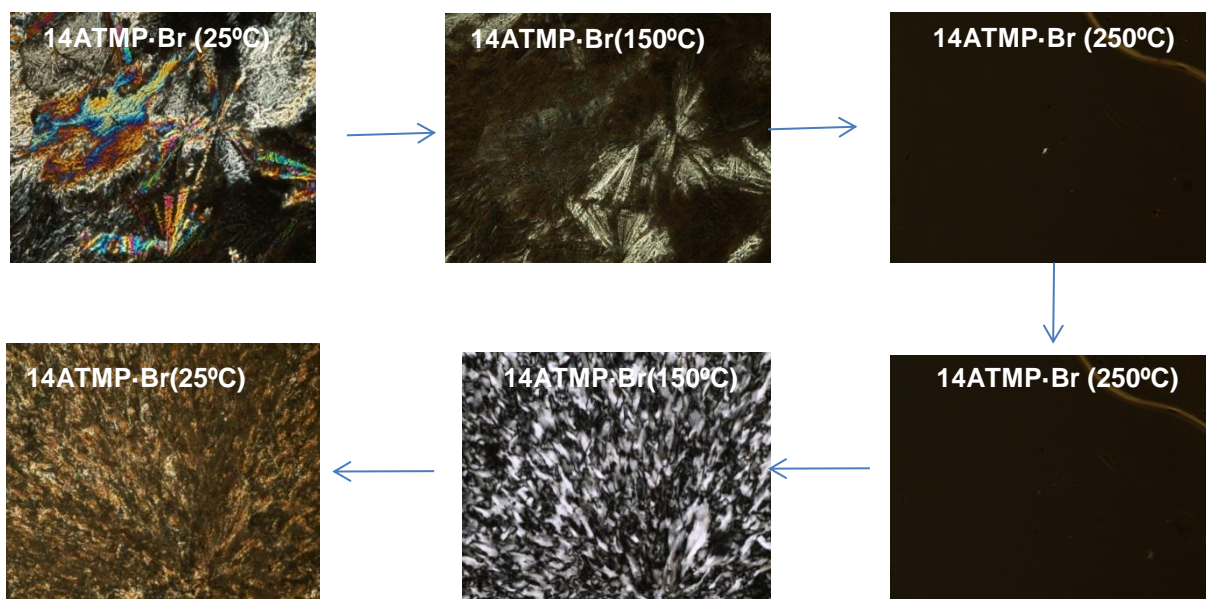
Figure. III.11. Micrographs recorded by POM from 14ATMP·Br at the indicated temperatures.
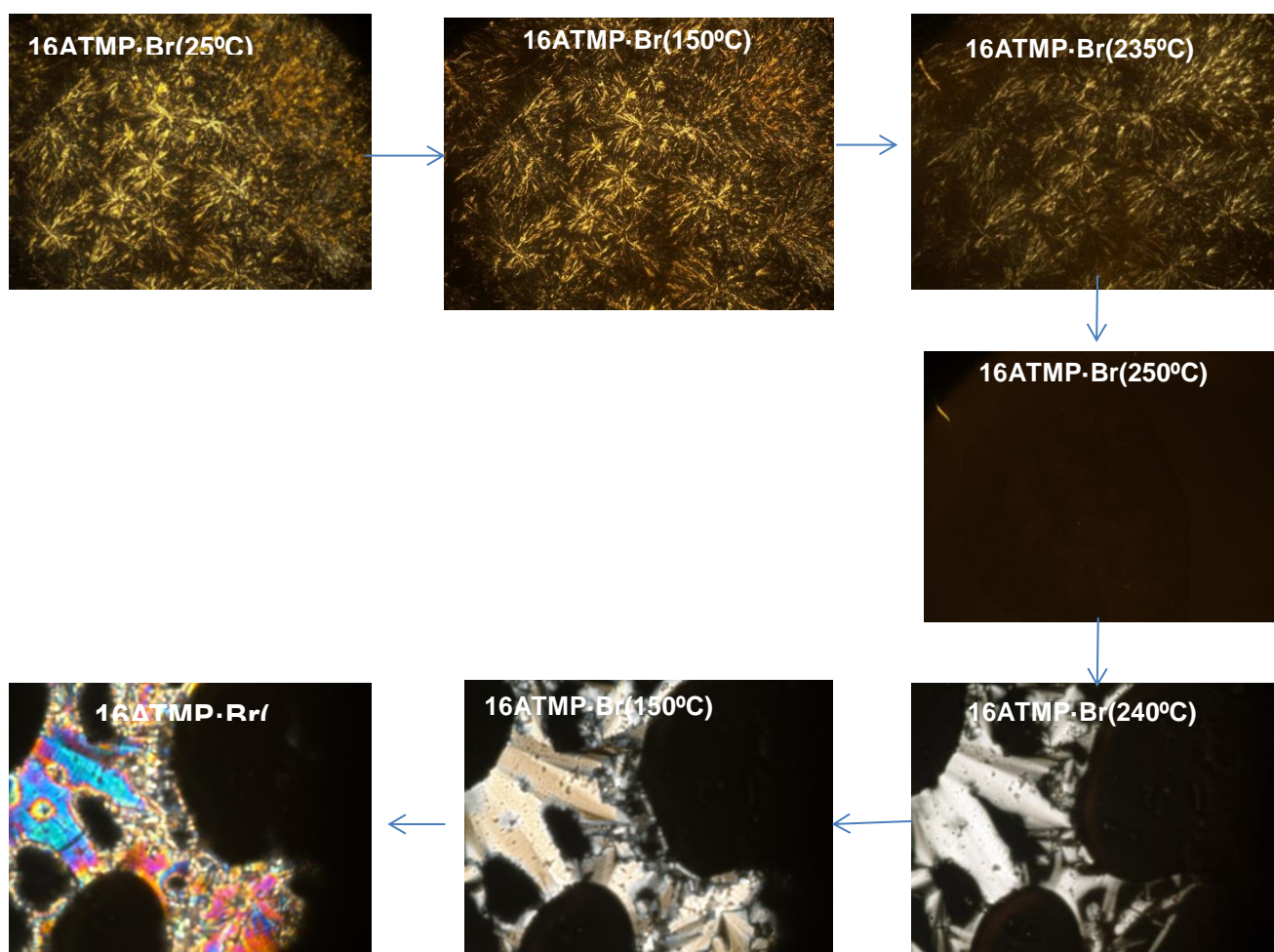
Figure. III.12. Micrographs recorded by POM from 16ATMP·Br at the indicated temperatures.

VII. SUPPLEMENTARY INFORMATION
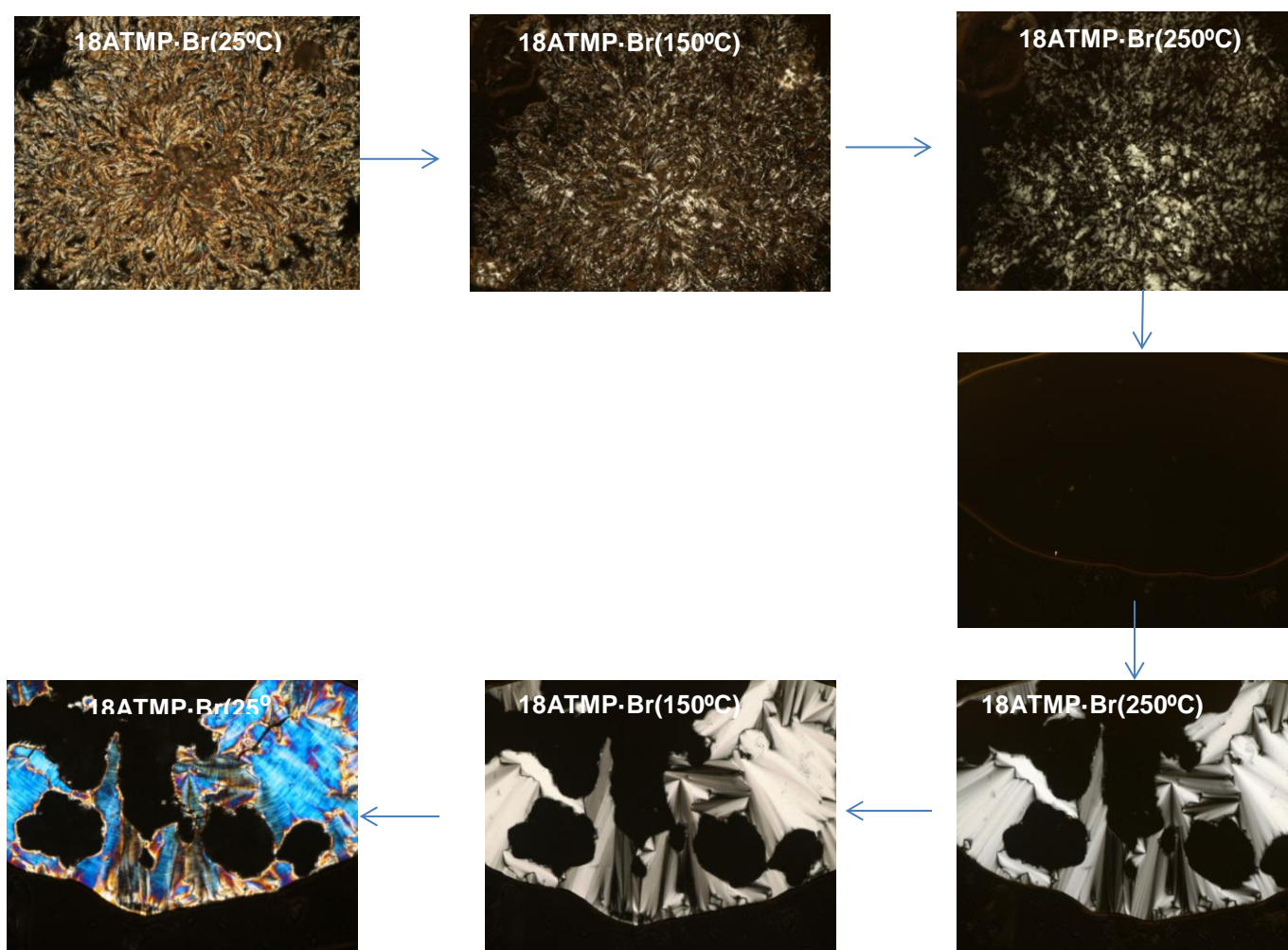
Figure. III.13. Micrographs recorded by POM from 18ATMP·Br at the indicated temperatures.
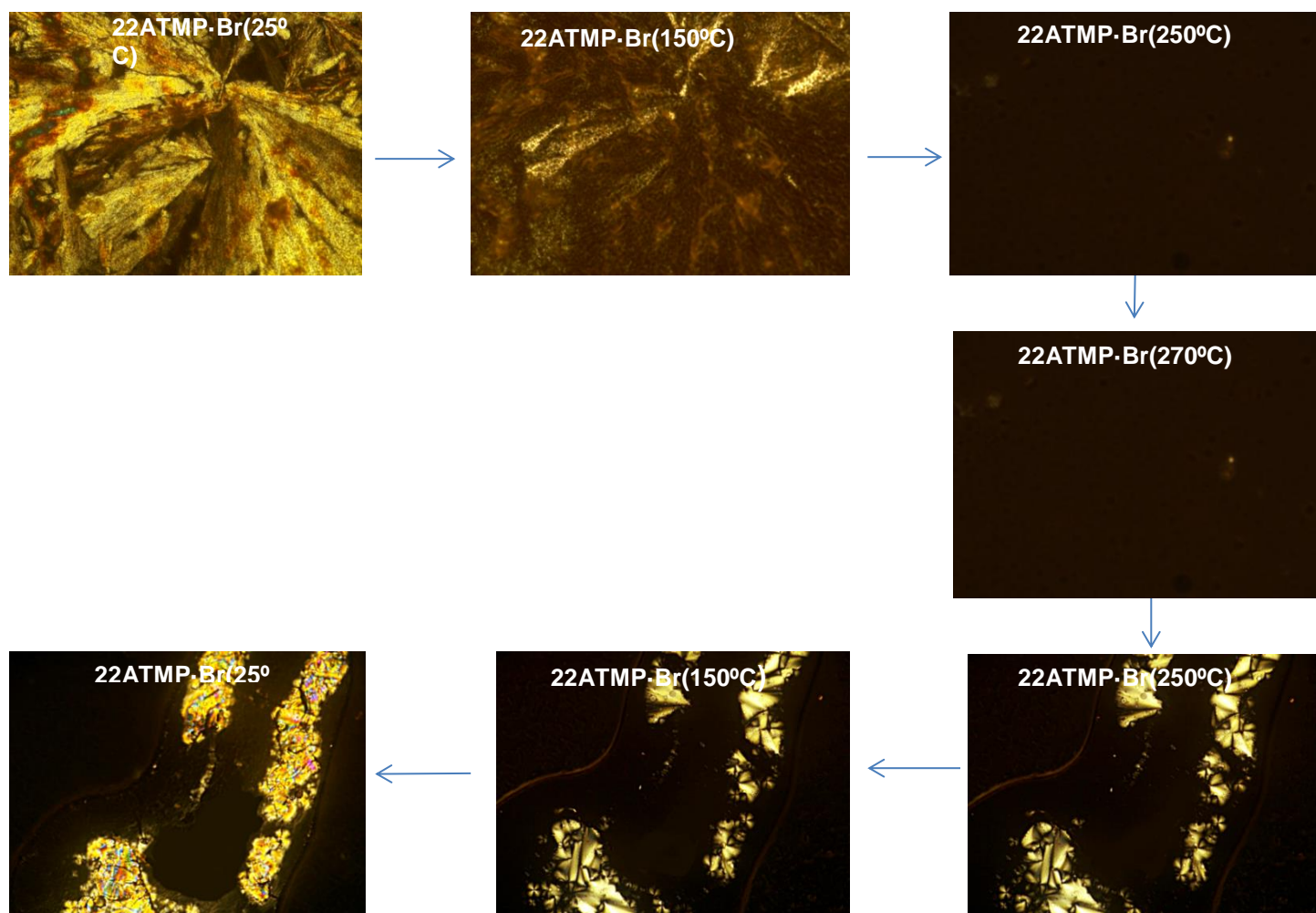
Figure. III.14. Micrographs recorded by POM from 12ATMP·Br at the indicated temperatures.

2.   Ionic complexs of *n*ATMP·PGGA

2.1 Chemical characterization
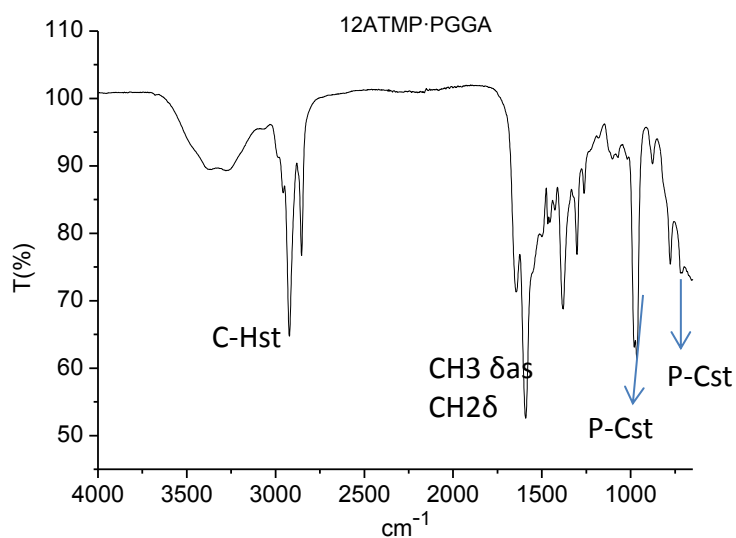
Figure VI.15. FTIR of 12ATMP·PGGA.
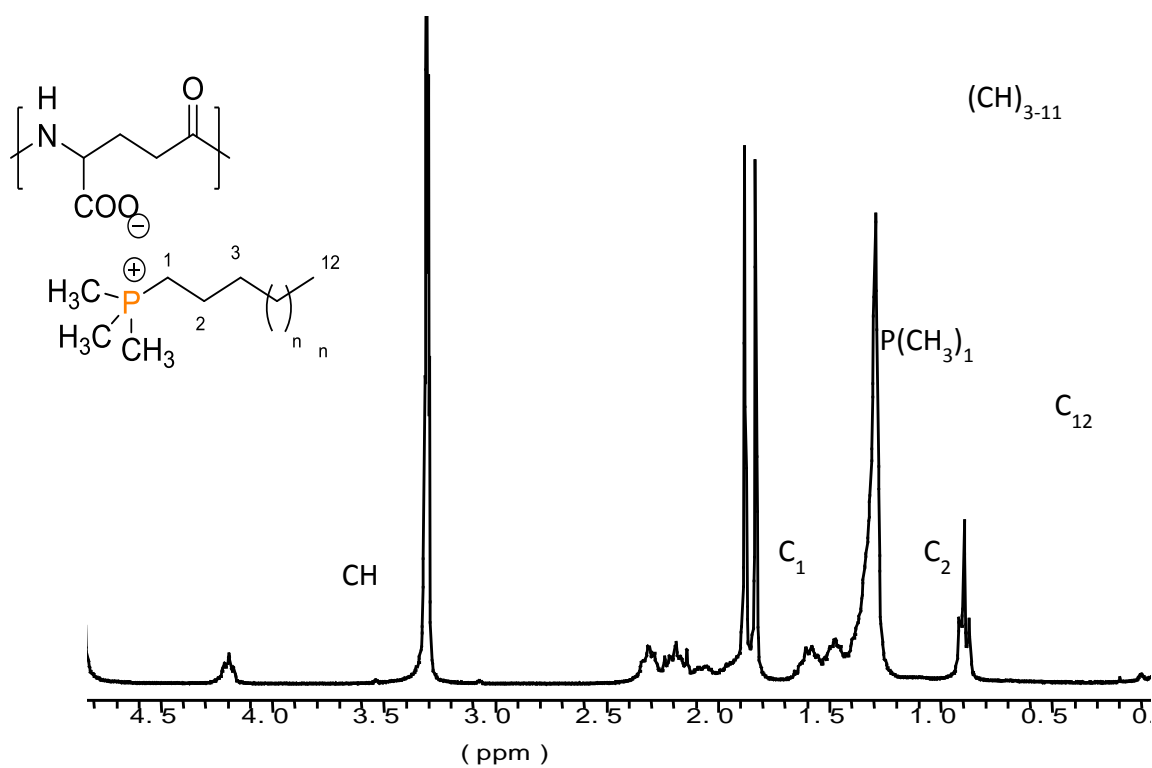
Figure VI.16. ^{1}HNMR spectrum of *12*ATMP·PGGA recorded at 25 ºC.
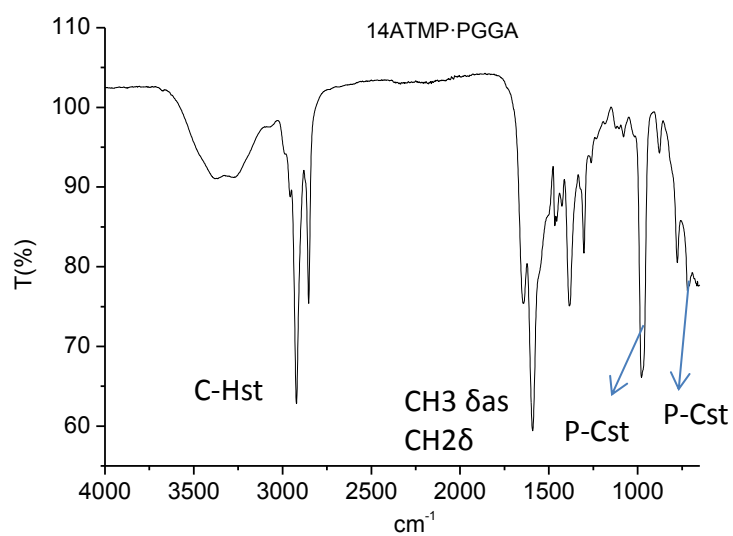
Figure VI.17. FTIR of 14ATMP· PGGA.
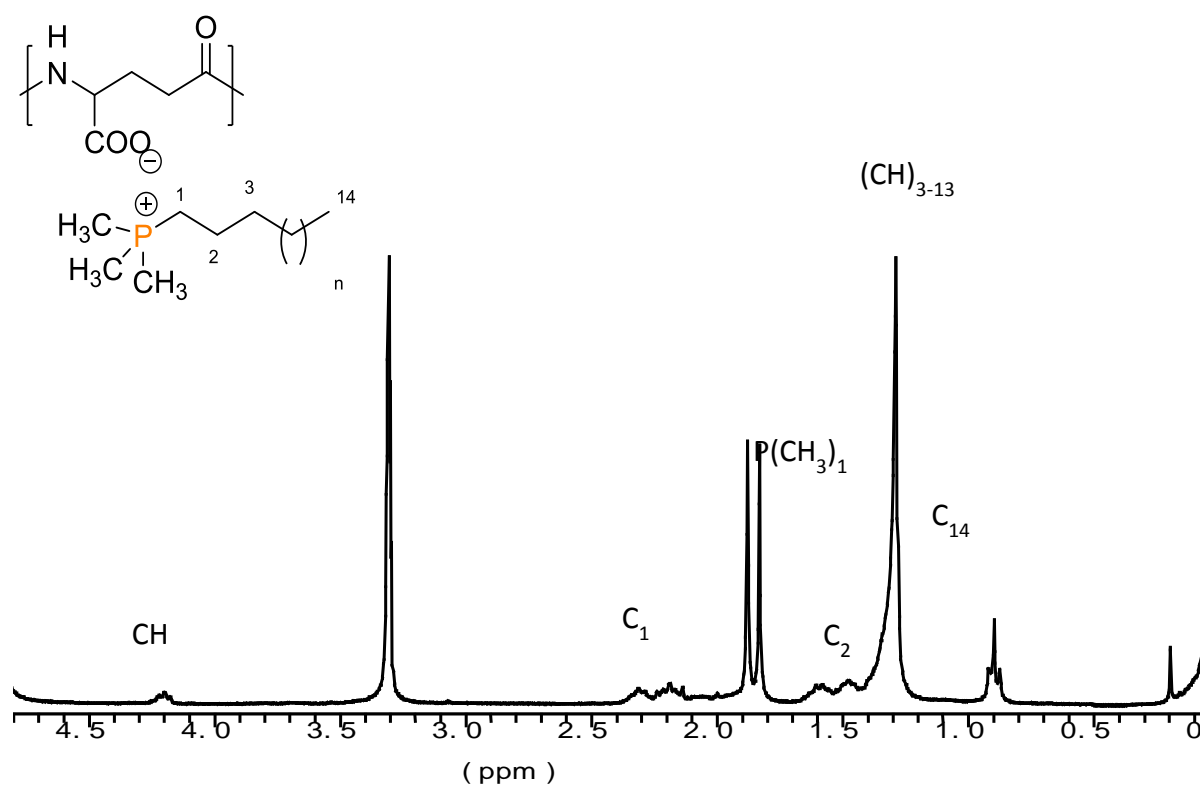
Figure VI.18. ^{1}HNMR spectrum of *14*ATMP·PGGA recorded at 25 °C.

VII. SUPPLEMENTARY INFORMATION
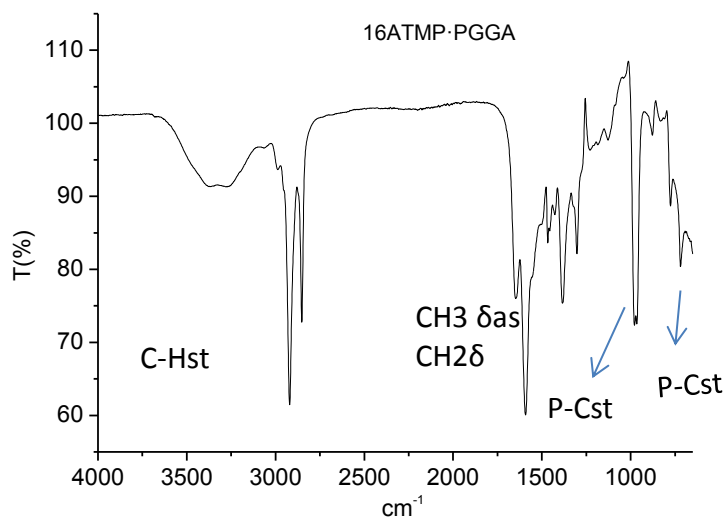
Figure VI.19. FTIR of 16ATMP· PGGA.
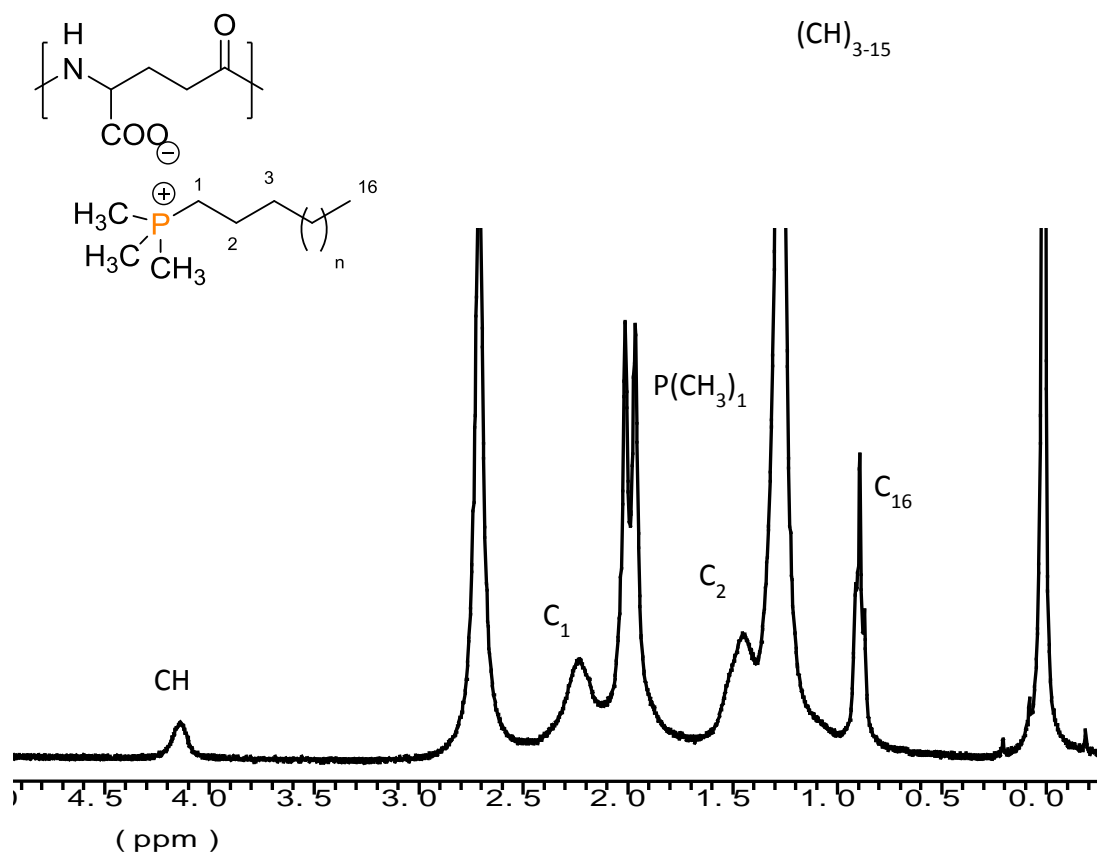
Figure VI.20. ^{1}HNMR spectrum of *16*ATMP·PGGA recorded at 25 ºC.

VII. SUPPLEMENTARY INFORMATION
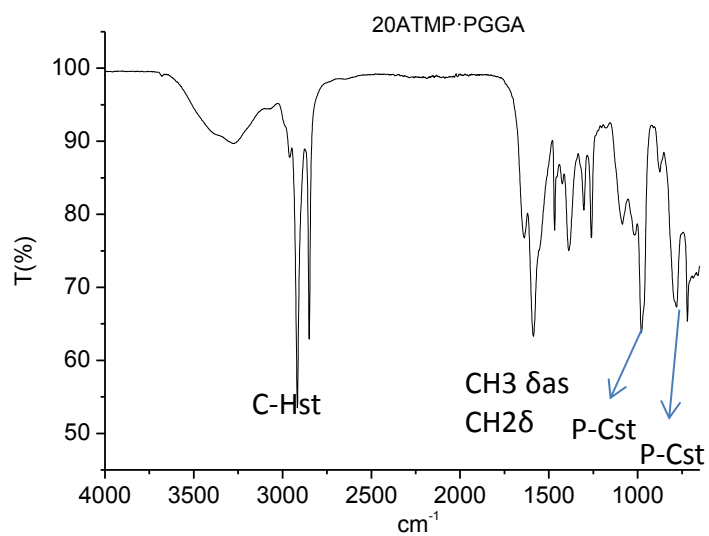
Figure VI.21. FTIR of 20ATMP· PGGA.
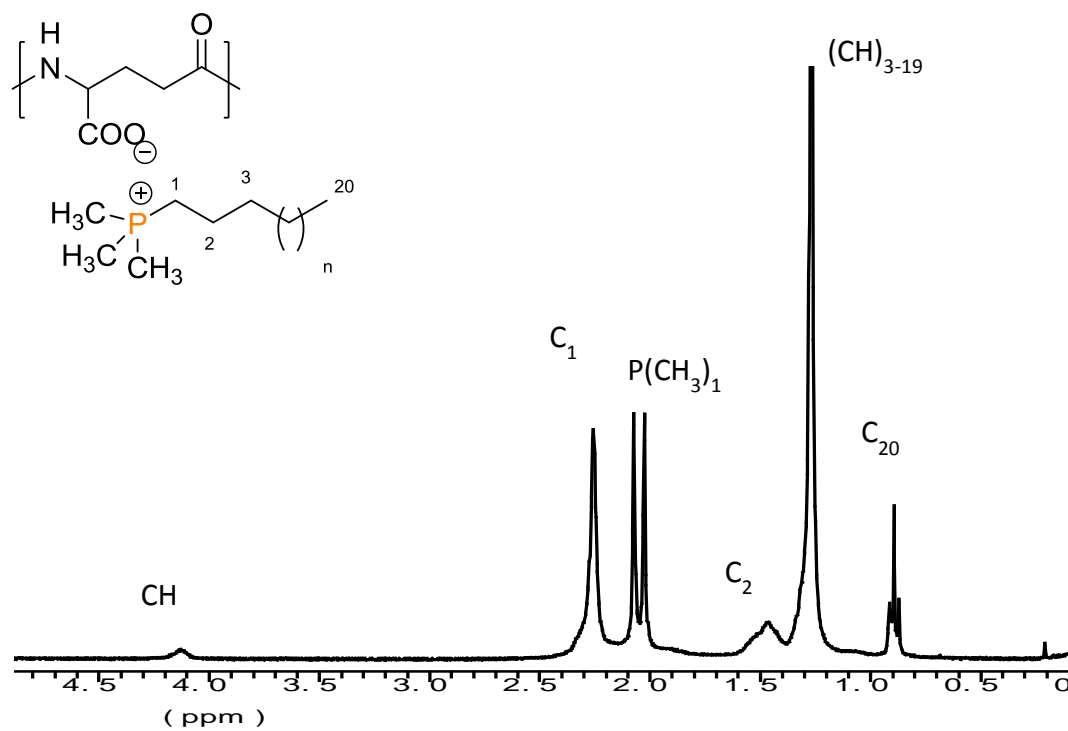
Figure VI.22. ^{1}HNMR spectrum of *20*ATMP·PGGA recorded at 25 ºC.

VII. SUPPLEMENTARY INFORMATION
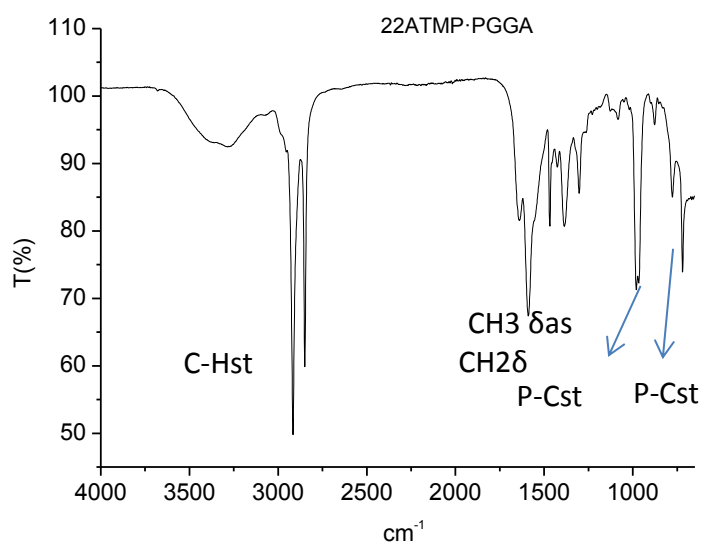
Figure VI.23. FTIR of 22ATMP· PGGA.
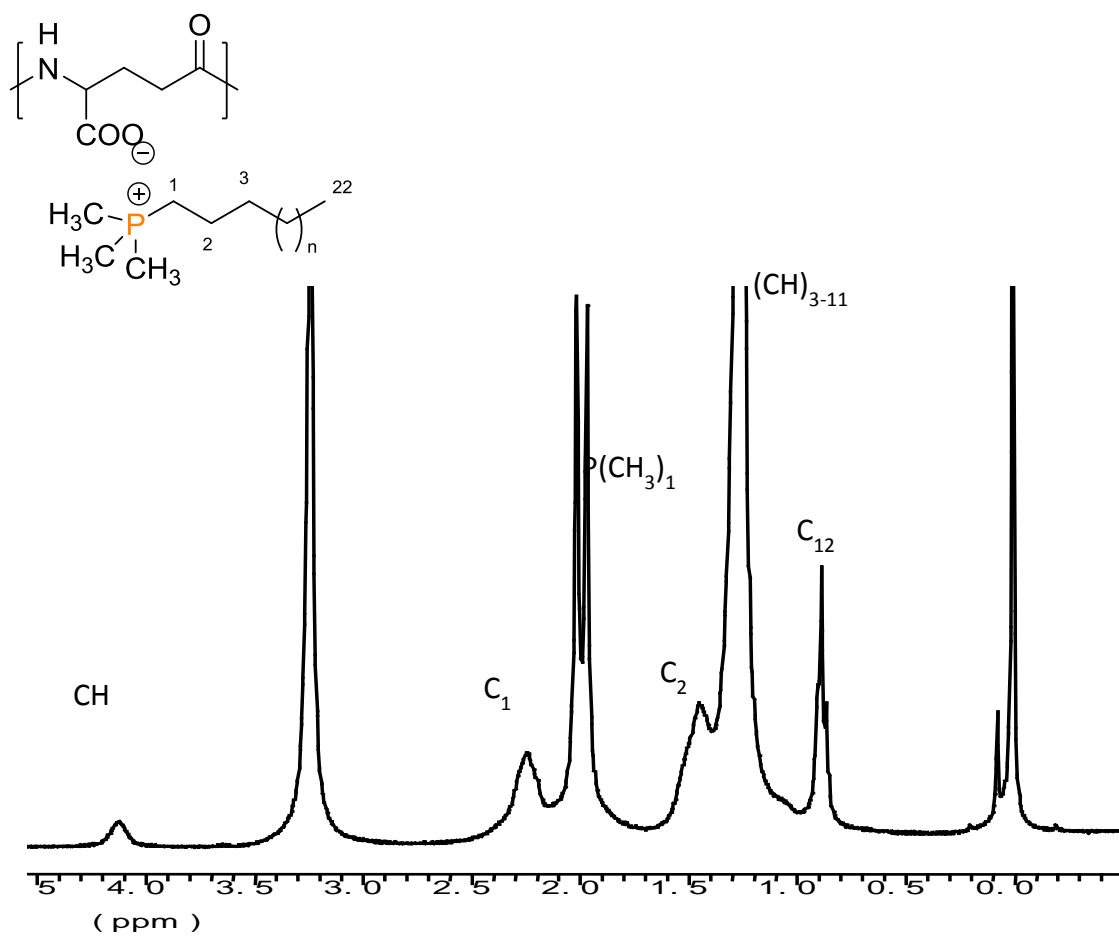
Figure VI.24. ^{1}HNMR spectrum of *22ATMP·PGGA* recorded at 25 ºC.

VII. SUPPLEMENTARY INFORMATION

3. Ionic complexes of *n*ATMP·HyalA

3.1 Chemical characterization
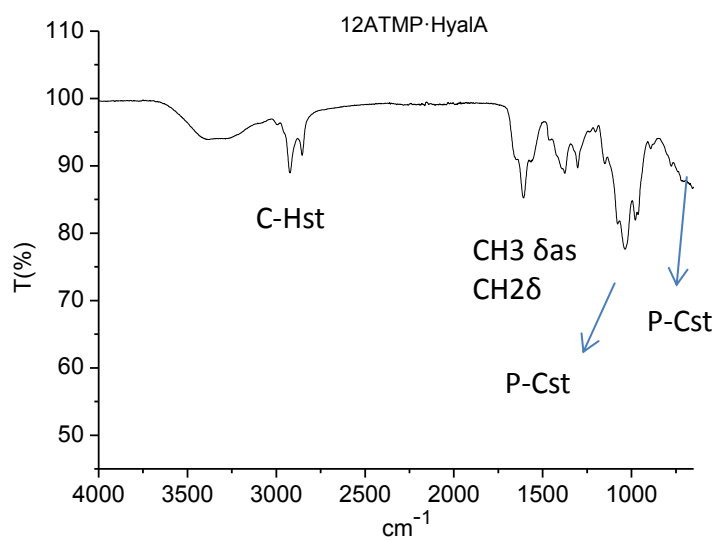
Figure VI.25. FTIR of 12ATMP·HyalA.
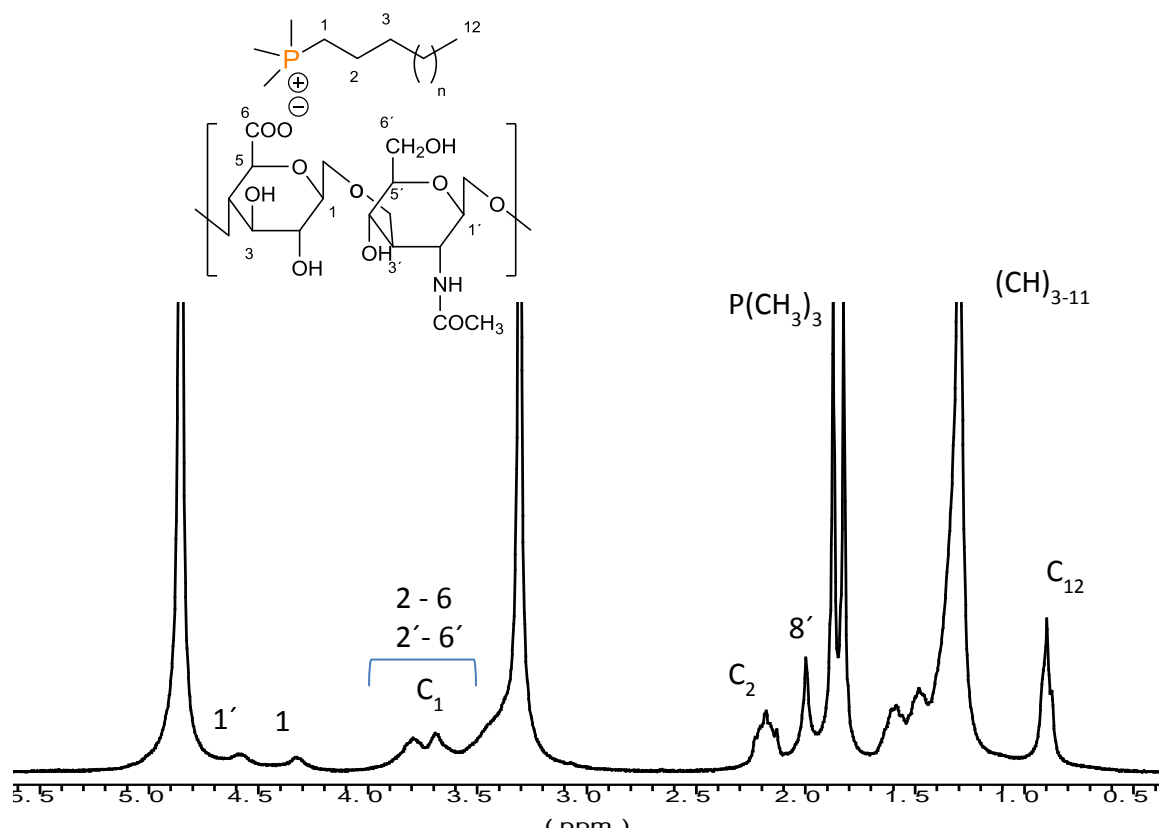
Figure VI.26. ^{1}HNMR spectrum of *12*ATMP·HyalA recorded at 25 ºC.
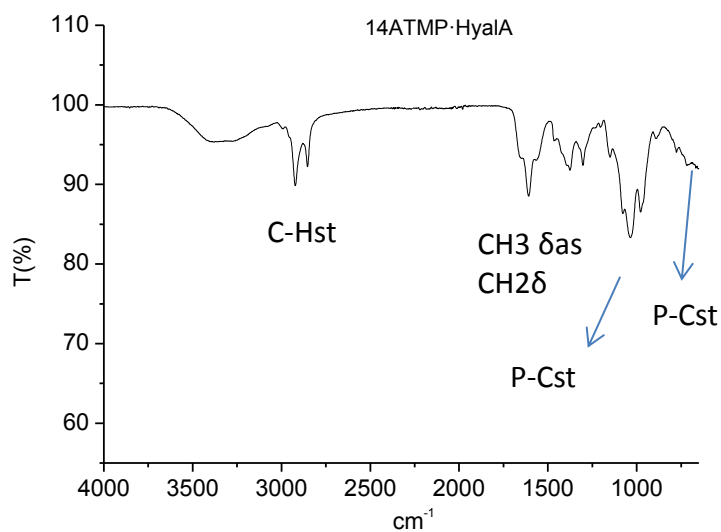
Figure VI.27. FTIR of 14ATMP·HyalA.
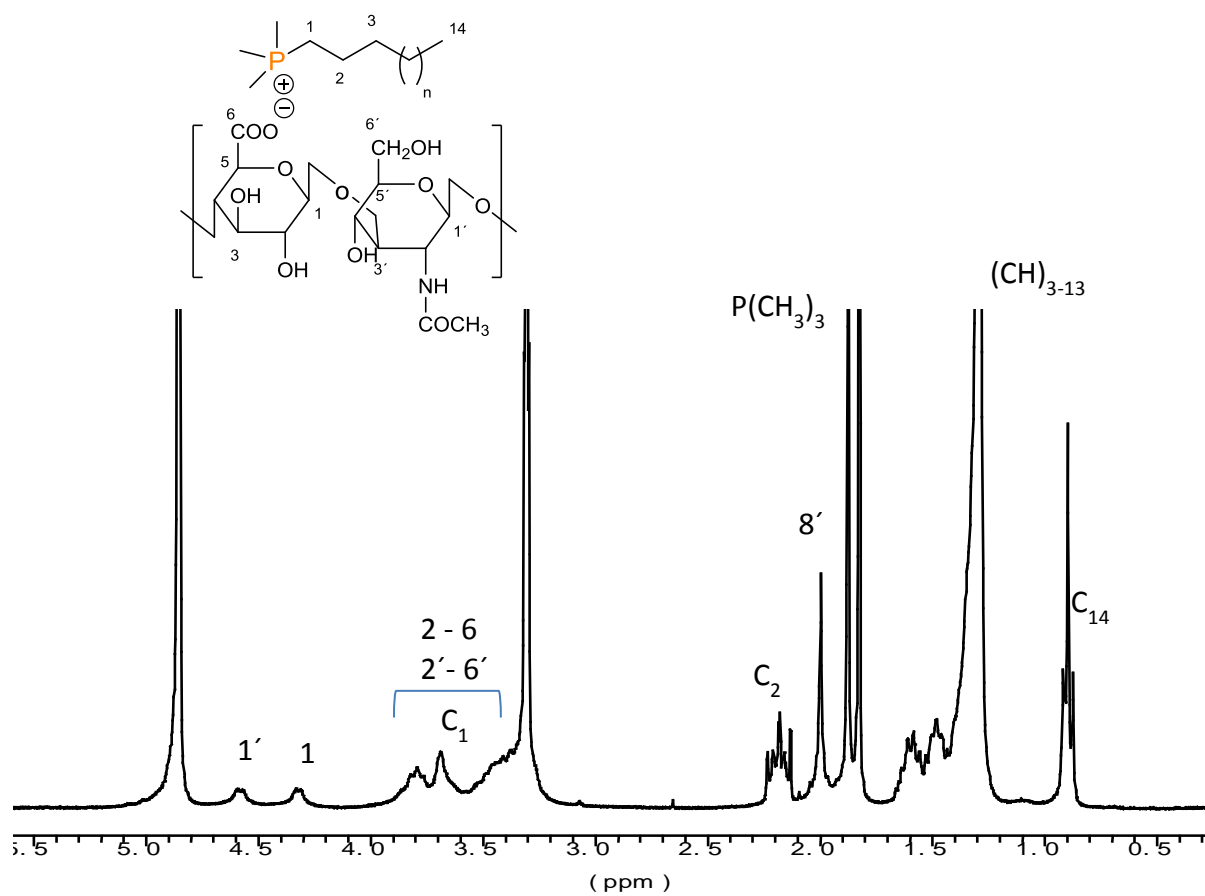
Figure VI.28. ^{1}HNMR spectrum of *14*ATMP·HyalA recorded at 25 ºC.

VII. SUPPLEMENTARY INFORMATION
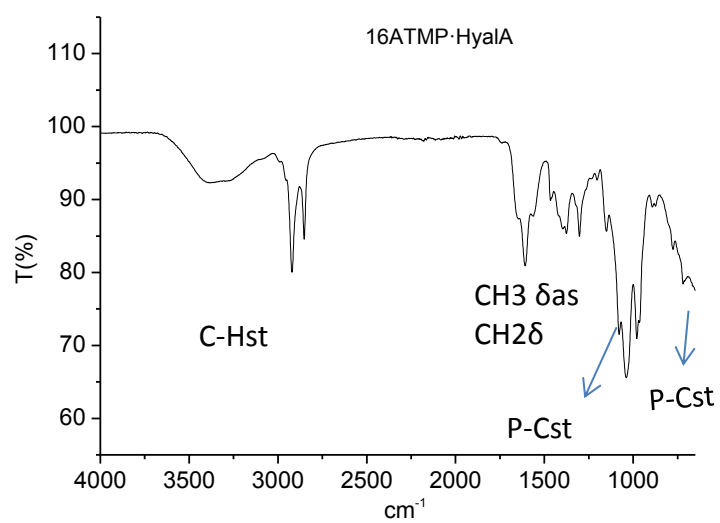
Figure VI.29. FTIR of 16ATMP·HyalA.
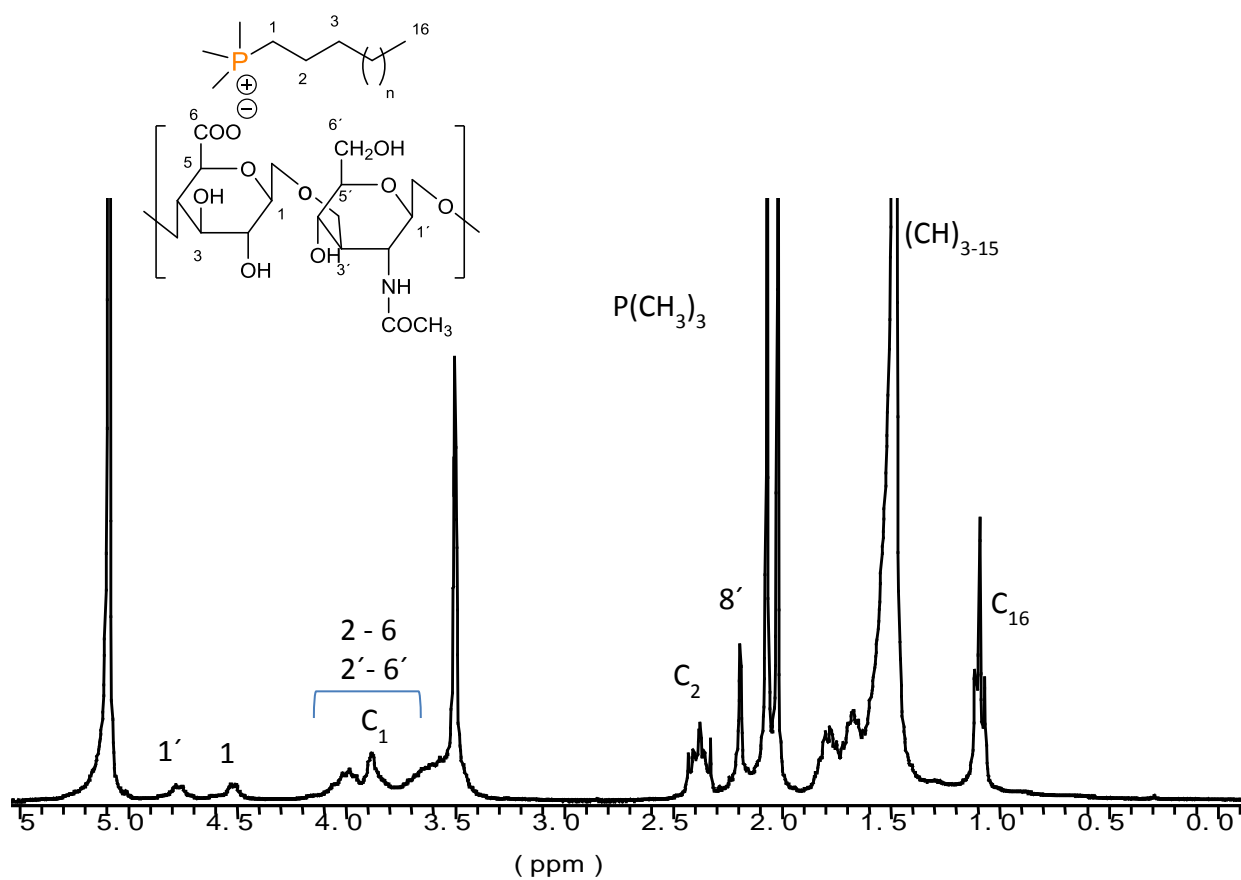
Figure VI.30. ^{1}HNMR spectrum of *16*ATMP·HyalA recorded at 25 ºC.

VII. SUPPLEMENTARY INFORMATION
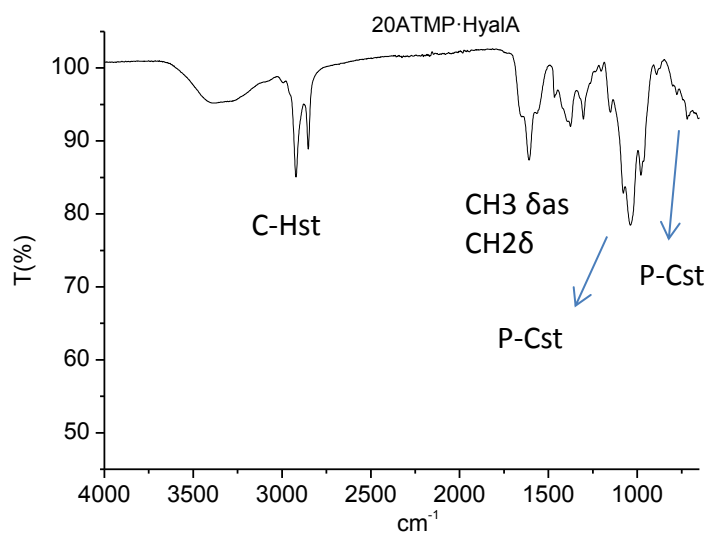
Figure VI.31. FTIR of 20ATMP·HyalA.
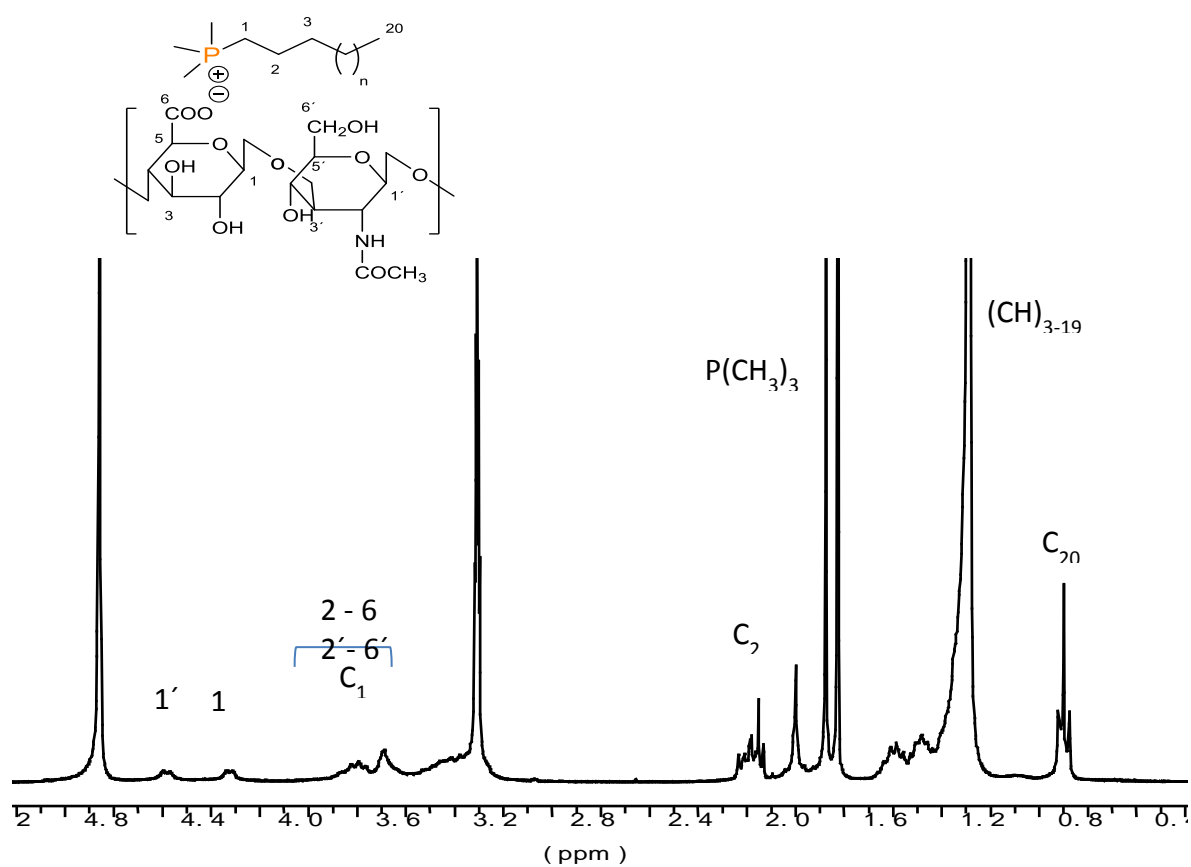
Figure VI.32. ^{1}HNMR spectrum of *20*ATMP·HyalA recorded at 25 ºC.

VII. SUPPLEMENTARY INFORMATION
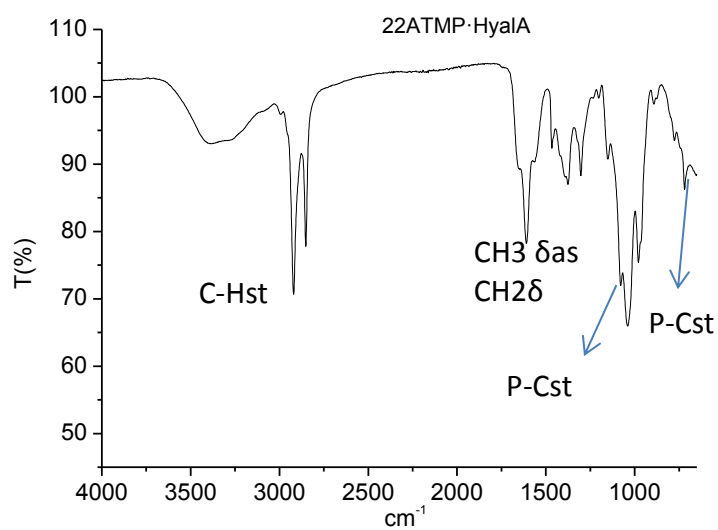
Figure VI.33. FTIR of 22ATMP·HyalA.
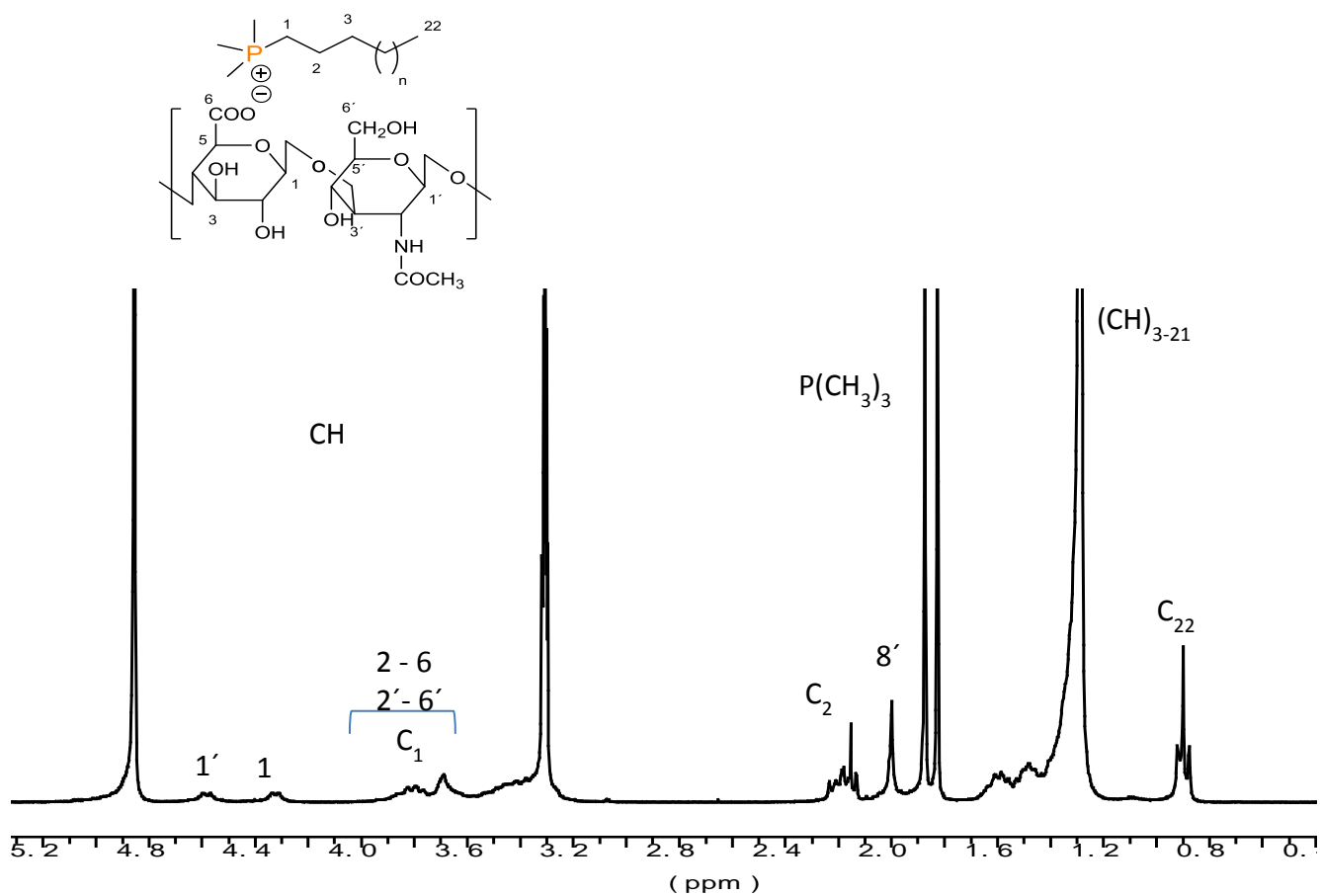
Figure VI.34. ^{1}HNMR spectrum of 22ATMP·HyalA recorded at 25 ºC.

VII. SUPPLEMENTARY INFORMATION

*